



**SYNTHESIS AND CHARACTERIZATION OF 4-  
VINYLPIRIDINE-FUNCTIONALIZED NATURAL  
RUBBER AS PH-RESPONSIVE MATERIALS**

**BY**

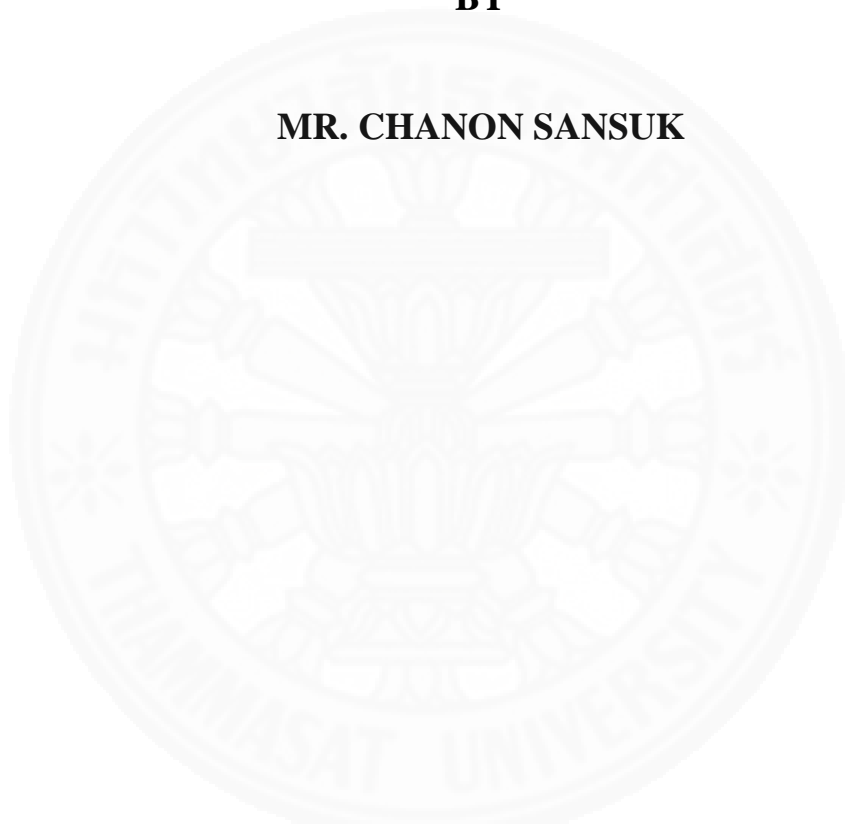
**MR. CHANON SANSUK**

**A THESIS SUBMITTED IN PARTIAL FULFILLMENT OF  
THE REQUIREMENTS FOR THE DEGREE OF  
MASTER OF SCIENCE (CHEMISTRY)  
DEPARTMENT OF CHEMISTRY  
FACULTY OF SCIENCE AND TECHNOLOGY  
THAMMASAT UNIVERSITY  
ACADEMIC YEAR 2016  
COPYRIGHT OF THAMMASAT UNIVERSITY**

**SYNTHESIS AND CHARACTERIZATION OF 4-  
VINYLPIRIDINE-FUNCTIONALIZED NATURAL  
RUBBER AS PH-RESPONSIVE MATERIALS**

**BY**

**MR. CHANON SANSUK**



**A THESIS SUBMITTED IN PARTIAL FULFILLMENT OF THE  
REQUIREMENTS FOR THE DEGREE OF  
MASTER OF SCIENCE (CHEMISTRY)  
DEPARTMENT OF CHEMISTRY  
FACULTY OF SCIENCE AND TECHNOLOGY  
THAMMASAT UNIVERSITY  
ACADEMIC YEAR 2016  
COPYRIGHT OF THAMMASAT UNIVERSITY**

THAMMASAT UNIVERSITY  
FACULTY OF SCIENCE AND TECHNOLOGY

THESIS

BY


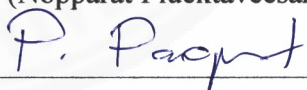
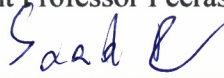
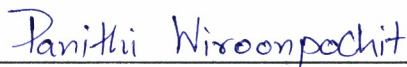
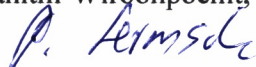
MR. CHANON SANSUK

ENTITLED

SYNTHESIS AND CHARACTERIZATION OF 4-VINYLPYRIDINE-  
FUNCTIONALIZED NATURAL RUBBER AS PH-RESPONSIVE MATERIALS

was approved as partial fulfillment of the requirements for  
the degree of master of science (chemistry)

on July 7, 2017

Chairman	 _____ (Nopparat Plucktaveesak, Ph.D.)
Member and Advisor	 _____ (Assistant Professor Peerasak Paoprasert, Ph.D.)
Member	 _____ (Associate Professor Sa-Ad Riyajan, Ph.D.)
Member	 _____ (Panithi Wiroonpochit, Ph.D.)
Dean	 _____ (Associate Professor Pakorn Sermasuk, M.Sc.)

Thesis Title	SYNTHESIS AND CHARACTERIZATION OF 4-VINYLPYRIDINE-FUNCTIONALIZED NATURAL RUBBER AS PH-RESPONSIVE MATERIALS
Author	Mr. Chanon Sansuk
Degree	Master of Science (Chemistry)
Major Field/Faculty/University	Chemistry Science and Technology Thammasat University
Thesis Advisor	Assistant Professor Peerasak Paoprasert, Ph.D.
Academic Years	2016

## ABSTRACT

Natural rubber (NR) is a renewable elastomer with excellent mechanical properties. Modification of NR *via* many chemical-based methods has been widely received much attention as it can improve the physical and chemical properties of NR and extend its application. This thesis research has demonstrated a method for introducing a pH-responsive function to NR using 4-vinylpyridine (4VP). Functionalization of 4VP onto NR *via* two methods: crosslinking and graft copolymerization, was described. The effects of varying the monomer/polymer concentration, initiator concentration, emulsifier concentration, reaction time, and reaction temperature on the reaction efficiency were investigated. It was found that the gel content of the crosslinking reaction reached 90% when using a P4VP concentration of 150 phr and a BPO concentration of 10 phr for 24 h at 90 °C. The grafting ratio of the grafting reaction achieved 31% when using a 4VP concentration of 100 phr, KPS concentration of 8 phr, and SDS concentration of 10 phr for 3 h at 90 °C. The 4VP-functionalized NRs were characterized using Fourier-transform infrared spectroscopy, proton nuclear magnetic resonance spectroscopy, and X-ray photoelectron spectroscopy techniques. The thermal properties of the resultant products were determined using thermogravimetric analyzer and differential scanning calorimeter. The pH-responsiveness of the obtained materials was studied using the water swelling

experiments and water contact angle measurement. The results showed that unlike the unmodified rubber, the 4VP-functionalized NRs were pH responsive in an acidic condition at pH below 4. Subsequently, the adsorption isotherm and the controlled-release behavior were studied to gain the mechanistic insights and explore the potentials for drug release applications. It was found that the dye adsorption on modified NR showed the Langmuir adsorption isotherm, suggesting a monolayer coverage of the dye. Moreover, the indigo carmine and carbon dot could also be released upon decreasing the pH of solution below 4. In summary, this research led to produce a new responsive rubber-based materials that can be used in biomedical and sensing applications.

**Keywords:** Natural rubber, 4-(vinylpyridine), Crosslinking, Grafting, pH-responsive materials

## ACKNOWLEDGEMENTS

I would like to express sincere thanks to my thesis advisor, Assistant Professor Peerasak Paoprasert, Ph.D. for his continued support throughout this research. In addition, the author is also grateful to Nopparat Plucktaveesak, Ph.D., Associate Professor Sa-Ad Riyajan, Ph.D., and Panithi Wiroonpochit, Ph.D. for serving as chairman and members of these thesis committee, respectively, and also giving me a beneficial guidance. All the comments and suggestions from the committee have been particularly valuable, and I have used them to fulfill this thesis research completely.

I am also thankful for the Faculty of Science and Technology, Thammasat University, Chulalongkorn University, Chiang Mai University, and the National Metal and Materials Technology Center (MTEC) for all instruments. Many thanks are also to all technical staffs of Department of Chemistry, Faculty of Science and Technology, Thammasat University for supporting. As well as, I am grateful to the scholarship for Talent Student, Faculty of Science and Technology, Thammasat University (2015-2016). Furthermore, I gratefully acknowledge the financial support provided by Thammasat University under the TU Research Scholar (2017).

Finally, I am most thankful to my beloved parents for their love and financial supports as well as to friend, especially Miss. Sopitcha Phetrong, for her helps during my study with a master degree.

The appreciation is expressed towards everyone who has encouraged suggestions and supports throughout this research.

Mr. Chanon Sansuk

## TABLE OF CONTENTS

	Page
ABSTRACT	(1)
ACKNOWLEDGEMENTS	(3)
LIST OF TABLES	(9)
LIST OF FIGURES	(10)
LIST OF ABBREVIATIONS	(14)
CHAPTER 1 INTRODUCTION	1
1.1 Statement of the problem	1
1.2 Research objectives	2
1.3 Scope and limitations of the study	3
CHAPTER 2 REVIEW OF LITERATURE	5
2.1 Natural rubber	5
2.1.1 Rubber plants	6
2.1.2 Exploitation	7
2.1.3 Compositions	7
2.1.4 Chemical formula	9
2.1.5 Physical properties	10
2.2 Deproteinization of natural rubber	11
2.3 Chemical modification of NR	14
2.3.1 Crosslinking of NR	15
2.3.2 Graft copolymerization of NR	18
2.4 pH responsive polymer	19

	(5)
2.4.1 Poly(4-vinylpyridine)	20
<b>CHAPTER 3 RESEARCH METHODOLOGY</b>	<b>24</b>
3.1 Materials	24
3.1.1 Chemical reagents	24
3.1.2 Glassware	24
3.1.3 Instrument and Apparatus	25
3.2 Methods and Preparation	26
3.2.1 Synthesis of P4VP-crosslinked NR	26
3.2.1.1 Preparation of Dried NR	26
3.2.1.2 Preparation of poly(4-vinylpyridine) (P4VP)	27
3.2.1.3 Preparation of P4VP-crosslinked NR (P4VP-NR)	27
3.2.1.4 Determination of the crosslink density	30
3.2.2 Synthesis of 4VP-grafted DPNR (4VP-g-DPNR)	31
3.2.2.1 Preparation of deproteinized natural rubber latex (DPNR latex)	31
3.2.2.2 Preparation of graft copolymerization between 4VP and DPNR latex (4VP-g-DPNR)	33
3.3 Characterization	35
3.3.1 Determination of the chemical structure and chemical elements of the functionalized products	35
3.3.1.1 Fourier Transform Infrared (FT-IR) spectroscopy	35
3.3.1.2 Nuclear Magnetic Resonance (NMR) spectroscopy	36
3.3.1.3 X-ray Photoelectron Spectroscopy (XPS)	37
3.3.1.4 CHN Element Analysis	38
3.3.2 Determination of the thermal properties of the functionalized products	39
3.3.2.1 Thermal Gravimetric Analysis (TGA)	39
3.3.2.2 Differential Scanning Calorimetry (DSC)	39
3.4 Determination of the pH responsiveness	40
3.4.1 The water swelling measurements	40



3.4.2 The contact angle measurement	41
3.5 Demonstration of the pH responsive releasing behavior of the functionalized products	42
3.5.1 Release of indigo carmine	42
3.5.2 Release of carbon quantum dots	43
3.6 Adsorption experiment	44
3.6.1 Adsorption isotherms	44
3.6.1.1 Langmuir adsorption isotherm	45
3.6.1.2 Freundlich adsorption isotherm	46
3.6.1.3 Temkin adsorption isotherm	48
3.6.1.4 Dubinin-Radushkevich adsorption isotherm	49
<b>CHAPTER 4 RESULTS AND DISCUSSION</b>	<b>51</b>
4.1 Synthesis and characterizations of P4VP-crosslinked NR (P4VP-NR)	51
4.1.1 Preparation of P4VP-NR	51
4.1.2 FT-IR characterization of P4VP-NR	54
4.1.3 XPS characterization of P4VP-NR	57
4.1.4 Effect of influential parameters on gel contents	59
4.1.4.1 Effect of P4VP concentration	59
4.1.4.2 Effect of BPO concentration	60
4.1.4.3 Effect of reaction temperature	61
4.1.4.4 Effect of reaction time	62
4.1.5 Determination of crosslink density of P4VP-NR	63
4.1.6 Determination of thermal properties of P4VP-NR	65
4.1.6.1 Thermal Gravimetric Analysis (TGA)	65
4.1.6.2 Differential Scanning Calorimetry (DSC)	67
4.1.7 Determination of pH responsiveness of P4VP-NR	69
4.1.7.1 The water swelling of P4VP-NR in pH solutions	69
4.1.7.2 The water contact angle of P4VP-NR	71
4.1.8 Demonstration of the pH responsive releasing behavior of P4VP-NR	73

4.1.8.1 Study the controlled release of indigo carmine from the resultant products	73
4.1.9 Study of adsorption isotherms	75
4.2 Synthesis and characterizations of 4VP-grafted DPNR (4VP- <i>g</i> -DPNR)	79
4.2.1 Preparation of deproteinized natural rubber latex	79
4.2.2 Preparation of 4VP-grafted DPNR	80
4.2.3 FT-IR characterization of 4VP- <i>g</i> -DPNR	82
4.2.4 XPS characterization of 4VP- <i>g</i> -DPNR	85
4.2.5 <sup>1</sup> H-NMR characterization of 4VP- <i>g</i> -DPNR	86
4.2.6 Effect of influential parameters on grafting ratio	88
4.2.6.1 Effect of 4VP concentration	88
4.2.6.2 Effect of KPS concentration	89
4.2.6.3 Effect of emulsifier concentration	90
4.2.6.4 Effect of reaction temperature	91
4.2.6.5 Effect of reaction time	92
4.2.7 Determination of thermal properties of 4VP- <i>g</i> -DPNR	93
4.2.7.1 Thermal Gravimetric Analysis (TGA)	93
4.2.7.2 Differential Scanning Calorimetry (DSC)	95
4.2.8 Determination of pH responsiveness of 4VP- <i>g</i> -DPNR	97
4.2.8.1 The water swelling of 4VP- <i>g</i> -DPNR in pH solutions	97
4.2.8.2 The water contact angle of 4VP- <i>g</i> -DPNR	99
4.2.9 Demonstration of the pH-responsive releasing behavior of 4VP- <i>g</i> -DPNR	101
4.2.9.1 Study the controlled release of indigo carmine from the resultant products	101
4.2.9.2 Study the controlled release of carbon quantum dots from the resultant nanocomposites	104
4.2.10 Study of adsorption isotherms	106
 CHAPTER 5 CONCLUSIONS AND RECOMMENDATIONS	 109
5.1 Conclusions	109

5.1.1 Synthesis and characterization of P4VP-crosslinked NR (P4VP-NR)	109
5.1.2 Synthesis and characterization of 4VP-grafted DPNR (4VP- <i>g</i> -DPNR)	110
5.2 Recommendations	111
REFERENCES	112
APPENDICES	124
APPENDIX A PREPARATION OF CROSSLINKED MATERIALS (P4VP-NR)	125
APPENDIX B PREPARATION OF GRAFTED MATERIALS (4VP- <i>g</i> -DPNR)	127
APPENDIX C DETERMINATION OF PH RESPONSIVENESS OF THE MATERIALS	130
APPENDIX D THE STUDY OF CONTROLLED RELEASE OF INDIGO CARMINE	135
APPENDIX E THE STUDY OF ADSORPTION ISOTHERMS	137
APPENDIX F PUBLICATION	139
BIOGRAPHY	154

## LIST OF TABLES

Tables	Page
1 Compositions of fresh NR latex and HANR latex [48].	8
2 Nitrogen content of treated-NR latex derived from several techniques of deproteinization.	12
3 Various types of monomers grafted onto NR.	18
4 Formulation and the range of investigated parameters in crosslink reaction (P4VP-NR).	30
5 Formulation and the range of investigated parameters in graft copolymerization (4VP-g-DPNR).	35
6 Mathematical equations for the isotherms and their linear forms.	45
7 The nature of adsorption process.	46
8 The nature of adsorption process [100, 103-105].	47
9 The comparison of the characteristic IR absorption bands of NR, P4VP, and the crosslinked material at a specific wavenumber ( $\text{cm}^{-1}$ ) [114].	55
10 Decomposition temperatures of P4VP-NR sample, in comparison with those of NR and P4VP.	66
11 Glass transition temperatures ( $T_g$ ) of P4VP-NR sample, in comparison with those of NR and P4VP.	68
12 Langmuir, Freundlich, Temkin and Dubinin-Radushkevich isotherm constants for the adsorption of indigo carmine onto P4VP-NR.	77
13 The C, H, and N data of NR and DPNR.	79
14 The comparison of the characteristic IR absorption bands of DPNR, P4VP, and 4VP-g-DPNR at a specific wavenumber ( $\text{cm}^{-1}$ ).	84
15 Degradation temperatures of 4VP-g-DPNR sample, in comparison with those of DPNR and P4VP.	94
16 Glass transition temperature ( $T_g$ ) of 4VP-g-DPNR sample, in comparison with those of NR and P4VP.	96
17 Langmuir, Freundlich, Temkin and Dubinin-Radushkevich isotherm constants for the adsorption of indigo carmine onto 4VP-g-DPNR.	107

## LIST OF FIGURES

Figures	Page
1 A structure of 4-vinylpyridine (4VP).	3
2 Photographic images of natural rubber latex from <i>Hevea brasiliensis</i> tree.	5
3 Examples of products made from NR [35-38].	6
4 Fractions of natural rubber latex after centrifugation [43].	9
5 A structure of isoprene and the arrangement of polyisoprene.	10
6 Chemical structure of natural rubber (cis-1,4-polyisoprene).	10
7 A model of rubber latex particle.	11
8 A schematic representation of the proposed deproteinization mechanism by (a) enzymatic treatment and (b) surfactant washing or physical treatment [58].	13
9 A schematic representation of the chemical modification of NR.	15
10 A Schematic representation of uncrosslinked and crosslink states [67].	16
11 A Schematic representation of vulcanization of NR with sulfur.	16
12 A peroxide crosslinking in NR.	17
13 (a) Schematic representation of the swelling and unswelling of pH-responsive polymer particles, and compositional reversibility of: (b) weakly basic and, (c) weakly acidic methacrylic polymers in response to solution pH changes [82].	19
14 Chemical structures of pH responsive polymers.	20
15 A chemical structure of poly(4-vinylpyridine) (P4VP).	21
16 (a) Illustration of protonated and deprotonated pyridyl groups on P4VP-g-CNC, and (b) contact angle measurement [91].	22
17 Photographs of pH-responsive behavior of P(MBA-co-4VP) 1D nanostructures immersed into buffer solutions of (a) pH 2.2 and (b) pH 11 respectively. (c) Dried sample and the same sample saturated by buffer solutions of (d) pH 2.2 and (e) pH 11, respectively [92].	22
18 The swelling percentage (%S) values of prepared hydrogels at different pHs (pH was adjusted by the addition of 0.1 M HCl, 0.1 M. NaOH) [28].	23
19 A schematic representation of the preparation of dried NR.	26

20 Synthesis of poly(4-vinylpyridine) from 4-vinylpyridine (4VP) and benzoyl peroxide (BPO) as a monomer and initiator, respectively.	27
21 A schematic representation of the preparation of P4VP-NR.	29
22 A schematic representation of the preparation of DPNR latex.	32
23 A schematic representation of the preparation of 4VP-g-DPNR.	34
24 A photograph of a Perkin Elmer FT-IR (Spectrum GX model) spectrometer.	36
25 An image of NMR spectrometer.	37
26 An image of an X-ray Photoelectron Spectrometer (AXIS ULTRA <sup>DLD</sup> , Kratos analyticle).	38
27 An image of a CHN-2000 LECO analyzer.	38
28 An image of a Mettler Toledo SDTA851e analyzer (TGA).	39
29 An image of a Mettler Toledo DSC822e differential scanning calorimeter (DSC).	40
30 An image demonstration of the determination of water contact angle in each samples.	41
31 An image of a water contact angle instrument.	41
32 An image of a UV-Visible spectrometer (UV-1700 PharmaSpec, SHIMADZU).	42
33 An image of a fluorescence spectrometer (FP-6200, JASCO).	43
34 Photographic image of (a) the gel formation, (b) crosslinked material, and (c) the insoluble of product in organic solvents, included toluene, chloroform, hexane, and tetrahydrofuran (THF).	52
35 A schematic representation of (a) the crosslinking reaction between natural rubber (NR) and poly(4-vinylpyridine) (P4VP), and photographic image of (b) NR, (c) P4VP, and (d) P4VP-NR, respectively.	53
36 FT-IR spectra of NR (black line), P4VP (red line), and P4VP-NR (gel content = 63%, blue line).	55
37 XPS survey scan spectra of NR and P4VP-NR (gel content = 63%).	58
38 XPS high-resolution spectra of N <sub>1s</sub> region of NR and P4VP -DPNR (gel content = 63%).	58
39 Gel content as a function of P4VP concentration.	59

40 Gel content as a function of BPO concentration.	60
41 Gel content as a function of reaction temperature.	61
42 Gel content as a function of reaction time.	62
43 Crosslink density as a function of (a) degree of swelling in toluene and (b) gel content, and (c) the degree of solvent swelling as a function of gel content.	64
44 TGA thermograms of NR, P4VP and P4VP-NR (gel content = 63%).	66
45 DSC thermograms of NR, P4VP and P4VP-NR (gel content = 63%).	68
46 Degree of swelling (%) of NR and P4VP-NR (gel content = 34% and 63%) in aqueous solutions with different pH values.	70
47 Swelling behavior of P4VP-NR (gel content = 63%) in aqueous solutions with pH 2 for 30 min.	70
48 Water contact angles of NR and P4VP-NR (gel content = 63%) at different pH values.	72
49 Water contact angles of P4VP-NR (gel content = 63%) sample after wetted with pH 2.	72
50 UV-visible spectra of NR and P4VP-NR (gel content = 63%) after immersion in dye solutions compared with standard dye solution.	74
51 Absorbance values of NR and P4VP-NR samples.	74
52 Relative absorbance as a function of immersion time.	75
53 Linear adsorption isotherms based on (a) Langmuir, (b) Freundlich, (c) Temkin, and (d) Dubinin-Radushkevich models.	77
54 Thermal decomposition of potassium persulfate.	81
55 The proposed mechanism of the grafting reaction between 4VP and DPNR.	81
56 Photograph of 4VP-g-DP NR. Sample size is approximately 1x1 cm <sup>2</sup> .	82
57 FT-IR spectra of DP NR (black line), P4VP (red line), and 4VP-g-DP NR (grafting ratio = 45%) (blue line).	83
58 XPS survey scan spectra of DP NR and 4VP-g-DP NR (grafting ratio = 45%).	85
59 XPS high-resolution spectra of N <sub>1s</sub> region of DP NR and 4VP-g-DP NR (grafting ratio = 45%).	86
60 <sup>1</sup> H-NMR spectra of (a) DP NR, (b) P4VP, and (c) 4VP-g-DP NR (grafting ratio = 45%)	87

61 Grafting ratio as a function of 4VP concentration.	88
62 Grafting ratio as a function of KPS concentration.	89
63 Grafting ratio as a function of emulsifier concentration.	90
64 Grafting ratio as a function of reaction temperature.	91
65 Grafting ratio as a function of reaction time.	92
66 TGA thermograms of DPNR, P4VP and 4VP- <i>g</i> -DPNR (grafting ratio = 45%).	94
67 DSC thermograms of DPNR, P4VP and 4VP- <i>g</i> -DPNR (grafting ratio = 45%).	96
68 Degree of swelling (%) of DPNR and 4VP- <i>g</i> -DPNR (grafting ratio = 16% and 45%) in aqueous solutions with different pH values.	98
69 Swelling behavior of 4VP- <i>g</i> -DPNR (grafting ratio = 45%) in aqueous solutions with pH 2 for 30 min.	98
70 Water contact angles of DPNR and 4VP- <i>g</i> -DPNR (grafting ratio = 45%) at different pH values.	100
71 (a) An image representation of protonated and deprotonated pyridyl groups on 4VP- <i>g</i> -DPNR and (b) water contact angles of 4VP- <i>g</i> -DPNR (grafting ratio = 45%) at pH 2 and 4.	100
72 UV-visible spectra of DPNR and 4VP- <i>g</i> -DPNR (grafting ratio = 45%) after immersion with dye solution compared with standard dye solution.	102
73 Interaction between 4VP- <i>g</i> -DPNR and indigo carmine molecule.	102
74 Absorbance values of DPNR and 4VP- <i>g</i> -DPNR samples.	103
75 Relative absorbance as a function of immersion time.	103
76 (a) A schematic of preparation of 4VP- <i>g</i> -DPNR/CQDs nanocomposite, and (b) a photograph of fluorescence intensity of DPNR/CQDs and 4VP- <i>g</i> -DPNR/CQDs nanocomposites after immersion in aqueous solutions at a range of pH 2-12 under the UV light.	105
77 Fluorescence spectra of the pH solutions from 2-12 after immersion with 4VP- <i>g</i> -DPNR/CQDs nanocomposite samples.	105
78 Linear adsorption isotherms based on (a) Langmuir, (b) Freundlich, (c) Temkin, and (d) Dubinin-Radushkevich models.	107



## LIST OF ABBREVIATIONS

Symbols/Abbreviations	Terms
NR	Natural rubber
NRL	Natural rubber latex
HANR	High-ammonia natural rubber
HANRL	High-ammonia natural rubber latex
DPNR	Deproteinized natural rubber
DPNRL	Deproteinized natural rubber latex
4VP	4-vinylpyridine
P4VP	Poly(4-vinylpyridine)
DRC	Dry rubber content
phr	Parts per hundred rubber
rpm	Revolutions per minute
°C	Degree Celsius
h	Hour
SDS	Sodium dedocyl sulfate
BPO	Benzoyl peroxide
KPS	Potassium persulfate
CHP	Cumyl hydroperoxide
TEPA	Tetraethylene pentamine
AIBN	Azobisisobutyronitrile
PE	Polyethylene
DSC	Differential scanning calorimetry
T <sub>g</sub>	Glass transition temperature
TGA	Thermal gravimetric analysis
XPS	X-ray photoelectron spectroscopy
<sup>1</sup> H-NMR	Proton nuclear magnetic spectroscopy
FTIR	Fourier transform infrared spectroscopy
CHN	Carbon Hydrogen Nitrogen

# CHAPTER 1

## INTRODUCTION

### 1.1 Statement of the problem

Natural rubber (NR) from *Hevea brasiliensis* tree is one of the most valuable renewable resources and sustainable materials. It has been attracting significant interests and used in many fields, including the automobile, consumer products, and medical sectors, mainly due to its outstanding elasticity and good mechanical properties [1]. In addition to its excellent properties, Thailand is ranked as the world leading producer and exporter because it produces and exports of raw and final products from NR with a production capacity of 3.1 – 3.2 million tons per year in which 88-90 percent of total production capacity is exported to foreign markets [2].

Although NR is a good supply in Thailand and possesses many excellent properties, at present, many countries including Thailand have been steadily facing the problem of rubber prices due to the oversupply and the falling demand [3, 4]. Moreover, the export of unmodified rubbers has had the tendency to decrease [5]. Therefore, it is necessary to find a new approach to produce and use more NR products. This motivates researchers to work on improving and modifying the NR properties for increasing its values and extending its applications.

*Cis*-1,4-polyisoprene, the main polymeric material of NR, consists of unsaturated double bonds on the main chain, which are considered to be similar to a simple olefin or alkene. As a result alkene-based reactions can be applied to NR. Nowadays, the modification for improving the properties of NR *via* many chemical-based methods, such as hydrogenation [6, 7], chlorination [8, 9], epoxidation [10, 11], bromination [12], sulfonation [13], crosslinking [14, 15], and grafting [16-22], have been reported, but the crosslinking and grafting methods have received most attention as they not only can improve the properties of NR and also add new properties to NR for producing a range of new rubber-based materials.

Among these modified rubber materials, the preparation of NR with stimuli-responsive functions providing smart materials is rare [23]. Stimuli responsive

materials are unique because they can sense to external stimuli or changes in ambient conditions, such as pH, temperature, light, ionic strength, electric field, and magnetic field [24-26], and then respond by changing in their physical or chemical properties, such as their size, shape, hydrophobicity/hydrophilicity, and degradation rate. Accordingly, adding responsive functions to the unique properties of NR will not only provide new stimuli-responsive elastomer materials, but also expand a range of applications of NR, for example to sensing devices and drug delivery systems.

In this thesis research, the methods for functionalizing 4-vinylpyridine (4VP) onto NR as pH responsive materials were demonstrated. Generally, 4VP-based polymers are known as pH-responsive materials that can potentially be used in many sensing and biomedical applications, such as in drug delivery and biosensors [27]. Furthermore, 4-vinylpyridine is a good ligand for the formation of complexes with metal ions, thereby allowing P4VP-based polymers to be used as metal absorbents [28-31] and catalyst ligands [32, 33]. To the best of our knowledge, no research to date has been carried out on functionalizing 4VP onto NR. Thus, integration of 4VP and NR will provide the responsive function to NR and expand the range of applications of rubber-based materials.

## **1.2 Research objectives**

1.2.1 To synthesize 4VP-functionalized NRs as pH responsive materials *via* crosslinking and grafting methods.

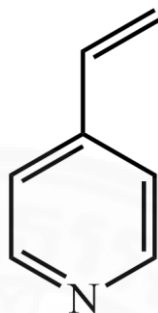
1.2.2 To study the effect of reaction conditions on reaction efficiency, such as the monomer/polymer concentrations, initiator concentration, emulsifier concentration, reaction time, and reaction temperature.

1.2.3 To characterize the chemical structure, chemical elements, and thermal property of 4VP-functionalized NRs.

1.2.4 To investigate the pH responsiveness of the resulting materials.

### 1.3 Scope and limitations of the study

1.3.1 Preparation of 4VP-functionalized NRs as pH-responsive materials by using two approaches: crosslinking and graft copolymerization methods.



**Figure 1** A structure of 4-vinylpyridine (4VP).

1.3.2 Study the effect of the following parameters on reaction efficiency.

- (a) Polymer/monomer concentration
- (b) Initiator concentration
- (c) Emulsifier concentration
- (d) Reaction temperature
- (e) Reaction time

1.3.3 Characterize the chemical structure and the chemical elements of the functionalized materials by the following techniques.

- (a) Fourier Transform Infrared Spectroscopy (FT-IR)
- (b) Proton Nuclear Magnetic Resonance Spectroscopy ( $^1\text{H-NMR}$ )
- (c) X-ray Photoelectron Spectroscopy (XPS)
- (d) CHN Elemental analysis

1.3.4 Evaluate the pH responsiveness property of the functionalized materials by the following experiments.

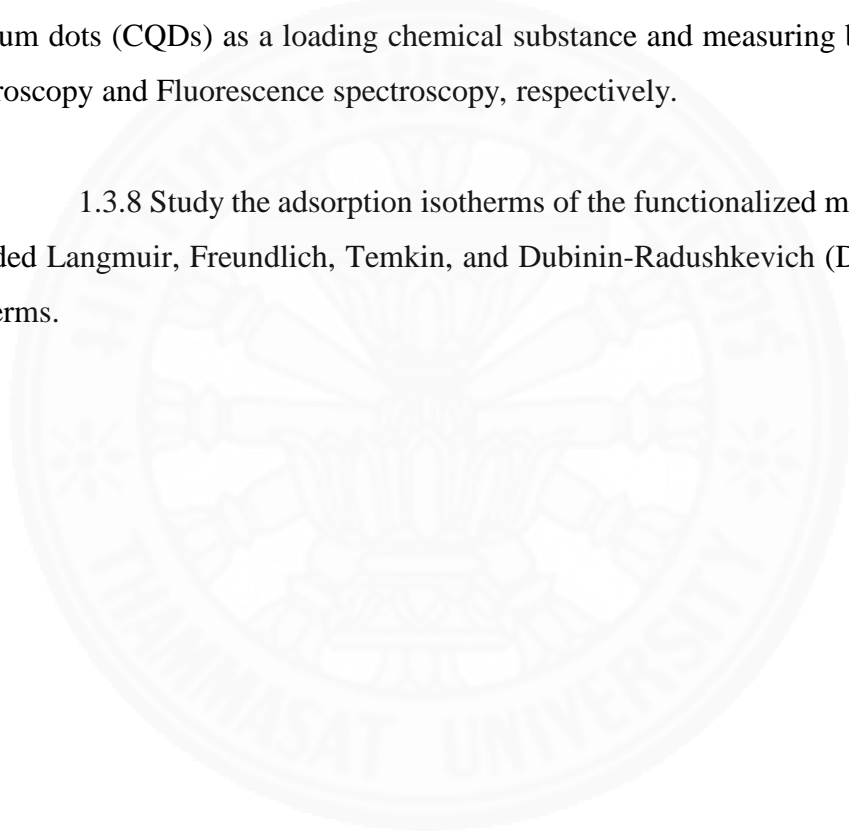
- (a) The water swelling experiment in pH solutions
- (b) The water contact angle measurement

1.3.5 Evaluate the thermal stability of the functionalized materials by Thermal Gravimetric Analysis (TGA).

1.3.6 Evaluate the glass transition temperature ( $T_g$ ) of the functionalized materials by Differential Scanning Calorimetry (DSC).

1.3.7 Study the controlled release behavior of the obtained pH-responsive materials in a different of pH media solutions by using an indigo carmine and carbon quantum dots (CQDs) as a loading chemical substance and measuring by UV-Visible spectroscopy and Fluorescence spectroscopy, respectively.

1.3.8 Study the adsorption isotherms of the functionalized materials, which included Langmuir, Freundlich, Temkin, and Dubinin-Radushkevich (DR) adsorption isotherms.



## CHAPTER 2

### REVIEW OF LITERATURE

#### 2.1 Natural rubber

Natural rubber (NR), consisting of *cis*-1,4-polyisoprene as a major polymeric material, is a useful material with a high amount of production and consumption throughout the world. NR is considered as a valuable renewable resource and sustainable elastic materials. It has been using as raw material in many industries, particularly for the manufacture of rubber tire industry, mainly due to its possessing of excellent mechanical properties including high elasticity, high tensile strength, and fatigue resistance and consumer products and medical sectors, such as footwear, rubber band, rubber toys, medical gloves, etc.[34].



**Figure 2** Photographic images of natural rubber latex from *Heavea brasiliensis* tree.





**Figure 3** Examples of products made from NR [35-38].

Nowadays, it is known that NR has significantly become one of the most economic agricultural products of Thailand, due to the large production capacity [2].

### 2.1.1 Rubber plants

More than 2,000 species of plants have been found to produce the polymeric product such *cis*-1,4-polyisoprene or NR [39]. However, the NR, which obtained from *Heavea brasiliensis* or the Pará rubber tree, is the most used available natural rubber resource. This plant produces NR in the milky white latex form.

The *Heavea brasiliensis* tree is a tropical hardwood tree with 30-40 meters of tall and native to the Amazon River basin in Brazil [40]. However, most of the world's natural rubber production mainly comes from the plantation in Southeast Asia, including Thailand, Indonesia, and Malaysia.

This type of rubber tree can be planted in the regions that have a tropical climate. It requires a 20 to 35 °C of temperature with a high humidity and well distributed rainfall. The rubber tree will grow up to 25-30 meter of tall. After they passed an initial growth phase to yield latex, generally from 5 to 7 years, the rubber tree

was harvested by the rubber tapping process. They could be tapped to give the latex for 15 to 30 years [41].

### 2.1.2 Exploitation

The freshly NR latex, obtained from *Hevea brasiliensis* tree by rubber tapping process, has a yield of approximately 30 % dry rubber content. After harvesting, an ammonia solution or ammonium hydroxide is usually added into fresh NR latex for inhibiting the bacteria growth. Furthermore, the ammonia can also prevent the premature coagulation of natural rubber latex at pH values closer to acid prior to transportation to the industries.

In general, NR could be served as a raw polymeric material to the processing industries through two forms of raw materials, including a latex form and coagulum or solid rubber form. For a latex form, almost all of the world's NR consumption is preferred to use a latex concentrate, which is usually carried out by centrifugation of the freshly latex (commonly containing of 30% dry rubber content). The commercial concentrated latex is shipped to the manufacturer as latex concentrate containing 60% dry rubber content, which is commonly called high-ammonia concentrated natural rubber latex (HANR latex). For a solid rubber raw material, the latex is processed into a sheet rubber, ribbed smoke sheet (RSS), crepe rubber, or block rubber, in which these types of conventional rubber material will further be converted to new forms or shapes for the desired applications [42].

### 2.1.3 Compositions

Natural rubber latex (NRL) from *Hevea brasiliensis* tree, also called *Hevea* latex, is obtained by rubber tapping process. The NRL is a colloid system, containing the rubber and non-rubber particles dispersed in water media (Table 1). The freshly *Hevea* latex has a pH of 6.5-7.0 and a density of 0.98 g/cm<sup>3</sup>. The total solids of fresh latex vary typically from 30 to 40%, depending on the clone, weather, simulation, tapping frequency, and other factors.

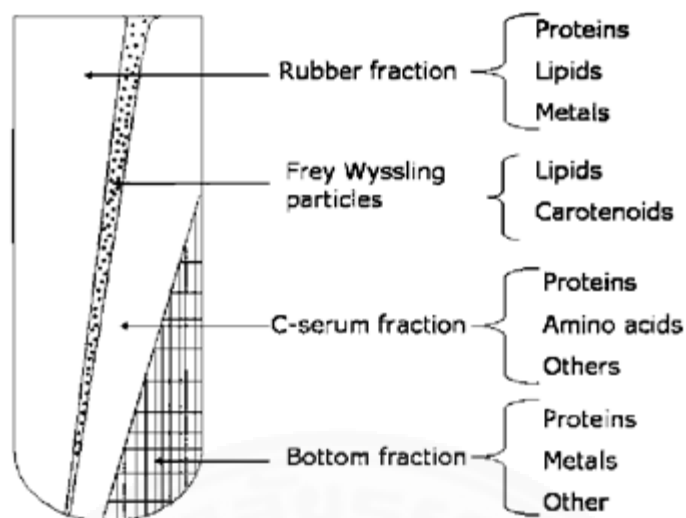


The freshly latex can be distributed into mainly three fractions, using ultracentrifugation. They contain the top fraction or rubber fraction, the C-serum fraction, and the bottom fraction as shown in Figure 4 [43]. The rubber fraction typically contains rubber hydrocarbon particle (*cis*-1,4-polyisoprene), proteins, lipids, and along with trace amounts of minerals. And the other fractions are dilute aqueous solutions which contain only non-rubber particles in many different classes of compounds, including carbohydrates, protein, amino acids, enzymes, and nitrogenous bases.

The rubber particles are generally found to be a spherical shape with a diameter ranging from approximately 50 nm to 2  $\mu\text{m}$  [44-46]. In addition to rubber particles, non-rubber particles components, such as proteins and phospholipids, play an important role in term of stabilizing the latex particles and contributing to the outstanding properties of NR [47].

**Table 1.** Compositions of fresh NR latex and HANR latex [48].

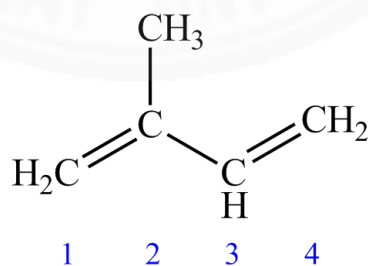
Constituents	Content, % w/w	
	Fresh NR latex	HANR latex
Total solid content	36	61.74
Dry rubber content	33	59.67
Proteinaceous substances	1-1.5	1.67
Resinous substances	1-2.5	<1
Inorganic salts (mineral, mainly K, P, and Mg)	0.5	<1
Ash	<1	0.4
Carbohydrates (Sugars)	1	<1
Ammonia	-	0.68
Water	60	37.49

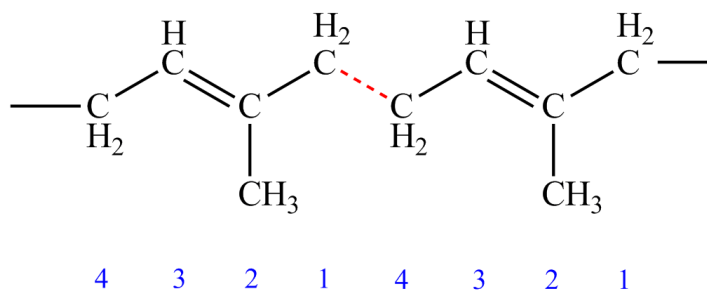


**Figure 4** Fractions of natural rubber latex after centrifugation [43].

#### 2.1.4 Chemical formula

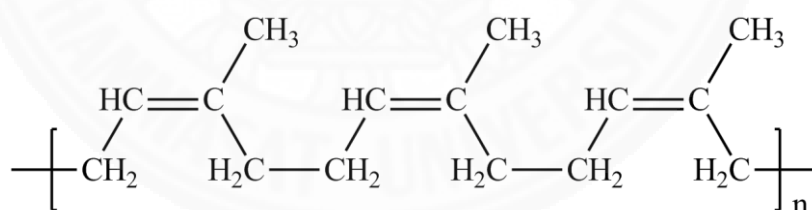
NR consists of *cis*-polyisoprene as the main polymeric material. Polyisoprene consists of isoprene repeating units as the formula of  $C_5H_8$  (Figure 5). The isoprene repeating units are linked together at carbon atoms 1 and 4 in a head-to-tail arrangement, which the head of one isoprene molecule connected with the tail of another isoprene molecule, to assemble a polymer chain.





**Figure 5** A structure of isoprene and the arrangement of polyisoprene.

*Cis*-polyisoprene contains double bonds along their backbone. The double bonds are prone to degradation upon exposure to heat, light, oxygen, and ozone [49, 50]. Upon exposure to these stimuli, undesirable reactions such as crosslinking and chain scission occur to the double bonds of *cis*-polyisoprene [51]. However, the chemical reactivity of the carbon–carbon double bond of NR is considered to be similar to that of simple olefins or alkene (C=C). Therefore all reactions with alkene may be applied to NR, including electrophilic addition at the carbon–carbon double bond and substitution reaction at the allylic position [52]. Hence, a means of improving the physical and chemical properties of NR can be achieved.



**Figure 6** Chemical structure of natural rubber (*cis*-1,4-polyisoprene).

### 2.1.5 Physical properties

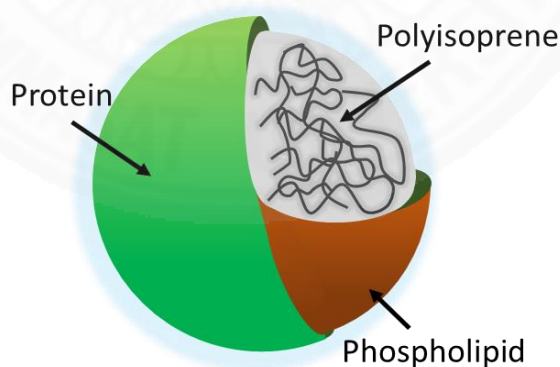
Macromolecules of NR are long chains and flexible. By considering the structure of NR, it comprises of carbon and hydrogen atoms, which are non-polar. As a result, the intermolecular interactions between chains are weak Van der Waals force. Furthermore, these interactions are further weakened because the *cis*-

configuration of all the double bonds do not permit the close interaction of polymer chains [53]. Thus, NR exhibits excellent elastic properties ( $T_g \sim -70\text{ }^\circ\text{C}$ ) and spontaneously crystallizes (maximum crystallization rate of approximately at  $-25\text{ }^\circ\text{C}$ ) also under influence of deformation forces already at relative prolongation of more than 80% [54]. In addition to excellent elasticity, NR has many other features as follow:

- Excellent dynamic properties with a low hysteresis loss.
- Good low temperature properties.
- Strong bonding to metal parts.
- High resistance to tear and abrasion.
- Ease of processing.

## 2.2 Deproteinization of natural rubber

Many of previous structural studies of NR showed that the rubber molecules mainly comprise of long chain of *cis*-1,4-polyisoprene surrounded by layer of proteins and phospholipids (Figure 7) [55, 56]. The surrounding proteins or phospholipids present a charged layer covering the rubber latex particle, accordingly stabilizing the latex particles against aggregation [57].



**Figure 7** A model of rubber latex particle.

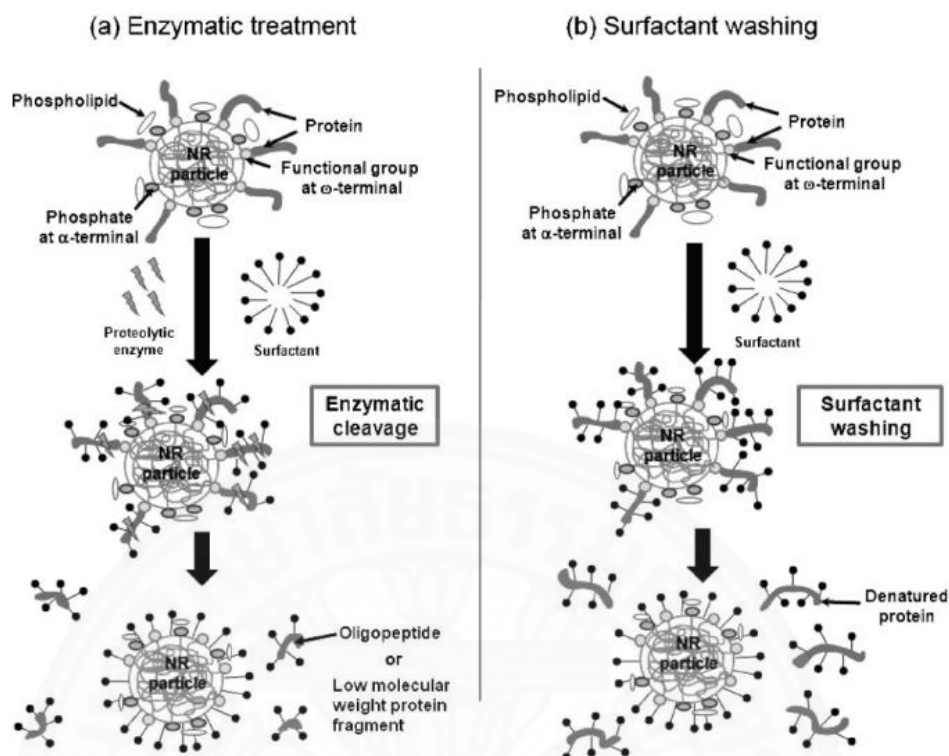
Unfortunately, the presence of these non-rubber components in the latex affects the utilization of NR. Firstly, the protein allergy risk in using NR products for some allergic

users has increased [58]. As a result, they created a demand for removing the protein or deproteinization from NR latex.

Several techniques have been reported for removing proteins from NR latex, depending on the substance and procedure that were used. The amount of proteins present in natural rubber latex after deproteinization can be investigated by determining the nitrogen content.

**Table 2** Nitrogen content of treated-NR latex derived from several techniques of deproteinization.

<b>Samples</b>	<b>Incubation time (min)</b>	<b>Incubation temperature (°C)</b>	<b>Nitrogen content (wt%)</b>	<b>Ref.</b>
Fresh NR latex (FNR)	-	-	0.650	[58]
Urea-treated NR latex (U-DPNR)	60	30	0.014-0.020	[44]
Enzymatic-treated NR latex (E-DPNR)	720	32	0.017-0.020	[44, 58, 59]
Saponified NR latex (SPNR)	180	70	0.120	[58]
Surfactant-washed NR latex (WSNR)	-	-	0.020-0.028	[44, 58]



**Figure 8** A schematic representation of the proposed deproteinization mechanism by (a) enzymatic treatment and (b) surfactant washing or physical treatment [58].

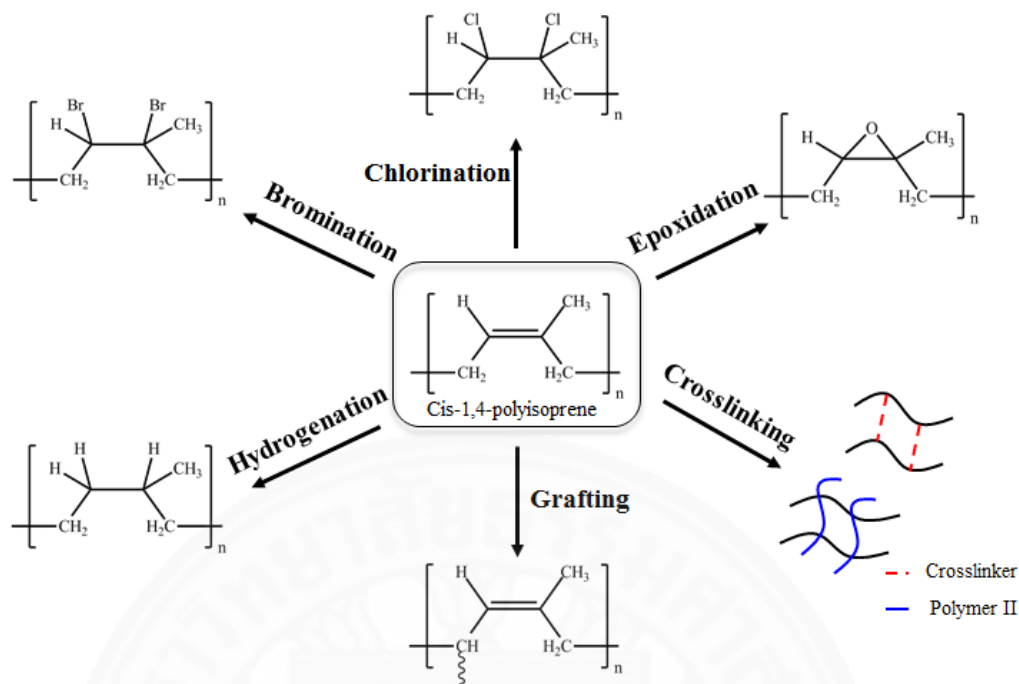
Aside from the allergy, many researchers have noted that the presence of proteins in NR latex may disturb the modification process of NR, such as graft copolymerization. They presumed that proteins affected the free-radical species by terminating the free radicals during grafting copolymerization, leading to lower grafting efficiency. Thus, they have verified these presumption by using the treated-DPNR latex to prepare graft copolymerization with various types of vinyl monomers. For example, **Kawahara et al.** prepared the deproteinized natural rubber latex (DPNRL) by using enzyme with surfactant. They found that the DPNR might be possible to achieve not only high conversion but also high grafting efficiency of monomer for the NR graft copolymerization in the latex form [60]. **Nakason et al.** reported that removing protein by enzymes can improve grafting efficiency of DPNR. Grafting efficiency of DPNR with MMA was higher than that of NR [61]. **Pukkate et al.** reported the use of urea and surfactant to reduce the nitrogen content. The grafting of urea-treated DPNR (U-

DPNR) with styrene has been carried out with tert-BuHP/TEPA as an initiator in latex state. The highest conversion for U-DPNR-*g*-PS copolymer were achieved at 1.5 mol/kg-rubber feed of styrene and grafting efficiency was more than 90% w/w [59]. **Kreua-ongarjnkool et al.** reported the preparation of DPNR by washing the HANR with SDS. It was found that DPNR was successfully prepared with the lowest nitrogenous content, and the grafting efficiency of DPNR-*g*-S/MMA was higher than that of NR-*g*-S/MMA [62].

From these studies, it can be concluded that the removing proteins from natural rubber latex should be considered as a process before modifying the natural rubber to achieve the high performance.

### 2.3 Chemical modification of NR

The chemical modification of NR can be carried out under various reaction conditions, such as in organic solution, aqueous, solid, and surface modifications. The reaction may be by one- or several-step modification to obtain the required properties [52]. Nowadays, many chemical-based methods for improving the properties of NR have been reported, such as hydrogenation [7], chlorination [8, 9], epoxidation [10, 11], bromination [12], sulfonation [13], crosslinking [14], and grafting [7, 17-22, 45, 62-66]. However, the crosslinking and grafting methods have received most attention as they can improve the properties of NR and also add new properties for producing a range of new rubber-based materials as mentioned earlier.



**Figure 9** A schematic representation of the chemical modification of NR.

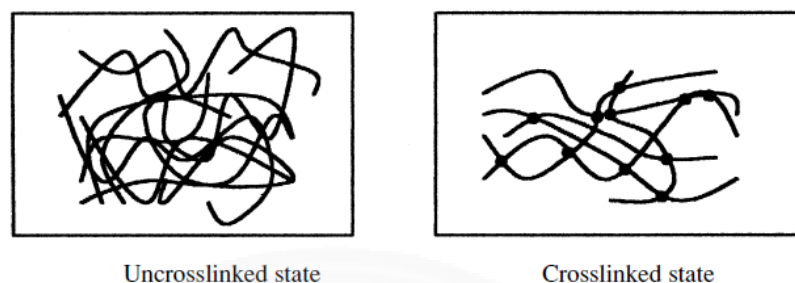
### 2.3.1 Crosslinking of NR

Crosslinking is a chemical process where long chains of rubber molecules are crosslinked or generated a network structure and transform the soft or weak plastic-like material into a strong elastic product with high and reversible deformability and good mechanical properties. The formation of network structure is one of the essential conditions for generating the elastomeric materials with good mechanical properties. It is now well known that many types of reaction can take place with unsaturated rubbers. NR can also be modified through crosslinking reaction, forming chemical bonds between the polymer chains and resulting in a network structure.

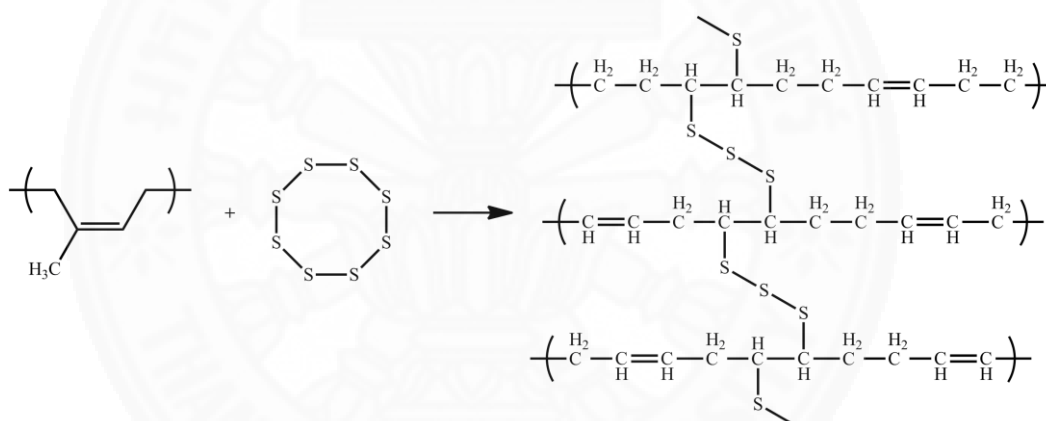
Charles Goodyear accidentally discovered the vulcanization process in 1839, by observing that NR can be crosslinked by using sulfur and heat. After the vulcanization process, the rubber loses its tackiness, becoming insoluble in solvents and more resistant to heat, light and aging processes. As a result, sulfur vulcanization has been the most widely used as a curing technique for rubbers, preferably for unsaturated



ones. However, the other curing methods can be used likewise, including resin, moisture, urethane, metal oxide, and radiation crosslinking [67].



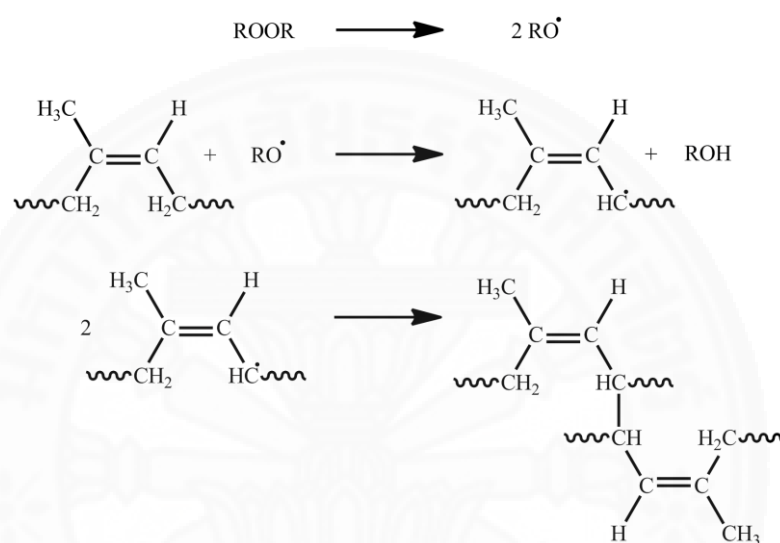
**Figure 10** A Schematic representation of uncrosslinked and crosslink states [67].



**Figure 11** A Schematic representation of vulcanization of NR with sulfur.

The use of free radical initiators such as peroxide compounds as a crosslinker for the crosslinking reaction has been reported, which is an interestingly alternative way due to a relatively simple chemistry. The advantage of using this type of initiators for crosslinking is that polymers having saturated and unsaturated hydrocarbon structure can be possibly crosslinked. For example, polyethylene (PE) is one type of polymers that many researchers have studied with peroxides [68]. In addition to PE, NR can be crosslinked by peroxides. The mechanism of this crosslinking reaction can be explained that the alkoxy radical derived from peroxide dissociation will abstract the hydrogen of NR *via* hydrogen abstraction reaction, followed by

pairwise combination of the resultant polymer radicals to give a crosslink structure, as shown in Figure 12. For saturated polymers, the reaction occurs through mainly two-step reactions: the chain scission reaction giving a polymer chain radicals and then the crosslinking between a pair of polymer chain radicals [69]. At present, many of peroxide compounds were employed for the crosslinking of polymers, such as dicumyl peroxide, di-tert-Butyl peroxide, dibenzoyl peroxide, etc.



**Figure 12** A peroxide crosslinking in NR.

In addition to self-crosslinking *via* vulcanization, NR can be crosslinked by generating a network structure with other polymers resulting in hybrid materials that can extend its applications. Examples of polymers that have been crosslinked or have formed interpenetrating network structures with NR including polystyrene [70], poly(methyl methacrylate) [71], poly(zinc dimethacrylate) [72], poly(vinyl alcohol) [73], poly(acrylic acid) [74], poly(carbonate urethane) [75], and polypropylene [76].

### 2.3.2 Graft copolymerization of NR

Besides crosslinking of NR with other polymers, NR can be modified through the graft copolymerization process. In general, graft copolymerization has attracted considerable attention as they can combine a variety of functional components into a single material. The graft copolymerization of a vinyl monomer onto NR is one of the most interesting and widely studied fields of research into adding value to NR. The thermal and chemical stability of NR is also improved due to the saturation of double bonds [77].

Graft copolymerization of NRs is usually carried out *via* free radical methods, which can be initiated by chemical initiators, high energy radiation, or UV illumination, under various conditions [78]. Both solid NR and NR latex have been used as precursors for modification, depending on the solubility of initiators and monomers. Moreover, several types of monomers, which were used to graft onto NR, have been reported.

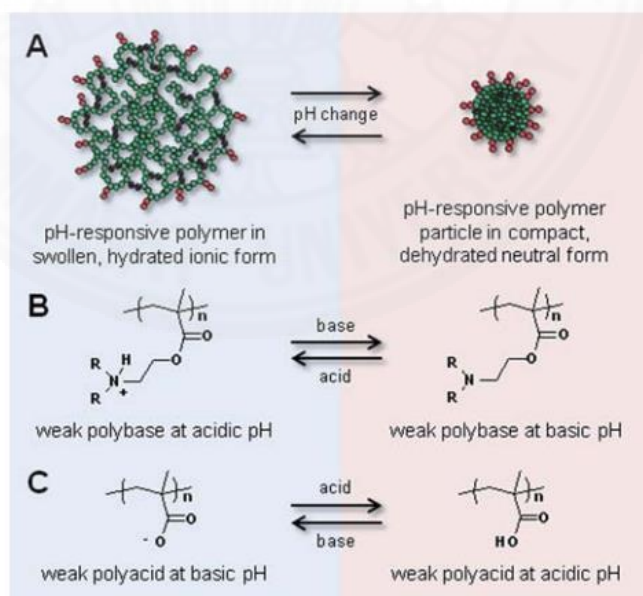
**Table 3** Various types of monomers grafted onto NR.

Monomers	Initiators	Application	Ref
Styrene	t-BHP/TEPA, CHPO/TEPA	To improve the resistance of heat and weathering ageing	[59, 63]
2-Hydroxyethyl methacrylate (HEMA)	CHPO/TEPA	To improve plywood adhesion	[65]
Methyl methacrylate (MMA)	CHPO/TEPA, K <sub>2</sub> S <sub>2</sub> O <sub>8</sub> / Na <sub>2</sub> S <sub>2</sub> O <sub>3</sub>	To improve the physical properties and reduced the tackiness of rubber	[19, 66, 79]
Dimethylaminoethyl Methacrylate (DMAEMA)	CHPO/TEPA	To provide strong interactions with inorganic fillers.	[64]

## 2.4 pH responsive polymer

The pH responsive polymers are materials which can respond to the changes in the pH of the surrounding medium by varying their dimensions. These materials will increase their size or collapse, depending on the pH of their environment. This behavior is exhibited due to the presence of functional groups in the polymer chain. In general, pH-sensitive polymers are polyelectrolytes that bear the weak acidic or basic groups in their structure that either accept or release protons in response to changes in environmental pH [80]. Thus, they can be divided based on their structure into two types as follows.

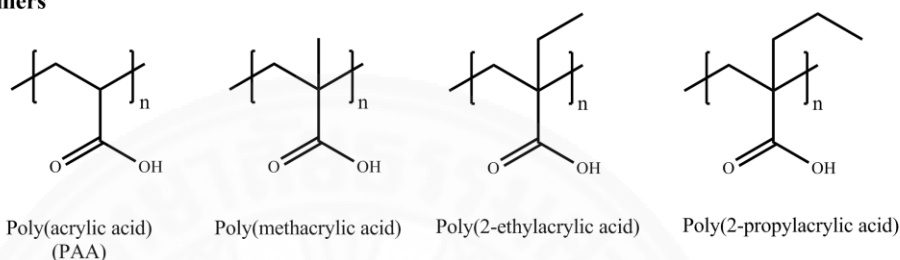
First, polyacidic polymers will be unswollen at low pH, since the acidic groups will be protonated. When increasing the pH, they will deprotonate and generate negatively charges, leading to a swelling behavior. The opposite behavior is found in polybasic polymers in which they will be swollen at low pH, since the basic groups will be protonated [81]. The pH-responsiveness at different pH varies with the type of polymers or copolymer compositions, depending on the  $pK_a$  or  $pK_b$  value of them.



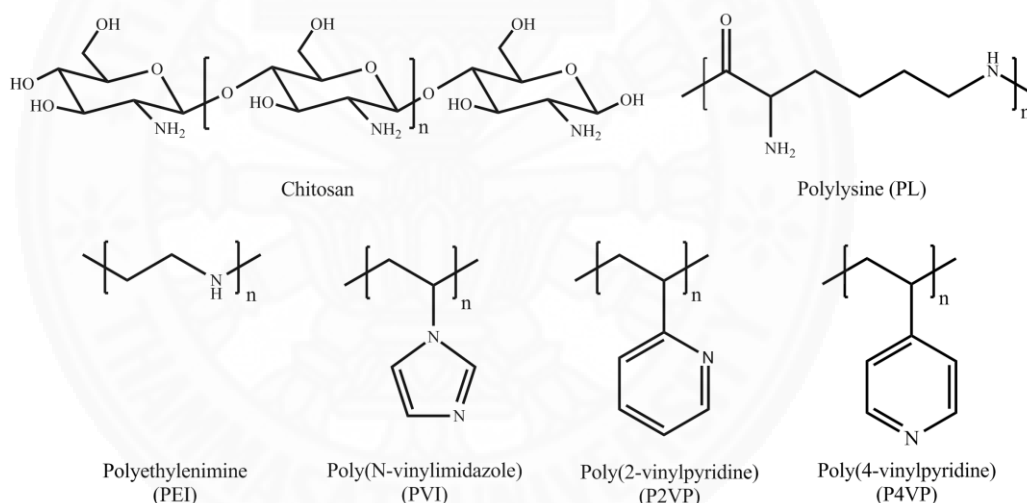
**Figure 13** (a) Schematic representation of the swelling and unswelling of pH-responsive polymer particles, and compositional reversibility of: (b) weakly basic and, (c) weakly acidic methacrylic polymers in response to solution pH changes [82].

Common pH-sensitive polymers with anionic groups are poly(carboxylic acids) as poly(acrylic acid) (PAA), poly(methacrylic acid), poly(2-ethylacrylic acid), and poly(2-propylacrylic acid). Well-known examples of cationic polyelectrolytes are poly(N-vinylimidazole) (PVI), polylysine (PL), polyethylenimine (PEI), chitosan, poly(2-vinylpyridine) (P2VP) and poly(4-vinylpyridine) (P4VP).

#### Polyacidic polymers



#### Polybasic polymers



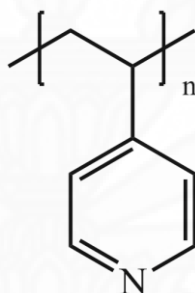
**Figure 14** Chemical structures of pH responsive polymers.

### 2.4.1 Poly(4-vinylpyridine)

In this work, we focused on poly(4-vinylpyridine), due to its outstanding pH responsive properties. P4VP is one of interesting responsive polymers that can change their chemical and morphological properties when the pH of the surrounding was changed. Naturally, P4VP is a weak base with a  $pK_a$  value of 4.7 [83]. The P4VP will present a hydrophilicity in an acidic environmental ( $pH < 4.7$ ) due to its

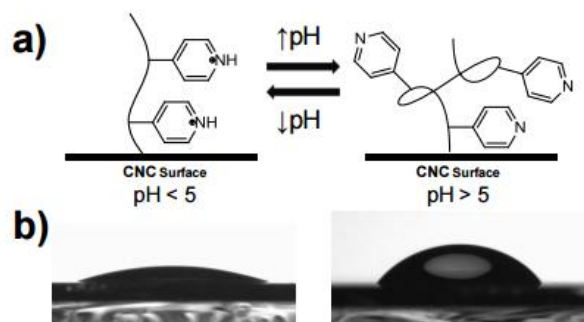
protonated state. This event promotes the P4VP polymeric chains to straighten up due to the electrostatic repulsion forces, resulting in the change of its physical properties such as an increasing in their size. In contrast, when it was in neutral or basic environmental ( $\text{pH} > 4.7$ ), leading to deprotonated (uncharged) state. P4VP becomes less hydrophilicity and presents an un-swollen behavior.

P4VP-based polymers are known as pH-responsive materials that can potentially be used in many applications, such as in drug delivery and biosensors [84]. Furthermore, 4-vinylpyridine is a good ligand for the formation of complexes with metal ions, thereby allowing P4VP-based polymers to be used as metal absorbents [85-88] and catalyst ligands [89, 90].



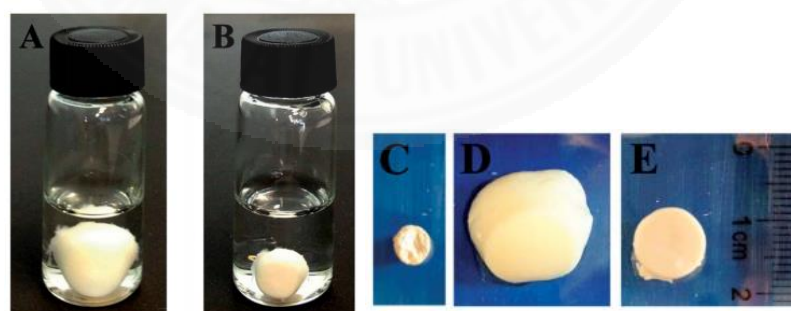
**Figure 15** A chemical structure of poly(4-vinylpyridine) (P4VP).

Different of P4VP-based copolymer were observed for providing a pH-responsive materials. For example, **Kan et al.** reported the synthesis of poly(4-vinylpyridine)-grafted cellulose nanocrystals (P4VP-g-CNCs). Then, they investigated the pH responsiveness by the water contact angle measurement. It was found that, the obtained materials showed the pH-responsiveness by controlling of wettability, depending on pH of environment [91].



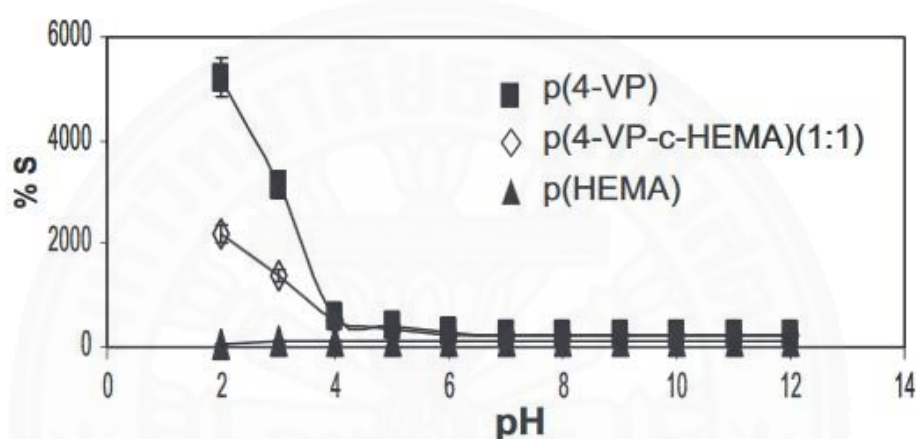
**Figure 16** (a) Illustration of protonated and deprotonated pyridyl groups on P4VP-*g*-CNC, and (b) contact angle measurement [91].

**Wen et al.** prepared poly(*N,N'*-methylenebisacrylamide-co-4-vinylpyridine) (P(MBA-4VP)). They observed the responsiveness using water swelling experiment in strong acid and base environment. The studies revealed that when immersing P(MBA-4VP-4) 1D nanostructures into buffer solutions of pH 2.2 and 11, the size of the P(MBA-4VP-4) gel decreased as the pH was increased from 2.2 to 11, due to the deprotonation of the 4VP pyridine groups. That means that P(MBA-4VP-4) 1D nanostructures became swollen in acidic environment, not in basic surroundings [92]. This result confirmed the pH-responsive behavior of P4VP.



**Figure 17** Photographs of pH-responsive behavior of P(MBA-co-4VP) 1D nanostructures immersed into buffer solutions of (a) pH 2.2 and (b) pH 11 respectively. (c) Dried sample and the same sample saturated by buffer solutions of (d) pH 2.2 and (e) pH 11, respectively [92].

In addition, **Ozay et al.** prepared a copolymer of 4-vinyl pyridine (4-VP) based hydrogels with 2-hydroxyethylmetacrylate (HEMA) *via* a redox polymerization technique. They tested the pH responsiveness of the obtained product *via* water swelling experiment in difference of pH solutions from 2 to 12. The study showed that as expected, P4VP based copolymer was susceptible to the pH of the environment, so the obtained copolymer was affected by changing its dimensions or degree of swelling when the pH of the surroundings was below 4 [28].



**Figure 18** The swelling percentage (%S) values of prepared hydrogels at different pHs (pH was adjusted by the addition of 0.1 M HCl, 0.1 M. NaOH) [28].

From this literature review, the introducing of 4VP into NR can provide the pH-responsive functions to NR and expand the range of applications of rubber-based materials.



## CHAPTER 3

### RESEARCH METHODOLOGY

#### 3.1 Materials

##### 3.1.1 Chemical reagents

High-ammonia NR latex (60% dry rubber content) was purchased from Department of Agriculture, Thailand. Indigo carmine and 4-Vinylpyridine (4VP,  $C_7H_7N$ , Assay 95%) were purchased from ACROS Organics™. 4VP was purified prior to polymerization by passing through a column containing aluminum oxide to remove the inhibitors and stabilizer, which were added for storage purposes. The purified 4VP was stored in a blown bottle and kept in refrigerator at  $-5\text{ }^{\circ}\text{C}$ . Acetic acid glacial ( $CH_3COOH$ , Assay 99.5%), Formic acid ( $HCOOH$ , Assay 99.5%), Potassium persulfate (KPS,  $K_2S_2O_8$ , Assay 99%), Sodium dodecyl sulfate (SDS, Assay 98%), Toluene (Assay 99.5%), and Urea ( $NH_2CONH_2$ , Assay  $99.0\pm 100.5\%$ ) were supplied from CARLO ERBA Reagent. Bis ( $\alpha,\alpha$ -dimethylbenzyl) peroxide (BPO,  $C_{18}H_{22}O_2$ , Assay 98%) was obtained from Merck Millipore Corporation and it was recrystallized using methanol before used. Chloroform ( $CHCl_3$ , Assay 98%) were purchased from RCI Labscan, Thailand, and deuterated chloroform ( $CDCl_3-d$ ) as an analytical grade was obtained from Cambridge Isotope, the United States. Diethyl ether ( $(CH_3CH_2)_2O$ , Assay 99.7%) was purchased from Panreac AppliChem ITW Companies. Acetone ( $C_3H_6O$ ), Dichloromethane ( $CH_2Cl_2$ ), Methanol ( $CH_3OH$ ), Potassium hydroxide (KOH) are commercially available. The distilled and deionized water (DI water) was used throughout experiments.

##### 3.1.2 Glassware

1. Beaker 100, 250, 600 mL
2. Round bottom flask 100, 250 mL
3. Condenser
4. Stirring rod

5. Glass funnel
6. Watch glass
7. Cylinder
8. Centrifuge tube
9. Dropper
10. Dropping funnel

### 3.1.3 Instrument and Apparatus

1. pH meter (Model: C860, Consort, TU)
2. Centrifuge (Model: Velocity 14R refrigerated centrifuge (Dynamica), TU)
3. Fourier transform infrared spectrometer (Model: Spectrum GX, Perkin Elmer, TU)
4. Nuclear magnetic resonance spectrometer (Model: AVANCE III HD NanoBay 400 MHz, BRUKER, TU)
5. X-ray photoelectron spectrometer (Model: AXIS Ultra DLD, Kratos Analytical Ltd., CMU)
6. CHN elemental analyzer (Model: CHN-2000 LECO instrument, CU)
7. Thermal gravimetric analyzer (Model: SDTA851e, Mettler Toledo, METC)
8. Differential scanning calorimeter (Model: DSC822e, Mettler Toledo, MTEC)
9. Contact angle instrument (Model: TL100 Theta Lite tensiometer, TU)
10. UV-Visible spectrometer (Model: UV-1700 PharmaSpec, SHIMADZU, TU)
11. Fluorescence spectrometer (Model: FP-6200, JASCO, TU)

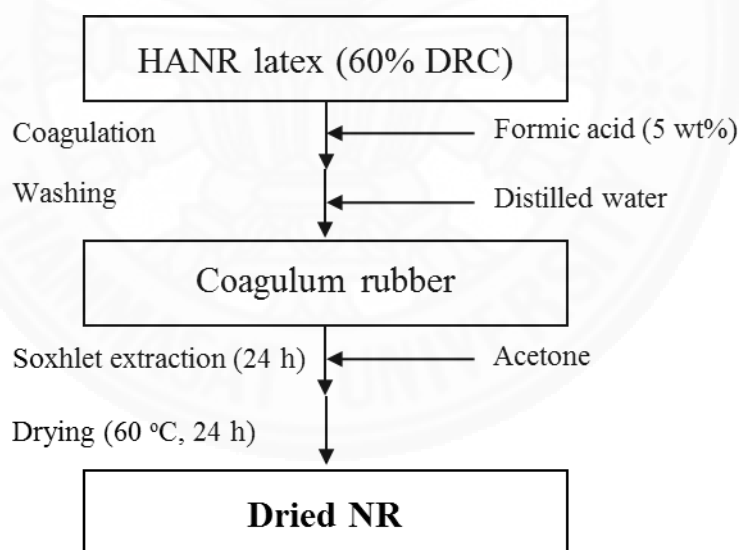
## 3.2 Methods and Preparation

In this thesis research, the method for modifying of natural rubber as pH responsive materials was divided into two approaches: crosslinking and grafting methods.

### 3.2.1 Synthesis of P4VP-crosslinked NR

#### 3.2.1.1 Preparation of Dried NR

Dried natural rubber (Dried NR) was prepared by coagulating HANR latex in 5 wt% formic acid and washing with distilled water for several times till the coagulated product was neutral. The coagulated rubber was dried in an oven at 60 °C overnight. Then, the dried rubber was purified by soxhlet extraction using acetone as solvent for 24 h to remove any contaminants before being dried again at 60 °C overnight.



**Figure 19** A schematic representation of the preparation of dried NR.

### 3.2.1.2 Preparation of poly(4-vinylpyridine) (P4VP)

Poly(4-vinylpyridine) (P4VP) was prepared by using 4-vinylpyridine (4VP) and benzoyl peroxide (BPO) as a monomer and initiator, respectively. First, the 4VP (10 g) and BPO (0.1 g) were placed in a 100-mL beaker under continuous agitation until the mixture became homogeneous mixture. The reaction mixture was then allowed to polymerize in a domestic microwave oven at 850 W for 8 min. Next, the resulting polymer was dissolved with dichloromethane, and the obtained polymer solution was subsequently precipitated with diethyl ether for purification. Finally, P4VP was filtered using vacuum filtration, followed by drying in a vacuum oven at 55 °C overnight to yield an orange-brown solid.



**Figure 20** Synthesis of poly(4-vinylpyridine) from 4-vinylpyridine (4VP) and benzoyl peroxide (BPO) as a monomer and initiator, respectively.

### 3.2.1.3 Preparation of P4VP-crosslinked NR (P4VP-NR)

A solution polymerization process was used to prepare the crosslinked materials between P4VP and NR. The preparation procedure of P4VP-NR was shown in Figure 21.

The as-prepared dried NR (1 g) was cut into tiny pieces and dissolved in chloroform (30 mL) in a 250-mL round bottom flask. A solution of P4VP (50-100 phr with respect to NR) in chloroform (15 mL) was then added. The reaction mixture was continuously stirred to obtain a homogeneous mixture, followed by heating

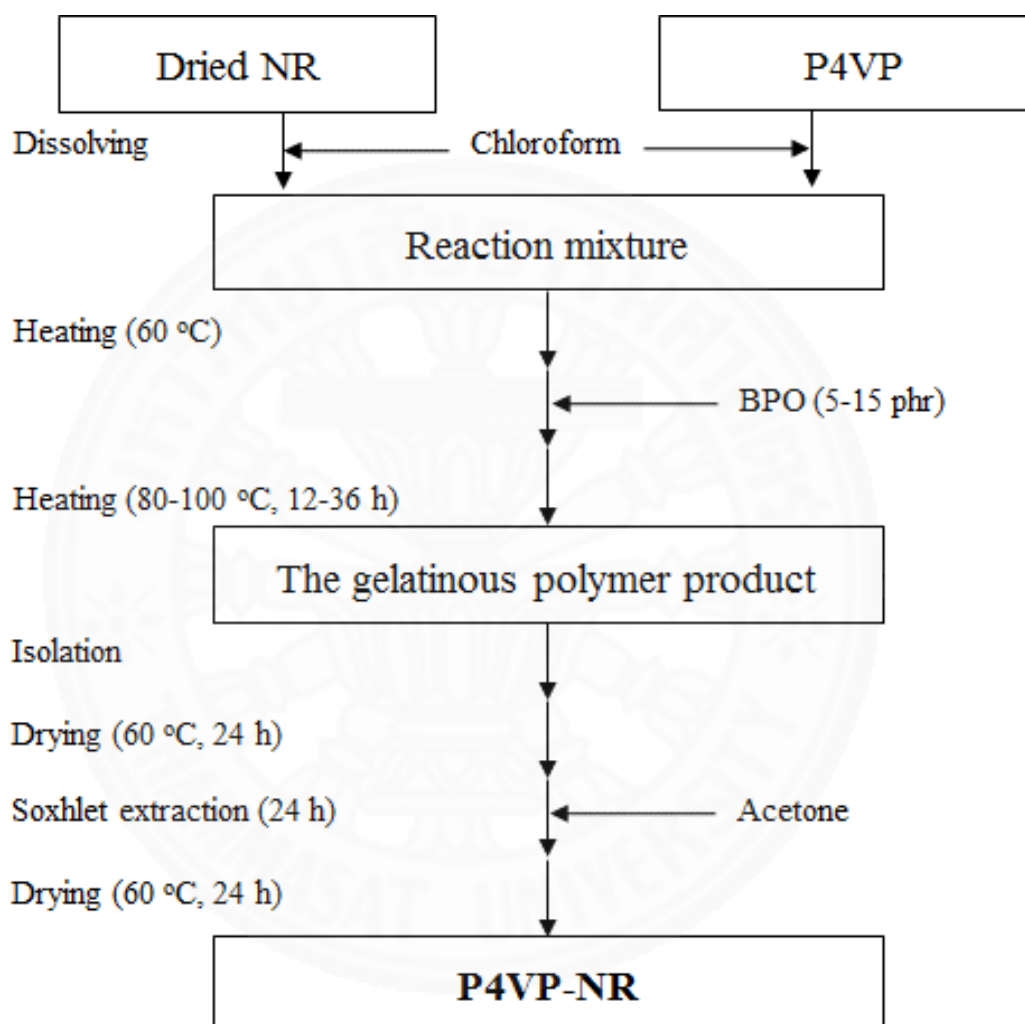
to approximately 60 °C. The BPO (5-10 phr with respect to NR) in chloroform (5 mL) was gradually added to the reaction while stirring. Then, the temperature was increased to a predetermined temperature (80-100 °C) for a specific amount of time (12-36 h) to obtain a gelatinous product. After finished the reaction, the reaction was cooled to room temperature. The gelatinous polymer product was separated, washed with plenty of chloroform, and dried under vacuum oven at 60 °C for 24 h. Subsequently, the resulting polymer was purified by soxhlet extraction in acetone for 24 h to remove the residue P4VP and any contaminants, followed by drying in an oven at 60 °C overnight until the weight was constant.

- **Gel content (%)**

In this work, the efficiency on this reaction was determined by the gel content, which is defined as the percentage of the weight of gel content polymers or the crosslinked polymers with respect to the weight of main polymeric substrate. In general, the gel content is used to determine the existence of branched or network structures in NR [58]. Based on this experiment, the obtained products had been extracted with acetone before being measured because acetone is a great solvent for dissolving the P4VP homopolymer. As a result, the remaining product would be only the crosslinked material between P4VP and NR. Accordingly, the gel content values can be likewise assumed as the ratio between crosslinked P4VP chains and NR. The gel content can be calculated from the following equation (1):

$$\text{Gel content (\%)} = \frac{W_2 - W_1}{W_1} \times 100 \quad (1)$$

where  $W_1$  and  $W_2$  are the weight of the dried rubber and the functionalized rubber, respectively.



**Figure 21** A schematic representation of the preparation of P4VP-NR.

**Table 4** Formulation and the range of investigated parameters in crosslink reaction (P4VP-NR).

Ingredients	Amount	
	phr <sup>a</sup>	g
<u>Main components</u>		
Dried NR	100	1
Poly(4-vinylpyridine), P4VP	50, 100, 150	0.5, 1, 1.5
<u>Initiators</u>		
Benzoyl peroxide, BPO	5, 10, 15	0.05, 0.1, 0.15
<u>Solvent</u>		
Chloroform (mL)	50	
<u>Reaction time (h)</u>	12, 24, 36	
<u>Reaction temperature (°C)</u>	80, 90, 100	

<sup>a</sup> parts per hundred of rubber

### 3.2.1.4 Determination of the crosslink density

To calculate the crosslink density of the P4VP-NR, each crosslinked rubber sample was immersed in toluene solution and kept in the dark at room temperature (25-30 °C) for a week. After reaching swelling equilibrium, the swollen gel samples were then isolated and weighed. Then, the weight of the sample was determined again after drying in a vacuum oven at 60 °C for 24 h. The crosslink density was calculated using the Flory-Rehner Equation (2) [93].

$$p_c = -\frac{1}{2V_s} \frac{\ln(1 - V_r^0) + V_r^0 + \chi(V_r^0)^2}{(V_r^0)^{\frac{1}{3}} - \frac{V_r^0}{2}} \quad (2)$$

where  $p_c$  is the crosslink density ( $\text{mol m}^{-3}$ ),  $V_s$  is the molar volume of toluene ( $1.069 \times 10^{-4} \text{ m}^3 \text{ mol}^{-1}$ ) at 25 °C,  $\chi$  is the interaction parameter ( $0.44 + 0.18V_r^0$ ), and  $V_r^0$  is the fraction of rubber in the swollen gel, which is calculated as follows equation (3):

$$V_r^0 = \frac{1}{1 + \frac{\rho_r}{\rho_s} \left( \frac{W_S - W_D}{W_D} \right)} \quad (3)$$

where  $\rho_s$  and  $\rho_r$  are the densities of toluene (0.87 g mL<sup>-1</sup>) and rubber (0.92 g mL<sup>-1</sup>), and  $W_S$  and  $W_D$  are the weights of the swollen and dried rubber, respectively [94].

### 3.2.2 Synthesis of 4VP-grafted DPNR (4VP-g-DPNR)

#### 3.2.2.1 Preparation of deproteinized natural rubber latex (DPNR latex)

The deproteinized natural rubber latex (DPNR latex) was prepared from the high-ammonia NR latex (HANR latex) using urea treatment [44], surfactant washing [58] and centrifugation methods as shown in Figure 22.

Firstly, the high-ammonia NR latex (HANR latex, 60% DRC) was incubated with 0.1 wt% urea in the presence of 1 wt% sodium dodecyl sulfate (SDS) at room temperature (25-30 °C) for 30 min. Then, the incubated rubber latex was centrifuged at 10,000 rpm at 25 °C for 60 min. The recovered cream fraction (top layer) was collected and then re-dispersed in 1 wt% of SDS solution for further washing the rubber particles. The washing procedure with surfactant was repeated twice using centrifugation methods. After collecting the last cream fraction, the DPNR was finally kept in 1 wt% SDS solution to prevent the aggregation of the rubber particles and obtain the DPNR latex with the final dry rubber content (DRC) of 28%.

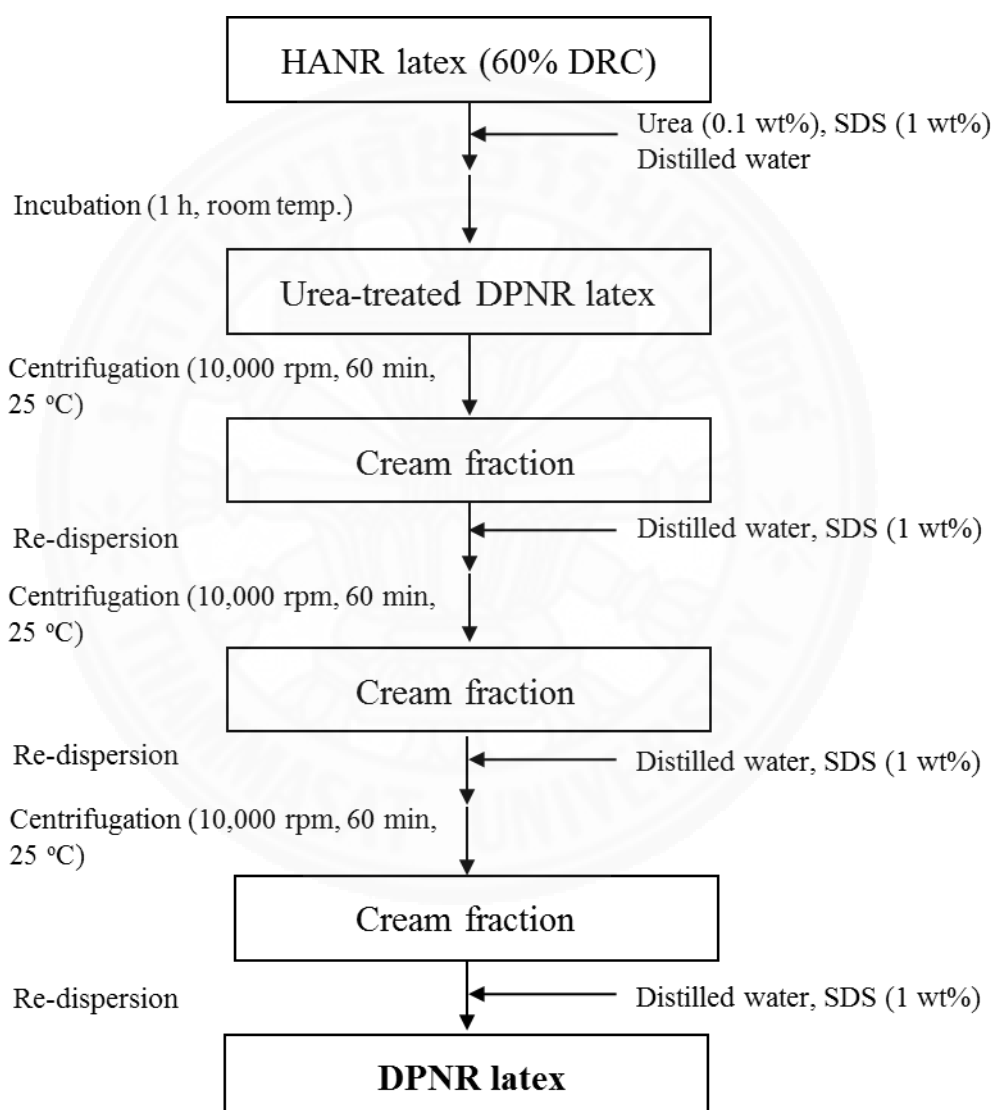
- **Dry rubber content (DRC, %)**

The final dry rubber content (DRC, %) was measured by coagulating a known amount of as-prepared DPNR latex with 5 wt% formic acid, washing with distilled water for several times. The weight of the dried rubber was then determined after drying in an oven at 60 °C for 24 h. The dry rubber content (DRC, %) was calculated from the following equation (4):



$$\text{The dry rubber content (DRC, \%)} = \frac{W_2}{W_1} \times 100 \quad (4)$$

where  $W_1$  and  $W_2$  are the weight in grams of DPNR latex taken for the test and the weight of dry coagulum, respectively.



**Figure 22** A schematic representation of the preparation of DPNR latex.

### 3.2.2.2 Preparation of graft copolymerization between 4VP and DPNR latex (4VP-g-DPNR)

An emulsion polymerization process was used to prepare the graft copolymerization between 4VP and DPNR. The preparation procedure of 4VP-g-DPNR was shown in Figure 23.

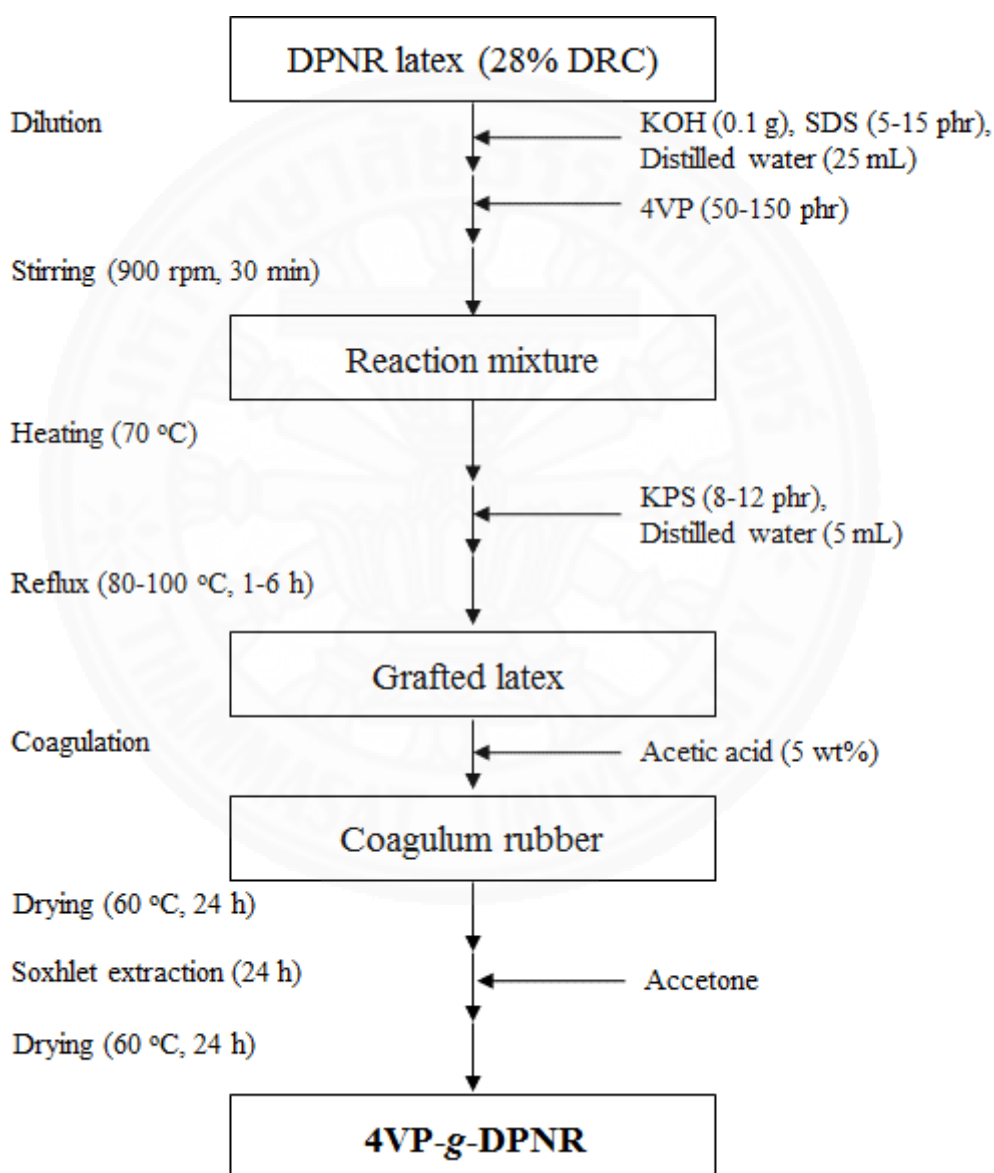
The DPNR latex (5 g) was firstly introduced into a 250 mL two-neck round-bottom flask equipped with a dropping funnel and reflux condenser, followed by dilution with DI water (5 mL). A solution of potassium hydroxide (KOH, 0.1 g) to maintain the pH of the latex above 10 and sodium dodecyl sulfate (SDS, 5-15 phr with respect to dry rubber content) as an emulsifier were then added. Subsequently, the 4VP (50-150 phr with respect to dry rubber content) monomer was slowly dropped into the reactor while stirring to prevent the aggregation of monomer. The reaction mixture was continuously stirred at a stirring speed of 900 rpm for 30 min in order to allow the rubber particles to swell with 4VP monomer and almost homogeneous mixture. When the reaction was heated up to approximately 70 °C, a solution of potassium persulfate (KPS, 8-12 phr with respect to dry rubber content) in distilled water as an initiator was added. The reactions were allowed to proceed the graft copolymerization under continuous stirring at a predetermined temperature (80-100 °C) for a specified amount of time (1-5 h). After finishing the reaction, the reactor was discharged. The grafted latex was coagulated with 5 wt% acetic acid, and the coagulum was washed with plenty of distilled water for several times before being dried up in an oven at 60 °C overnight. The obtained product was purified by soxhlet extraction in acetone for 24 hours to remove the residue 4VP monomer, P4VP homopolymer, and any contaminants, followed by drying again in a vacuum oven at 60 °C for 24 hours.

- **Grafting ratio (%GR)**

In this work, the efficiency on this reaction was determined by the grafting ratio (%) that is the ratio of the number of grafted polymer chains onto backbone chains. The grafting ratio was calculated from the following equation (5):

$$\text{Grafting ratio (\%GR)} = \frac{I_{8.5/2}}{I_{5.1}} \times 100 \quad (5)$$

where  $I_{8.5}$  and  $I_{5.1}$  are the integrated area under a signal that derived from  $^1\text{H-NMR}$  of the unsaturated proton of pyridine ring of 4VP unit ( $\text{N}=\text{C}-\text{H}$ ) and the unsaturated methyne proton of polyisoprene unit ( $\text{C}=\text{C}-\text{H}$ ), respectively.



**Figure 23** A schematic representation of the preparation of 4VP-g-DPNR.

**Table 5** Formulation and the range of investigated parameters in graft copolymerization (4VP-*g*-DPNR).

Ingredients	Amount	
	phr <sup>a</sup>	g
<u>Main components</u>		
DPNR latex	100	1.4 <sup>b</sup>
4-vinylpyridine, 4VP	50, 100, 150	0.7, 1.4, 2.1
<u>Initiators</u>		
Potassium persulfate, KPS	8, 10, 12	0.1, 0.14, 0.17
<u>Emulsifier</u>		
Sodium dedocyl sulfate, SDS (g)	5, 10, 15	0.07, 0.14, 0.21
<u>Others</u>		
Potassium hydroxide, KOH (g)		0.1
Distilled water (mL)		30
<u>Reaction time (h)</u>		1, 3, 5
<u>Reaction temperature (°C)</u>		80, 90, 100

<sup>a</sup> parts per hundred of rubber

<sup>b</sup> weigh of dry rubber calculated from 5 g of deproteinized natural rubber latex (DPNR latex) with 28 %DRC

### 3.3 Characterization

#### 3.3.1 Determination of the chemical structure and chemical elements of the functionalized products

##### 3.3.1.1 Fourier Transform Infrared (FT-IR) spectroscopy

The Fourier Transform Infrared (FT-IR) spectroscopy is a technique that basically and widely used to prior determine the chemical structures of the materials. Since the characteristic adsorption of infrared irradiation and the vibration frequency in each molecules is rather different, the structural characterization of functional groups of analyzed materials are obtained [95]. All of FT-IR spectra were

recorded using a Perkin Elmer FT-IR spectrometer (Spectrum GX model) with a resolution of  $4\text{ cm}^{-1}$ , measured in the range of  $4000\text{-}400\text{ cm}^{-1}$ . The P4VP sample was mixed with KBr and pressed to a plate for measurement, and the rubber samples were prepared by dissolving them with deuterated chloroform ( $\text{CDCl}_3\text{-}d$ ) followed by casting the obtained solution as a thin film onto NaCl salt windows before the measurement.



**Figure 24** A photograph of a Perkin Elmer FT-IR (Spectrum GX model) spectrometer.

### 3.3.1.2 Nuclear Magnetic Resonance (NMR) spectroscopy

Nuclear magnetic resonance (NMR) spectroscopy is a potential technique that commonly used to determine a unique structure of compounds through the magnetic properties of certain nuclei of atoms [96]. In this study, a proton nuclear magnetic resonance spectroscopy ( $^1\text{H}$ -NMR) was chosen to confirm the structure of the obtained products. All of  $^1\text{H}$ -NMR spectra were obtained using a Bruker Avance III HD NanoBay 400 MHz spectrometer. The rubber samples were prepared by dissolving them with deuterated chloroform ( $\text{CDCl}_3\text{-}d$ ) to a concentration of 5-10 %w/w solution before measurement.



**Figure 25** An image of NMR spectrometer.

### 3.3.1.3 X-ray Photoelectron Spectroscopy (XPS)

X-ray photoelectron spectroscopy (XPS) is a surface characterization technique. It is extensively used to analyze the elemental composition of the surface in many fields of research study. Generally, the XPS spectra are obtained by irradiating a material with a beam of X-rays and measuring the kinetic energy and number of electrons that escape from the analyzed materials. This technique is used to analyze many of substrates and materials, such as inorganic compounds, metal alloys, polymers, catalysts, glasses, ceramics, and many others [97].

In this study, the surface elements of the samples were obtained using an X-ray photoelectron spectrometer (XPS; AXIS ULTRA<sup>DLD</sup>, Kratos analyticle, Manchester, UK). The samples were cut into approximately of 1.0x1.0 cm<sup>2</sup> and kept in desiccator to prevent a moisture before measured. The base pressure in the XPS analysis chamber was about 5×10<sup>-9</sup> torr. The samples were excited using X-ray hybrid mode at a 700×300 μm spot area with a monochromatic Al K<sub>α1,2</sub> radiation at 1.4 keV. The X-ray anode was run at 15 kV 10 mA 150 W. The photoelectrons were detected with a hemispherical analyzer positioned at an angle of 45° with respect to the sample surface. The chemical composition of the samples was measured using a PANalytical X-ray fluorescent spectrometer in semi-quantitative analysis mode.



**Figure 26** An image of an X-ray Photoelectron Spectrometer (AXIS ULTRA<sup>DLD</sup>, Kratos analyticle).

#### 3.3.1.4 CHN Element Analysis

CHN Analyzer is an instrument that used to determine the elemental concentrations, such as carbon (C), hydrogen (H) and nitrogen (N) in an analyzed sample. It works by using a combustion process to oxidize the sample into any simple compounds, and then those compounds were detected with a thermal conductivity detection or infrared spectroscopy [98]. The CHN element analysis was obtained using a CHN-2000 LECO instrument. The samples were prepared by casting the NR and DPNR latex into a watch glass, and leaving at room temperature (25-30 °C) for 24 h. After that, the samples were peeled off and cut into approximately of 1.0x1.0 cm<sup>2</sup>, followed by keeping in desiccator to prevent a moisture before measured.

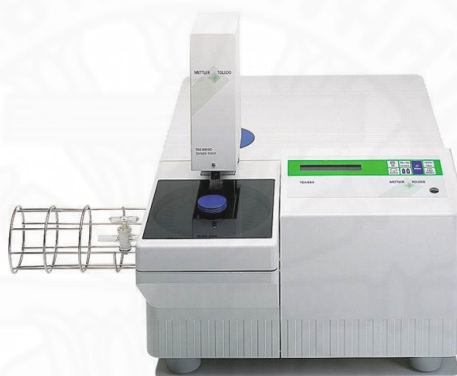


**Figure 27** An image of a CHN-2000 LECO analyzer.

### 3.3.2 Determination of the thermal properties of the functionalized products

#### 3.3.2.1 Thermal Gravimetric Analysis (TGA)

In this study, the TGA was used to determine the thermal stability of the functionalized products. TGA thermograms of the samples were carried out using a Mettler Toledo SDTA851e analyzer. The samples were prepared by cutting them into a small piece of  $1.0 \times 1.0 \text{ cm}^2$ . The samples were heated at a rate of  $10 \text{ }^\circ\text{C min}^{-1}$  under a nitrogen atmosphere and measured in the range of 30-600  $^\circ\text{C}$ .



**Figure 28** An image of a Mettler Toledo SDTA851e analyzer (TGA).

#### 3.3.2.2 Differential Scanning Calorimetry (DSC)

The glass transition temperatures ( $T_g$ ) of the samples were obtained using a Mettler Toledo DSC822e differential scanning calorimeter. Before being measured, the rubber samples were prepared by cutting them into a small piece of  $1.0 \times 1.0 \text{ cm}^2$ . The samples were heated at a rate of  $10 \text{ }^\circ\text{C min}^{-1}$  under a nitrogen atmosphere and measured in the range from -60  $^\circ\text{C}$  to 170  $^\circ\text{C}$ .





**Figure 29** An image of a Mettler Toledo DSC822e differential scanning calorimeter (DSC).

### 3.4 Determination of the pH responsiveness

#### 3.4.1 The water swelling measurements

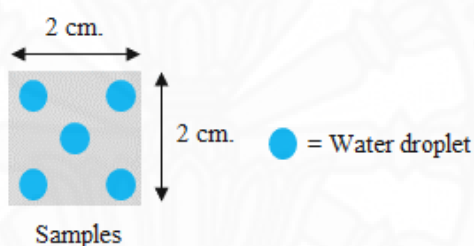
The samples were cut into small pieces of approximately 1.0x1.0 cm<sup>2</sup> and compressed by sandwiching them between two glass slides in order to remove air bubbles and reduce the roughness, followed by heating in an oven at 60 °C overnight. Then, the samples were weighed and immersed in different pH solutions from 2 to 12, which were adjusted by using 0.1 M HCl and 0.1 M NaOH, at ambient temperatures (25-30 °C) for 24 h. After withdrawing the samples from those pH solutions, the excess water on the surface was removed with filter paper by gently compression. The weight of swollen samples were measured, and the degree of swelling (%S) was calculated to determine the pH responsiveness as follow equation (6):

$$\text{The degree of swelling (\%S)} = \frac{W_2 - W_1}{W_1} \times 100 \quad (6)$$

where  $W_1$  and  $W_2$  are the weight of samples before and after water immersion, respectively.

### 3.4.2 The contact angle measurement

The samples were cut into a piece of approximately 2.0x2.0 cm<sup>2</sup> and compressed by sandwiching them between two glass slides to remove air bubbles and reduce the roughness, followed by heating in an oven at 60 °C overnight. Then, the samples were immersed in a range of different pH solutions from 2 to 12 at ambient temperatures (25-30 °C) for 24 h. After withdrawing the samples from those pH solutions, the excess water on the surface was gently blotted dry with filter paper. Then, the distilled water from syringe was dropped on surface of the sample and the angle of droplet was subsequently determined. Based on this experiment, the size of each water droplet was 8 μL, and it was dropped on 5 positions of each sample in order to calculate the average, as shown in Figure 30. In this study, the water contact angle was measured using a TL100 Theta Lite tensiometer instrument.



**Figure 30** An image demonstration of the determination of water contact angle in each samples.



**Figure 31** An image of a water contact angle instrument.

### 3.5 Demonstration of the pH responsive releasing behavior of the functionalized products

#### 3.5.1 Release of indigo carmine

The unmodified and modified rubber samples were cut into a piece of approximately  $1.0 \times 1.0 \text{ cm}^2$  and compressed by sandwiching them between two glass slides to remove air bubbles and reduce the roughness, followed by heating in an oven at  $60 \text{ }^\circ\text{C}$  overnight. The samples were then immersed in an aqueous solution of indigo carmine (20 ppm), a model water-soluble anionic drug, at room temperatures ( $25\text{-}30 \text{ }^\circ\text{C}$ ) for 2 weeks. After reaching an equilibrium adsorption, the rubber samples were withdrawn and dried in a vacuum oven at  $60^\circ\text{C}$  for 24 h. To investigate the releasing behavior, the rubber samples were placed in a range of different pH solutions from 2 to 10 at room temperature ( $25\text{-}30 \text{ }^\circ\text{C}$ ) for a specified amount of time (0.5-3 h) and those of pH solutions containing dye were withdrawn for measurement using UV-visible spectrometer at a  $\lambda_{\text{max}}$  corresponding to the maximum adsorption for the dye solution ( $\lambda_{\text{max}} = 610 \text{ nm}$ ).



**Figure 32** An image of a UV-Visible spectrometer (UV-1700 PharmaSpec, SHIMADZU).

### 3.5.2 Release of carbon quantum dots

In this experiment, the 4VP-*g*-DPNR/CQDs and DPNR/CQDs nanocomposites were firstly prepared. The 4VP-*g*-DPNR and DPNR sample (10 g) were dissolved with chloroform (50 mL). Carbon quantum dots<sup>a</sup> (CQDs, 0.1 g), prepared from water hyacinth, were then dispersed in each of the as-prepared polymer solutions under continuously stirring for 24 h to obtain an evenly dispersed mixture. The resultant polymer solutions were poured onto a glass plate and left to gradually evaporate at ambient temperature (25-30 °C). When the polymer mixture was dried, the obtained polymer sheets with the embedded CQDs were peeled off and cut into small pieces of rectangle shape (1.5 g/piece). The 4VP-*g*-DPNR/CQDs and DPNR/CQDs nanocomposites were placed in a range of pH solution from 2 to 12 at room temperature (25-30 °C) for 24 h. To investigate the releasing properties of CQDs in each of pH, those pH solutions were withdrawn for measurement using fluorescence spectrometer. The  $\lambda_{\text{excitation}}$  of this CQDs was 320 nm that corresponded to the suitable absorbance of CQDs.



**Figure 33** An image of a fluorescence spectrometer (FP-6200, JASCO).

---

<sup>a</sup> The CQDs was prepared using the following procedure. In brief, water hyacinth was pre-treated by washing, sun drying, and grinding. After that, the obtained water hyacinth powder was refluxed with nitric acid for 24 h, followed by pyrolysis at 250 °C. The resulting crude product was filtered. Then, the product was purified by dialysis, centrifuged, and freeze-dried.

### 3.6 Adsorption experiment

An indigo carmine stock solution of 1000 ppm was firstly prepared by dissolving indigo carmine (1 g) in deionized water (1 L). The working solutions (10-200 ppm) were prepared by dilution the stock solution with deionized water. The equilibrium adsorption of indigo carmine was carried out by introducing 0.25 g of the samples with 10 mL of different concentration of dye solutions from 10 to 200 ppm. Then, the bottles were sealed and placed in a laboratory shaker at room temperature (25-30 °C) for 2 weeks in order to reach the equilibrium adsorption. The concentration of the residual dye was subsequently measured using UV-visible spectrometer at a  $\lambda_{\max}$ , corresponding to the maximum adsorption for the dye solution ( $\lambda_{\max}= 610$  nm). Calibration curve was constructed between absorbance and concentration of the dye solution to obtain absorbance-concentration profile.

The amount of adsorbed indigo carmine was calculated based on a mass balance equation as given by the following equation (7) [99, 100]:

$$Q_e = \frac{(C_0 - C_e)V}{W} \quad (7)$$

where  $Q_e$  (mg/g) is the equilibrium adsorption capacity of dry weight of the adsorbent,  $C_0$  (mg/L) is the initial concentration of indigo carmine in the solution,  $C_e$  (mg/L) is the final or equilibrium concentration of indigo carmine in the solution,  $V$  (L) is the volume of the solution, and  $W$  (g) is the dry weight of rubber sample.

#### 3.6.1 Adsorption isotherms

In this study, the Langmuir, Freundlich, Temkin, and Dubinin-Radushkevich adsorption isotherms were used to investigate an adsorption process between the adsorbate molecules and the adsorbent surface, such as the adsorption process of indigo carmine onto the obtained products. The mathematical equations of these four models were summarized as shown in Table 6 [100-102]. The description of those isotherms were also mentioned at below.

**Table 6** Mathematical equations for the isotherms and their linear forms.

Isotherm	Equation	Linear form
Langmuir	$Q_e = \frac{Q_0 K_L C_e}{1 + K_L C_e}$	$\frac{1}{Q_e} = \frac{1}{Q_0} + \frac{1}{Q_0 K_L C_e}$
Freundlich	$Q_e = K_f C_e^{\frac{1}{n}}$	$\log Q_e = \log K_f + \frac{1}{n} \log C_e$
Temkin	$Q_e = \frac{RT}{b_T} \ln(A_T C_e)$	$Q_e = B \ln A_T + B \ln C_e$
Dubinin-Radushkevich	$Q_e = (q_s) \exp(-K_{ad} \varepsilon^2)$	$\ln Q_e = \ln(q_s) - (K_{ad} \varepsilon^2)$

### 3.6.1.1 Langmuir adsorption isotherm

The Langmuir adsorption isotherm is commonly used to describe the formation of monolayer coverage on the surface of the adsorbent, where the adsorbent contains a certain number of active sites. From these basic assumptions, this isotherm can be represented by the following equation (8):

$$Q_e = \frac{Q_0 K_L C_e}{1 + K_L C_e} \quad (8)$$

Then, the Langmuir equation (8) can be converted into a linear form (9) for plotting the data and determining of their parameters easily:

$$\frac{1}{Q_e} = \frac{1}{Q_0} + \frac{1}{Q_0 K_L C_e} \quad (9)$$

where  $C_e$  = the equilibrium concentration of adsorbate (mg/L)

$Q_e$  = the amount of dye adsorbed per gram of the adsorbent at equilibrium (mg/g)

$Q_0$  = the maximum monolayer coverage capacity (mg/g)

$K_L$  = the Langmuir isotherm constant (L/mg)

The values of  $Q_0$  and  $K_L$  were calculated from the slope and intercept of the linear regression equation of Langmuir plot (9) between  $1/Q_e$  and  $1/C_e$ . Moreover, the significant characteristic of this isotherm can be expressed in terms of a separation factor or equilibrium factor ( $R_L$ ) which was computed from the following equation (10):

$$R_L = \frac{1}{(1 + K_L C_0)} \quad (10)$$

where  $C_0$  = the initial concentration of adsorbate in solutions (mg/L)

$K_L$  = the Langmuir isotherm constant (L/mg)

The  $R_L$  value or the equilibrium factor was used to indicate the adsorption nature or probability of adsorption process, which was defined in Table 7.

**Table 7** The nature of adsorption process.

<b><math>R_L</math> value</b>	<b>Adsorption process</b>
$R_L > 1$	Unfavorable
$R_L = 1$	Linear
$0 < R_L < 1$	Favorable
$R_L = 0$	Irreversible

### 3.6.1.2 Freundlich adsorption isotherm

The Freundlich adsorption isotherm describes the adsorption characteristics based on multilayer adsorption. From this assumption, the data can be fitted by the empirical equation proposed by Freundlich as given in the following equation (11):

$$Q_e = K_f C_e^{\frac{1}{n}} \quad (11)$$

Then, the Freundlich equation (11) can be changed into linear form (12) for plotting the data and determining their parameters:

$$\log Q_e = \log K_f + \frac{1}{n} \log C_e \quad (12)$$

where  $K_f$  = the Freundlich isotherm constant (mg/g)

$n$  = the adsorption intensity

$C_e$  = the equilibrium concentration of adsorbate (mg/L)

$Q_e$  = the amount of dye adsorbed per gram of the adsorbent at equilibrium (mg/g)

Based on this isotherm, the values of  $K_f$  and  $n$  can be examined from the intercept and slope of the linear regression equation that derived by plotting of  $\log Q_e$  versus  $\log C_e$ , respectively. These constants are the essential characteristic parameters of the adsorbent-adsorbate system, in which  $K_f$  is an indicator of adsorption capacity. In addition,  $1/n$  or  $n$  are known as a heterogeneity parameter that is an indicator of a function of the strength adsorption in the system and the favorability of adsorption. The indication of  $1/n$  and  $n$  value are assigned in Table 8.

**Table 8** The nature of adsorption process [100, 103-105].

<b>n value</b>	<b>Adsorption process</b>
$1/n > 1$	Cooperative adsorption
$1/n < 1$	Normal adsorption
$n = 1$	The partition between the two phases are independent of the concentration
$n > 1$	Favorable adsorption condition
$1 < n < 10$	Beneficial adsorption



### 3.6.1.3 Temkin adsorption isotherm

The Temkin adsorption isotherm is used to describe the indirect effects on adsorbate/adsorbent interaction, such as heat, which can influence the interaction of adsorption isotherm. This model can be represented by the following equation (13):

$$Q_e = \frac{RT}{b} \ln(A_T C_e) \quad (13)$$

Then, the equation (13) can be rearranged into linear form as shown in equation (14):

$$Q_e = B \ln A_T + B \ln C_e \quad (14)$$

$$B = \frac{RT}{b_T} \quad (15)$$

where  $A_T$  = the Temkin isotherm equilibrium binding constant (L/g)

$b_T$  = the Temkin isotherm constant

$R$  = the universal gas constant (8.314J/mol K)

$T$  = the absolute temperature at 301K

$B$  = the constant related to heat of sorption (J/mol)

$C_e$  = the equilibrium concentration of adsorbate (mg/L)

$Q_e$  = the amount of dye adsorbed per gram of the adsorbent at equilibrium (mg/g)

In this isotherm, the characteristic constants were obtained by plotting the  $Q_e$  versus  $\ln C_e$  and then each of constants were determined by the slope and intercept from the given linear regression equation.

### 3.6.1.4 Dubinin-Radushkevich adsorption isotherm

Lastly, the Dubinin-Radushkevich (DRK) can be applied to express the adsorption model on both homogeneous and heterogeneous surfaces based on pore filling mechanism. This model can be expressed by the following equation (16):

$$Q_e = (q_s) \exp(-K_{ad}\varepsilon^2) \quad (16)$$

Then, the equation (16) can be rewritten into linear form as shown in equation (17):

$$\ln Q_e = \ln(q_s) - (K_{ad}\varepsilon^2) \quad (17)$$

where  $q_s$  = the theoretical isotherm saturation capacity (mg/g)

$K_{ad}$  = the Dubinin–Radushkevich isotherm constant ( $\text{mol}^2/\text{J}^2$ )

$Q_e$  = the amount of dye adsorbed per gram of the adsorbent at equilibrium (mg/g)

$\varepsilon$  = the Dubinin–Radushkevich isotherm constant, which can be calculated from the given equation below (18):

$$\varepsilon = RT \ln \left[ 1 + \frac{1}{C_e} \right] \quad (18)$$

where  $R$  = the universal gas constant ( $8.314 \text{ J mol}^{-1} \text{ K}^{-1}$ )

$T$  = the absolute temperature (301 K)

$C_e$  = the adsorbate equilibrium concentration ( $\text{mg L}^{-1}$ )

From the DRK adsorption isotherm, the constant values of  $K_{ad}$  and  $q_s$  were estimated from the slope and intercept of the linear regression equation obtained from the plotting of  $\ln Q_e$  against  $\varepsilon^2$ . However, the important characteristic parameter, which is often used to determine the physical and chemical adsorption behaviors, is the apparent mean free energy ( $E$ ). It is reported that if the  $E$  value is less than  $8 \text{ kJ mol}^{-1}$ , it can be indicated as the physical adsorption. On the other hand, if it is

found to be in the range between 8 to 16 kJ mol<sup>-1</sup>, it will be considered as the chemical adsorption or ionic exchange [106, 107]. The E value can be calculated from the following equation (19):

$$E = \left[ \frac{1}{\sqrt{2K_{ad}}} \right] \quad (19)$$



## CHAPTER 4

### RESULTS AND DISCUSSION

In this thesis research, the 4-vinylpyridine-functionalized natural rubbers as pH responsive materials including P4VP-NR and 4VP-*g*-DPNR were prepared *via* two chemical-based methods, which were the crosslinking and grafted copolymerization methods, respectively. The functional groups and chemical elements of the resulting polymers were characterized using Fourier transform infrared spectroscopy (FT-IR), X-ray photoelectron spectroscopy (XPS), proton nuclear magnetic spectroscopy ( $^1\text{H-NMR}$ ), and CHN elemental analysis. After characterization, the effect of influential parameters on both reactions, which consisted of the monomer/polymer concentrations, the initiator concentration, the emulsifier concentration, the reaction temperature, and the reaction time, were studied. For the crosslinked material, the crosslink density was further determined. In addition, the thermal properties such as decomposition temperature and glass transition temperature ( $T_g$ ) of the resulting polymers were also characterized using thermal gravimetric analyzer (TGA) and differential scanning calorimeter (DSC), respectively. Finally, the pH responsiveness of the obtained products were determined by the water swelling experiment and the water contact angle measurement, and the controlled-release of indigo carmine and carbon quantum dots in a different pH solutions had been further verified in order to demonstrate the pH responsive releasing behavior before the adsorption isotherms were studied.

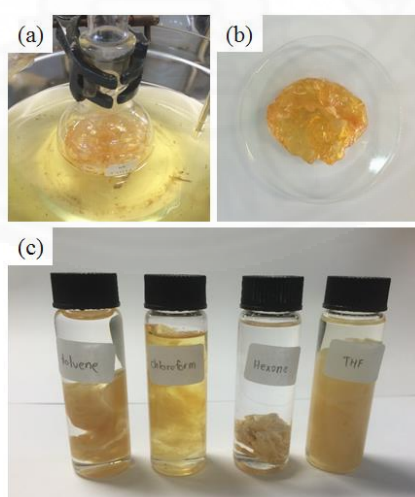
#### 4.1 Synthesis and characterizations of P4VP-crosslinked NR (P4VP-NR)

##### 4.1.1 Preparation of P4VP-NR

In this method, a crosslinked polymer (P4VP-NR) between poly(4-vinylpyridine) (P4VP) and natural rubber (NR) was prepared *via* a solution polymerization method in which the using of organic solvent system. Before the crosslinking, dried NR was firstly prepared by coagulating natural rubber latex in an acidic solution, followed by purification with acetone. After that, P4VP was subsequently prepared by polymerization of 4-vinylpyridine in the presence of benzoyl

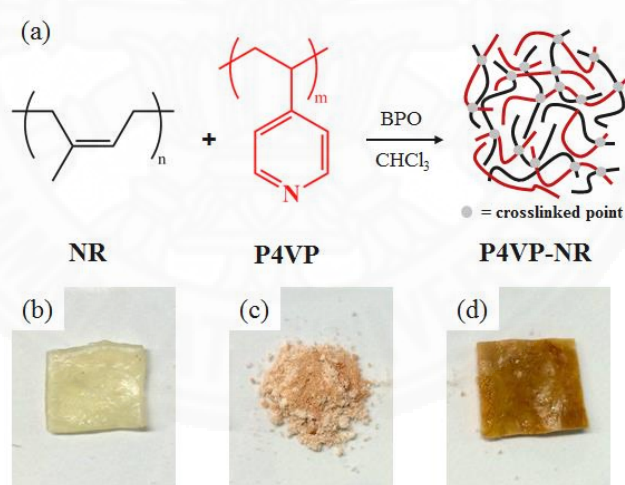
peroxide (BPO) as an initiator to yield an orange-brown solid (Figure 35c) with a conversion of 60%. The obtained P4VP was characterized using  $^1\text{H-NMR}$  and FT-IR spectroscopy. It was found that  $^1\text{H-NMR}$  of pure P4VP showed signals at around 6.5 and 8.5 ppm which belonged to the aromatic protons of the pyridine rings. Moreover, the FTIR spectrum of the P4VP showed signals at 2927, 1604, and  $1417\text{ cm}^{-1}$ , which corresponded to C-H stretches, C=N stretches, and C=C stretches, respectively. These results from  $^1\text{H-NMR}$  and FT-IR are consistent with a previous report [108].

Afterwards, the as-prepared P4VP and dried NR were introduced to the reaction using BPO as an initiator for crosslinking and chloroform as a solvent, which both P4VP and NR are readily soluble in this solvent. When the reaction finished, an insoluble polymer was formed, indicating the formation of a gel or crosslinked material (Figure 34a, b). From this phenomenon, it can be explained by the followings. In general, the crosslinking turned a polymer solution to a solid or insoluble product, because the polymer chains in the reaction are tied together by covalent bond, which lead to the extension of polymeric chain in multidimensional directions, giving a network structure. Therefore, the ability of polymeric chains to freely move is restricted as well as the gel-like feature and insolubility of polymer have formed [109].



**Figure 34** Photographic image of (a) the gel formation, (b) crosslinked material, and (c) the insoluble of product in organic solvents, included toluene, chloroform, hexane, and tetrahydrofuran (THF).

It is known that free radical initiators such as peroxide compounds can be used as crosslinking agents in NR because they can create free radicals on polymer chains *via* hydrogen abstraction processes [110-113]. And the formation of those free radicals on polymer chain leads to the crosslinking reaction between that polymer chains (Figure 35a). After purification by soxhlet extraction, photographs of the P4VP-NR were taken and compared with the pure NR and P4VP samples as shown in Figure 35b, c, and d. The NR sample was slight yellow and the P4VP powder was light orange-brown. In contrast, the P4VP-NR sample was found to be darker than both samples, initially indicating that P4VP-NR was not the same material as P4VP or NR. Furthermore, P4VP and NR are soluble in some organic solvents, for example chloroform and toluene, but the P4VP-NR sample did not dissolve in any solvents, but could only be swollen in some organic solvents, such as chloroform and toluene as shown in Figure 34c. This swelling event also suggested the formation of crosslinked material as mentioned above.



**Figure 35** A schematic representation of (a) the crosslinking reaction between natural rubber (NR) and poly(4-vinylpyridine) (P4VP), and photographic image of (b) NR, (c) P4VP, and (d) P4VP-NR, respectively.

In this approach, the using of dried NR instead of latex is advantageous for the production of crosslinked materials because it can be processed and controlled easily, which does not require surfactants and stabilizers to maintain the

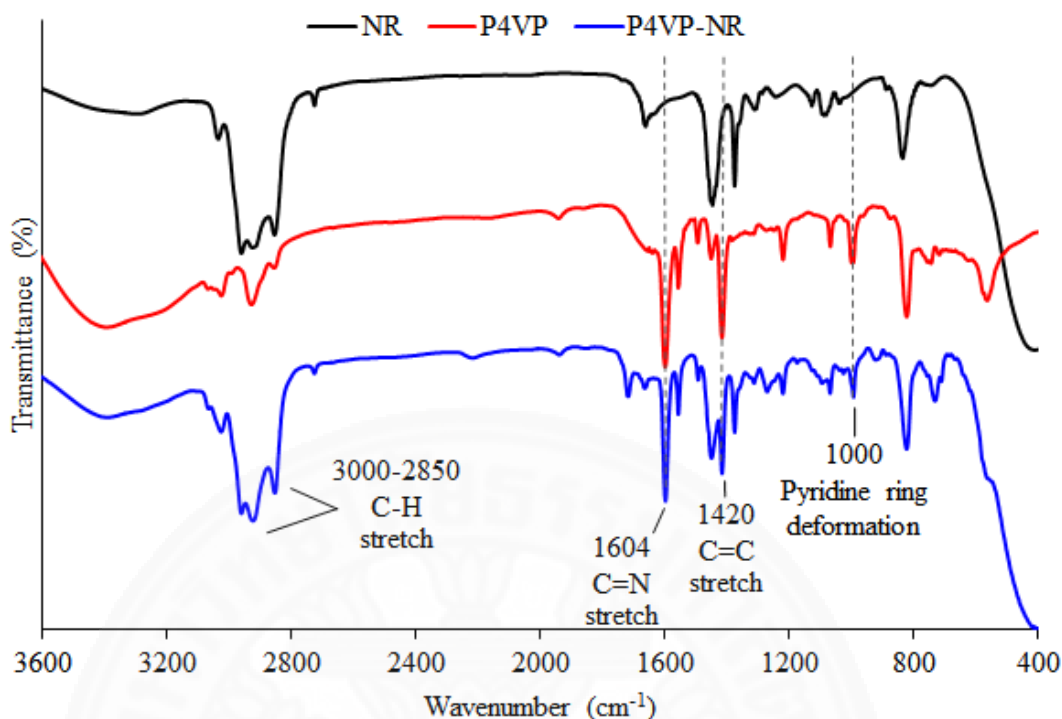
latex state. In addition, P4VP can be only dissolved in organic solvent such as chloroform and toluene, as a result the P4VP cannot proceed in latex form. Another advantage is that a pure product is obtained after removal of the solvent because the resulting polymer is an insoluble product, which will precipitate out of the medium easily.

The functionalized product was subsequently investigated *via* FT-IR and XPS techniques. Moreover, due to the lower solubility of crosslinked product in organic solvents, hence the nuclear magnetic resonance (NMR) could not be used to characterize the crosslinked product.

#### 4.1.2 FT-IR characterization of P4VP-NR

To verify the functional groups or structural characterization, the FT-IR spectrum of the crosslinked material (P4VP-NR) was obtained after purification and compared with that of the unmodified NR and P4VP as shown in Figure 36. Moreover, the comparison of the characteristic IR absorption bands of all samples at a specific wavenumber ( $\text{cm}^{-1}$ ) was shown in Table 9.

It was found that the unmodified NR sample (black line) showed the main signals which located at 3000 to 2850, 1661, and 835  $\text{cm}^{-1}$  corresponding to C-H stretching, C=C stretching, and olefinic C-H bending, respectively. However, the FT-IR spectra of the crosslinked material (blue line) showed signatures of both P4VP and NR, especially the signals at 1604  $\text{cm}^{-1}$ , 1420  $\text{cm}^{-1}$ , and 1000  $\text{cm}^{-1}$ , which corresponded to C=N stretching, C=C stretching, and pyridine ring deformation, respectively. Therefore, this confirmed the presence of P4VP in the crosslinked material as these three signals are not present in the spectra of the unmodified NR.



**Figure 36** FT-IR spectra of NR (black line), P4VP (red line), and P4VP-NR (gel content = 63%, blue line).

**Table 9** The comparison of the characteristic IR absorption bands of NR, P4VP, and the crosslinked material at a specific wavenumber (cm<sup>-1</sup>) [114].

Type of bonds	Wavenumber (cm <sup>-1</sup> )		
	NR	P4VP	P4VP-NR
O-H stretching (broad, moisture)	3600-3300	3600-3300	3600-3300
N-H stretching (protein)	3360	-	N/A
=C-H stretching	3037	3034	2995
CH <sub>3</sub> asymmetric stretching	2960	2927	2932
CH <sub>2</sub> asymmetric stretching	1917	N/A	1948
CH <sub>2</sub> symmetric stretching	2851	2854	2851
C=C stretching	1661	-	1661
CH <sub>2</sub> scissoring	1446	1452	1451



CH <sub>3</sub> asymmetric deformation	1375	-	1376
CH <sub>2</sub> wagging	1308	-	1312
CH <sub>2</sub> twisting	1261	N/A	1272
CH <sub>2</sub> wagging	1126	N/A	N/A
C-CH <sub>2</sub> stretching	1093	1069	1070
C-CH <sub>3</sub> stretching	1040	N/A	N/A
CH <sub>3</sub> rocking	927	N/A	924
CH <sub>3</sub> wagging	888	N/A	854
=C-H wagging	835	824	824
CH <sub>2</sub> rocking	743	744	733
C=C stretching of aromatic pyridine ring	-	1604	1600
C=N stretching of aromatic pyridine ring	-	1417	1420
Pyridine ring deformation	-	1000	993

---

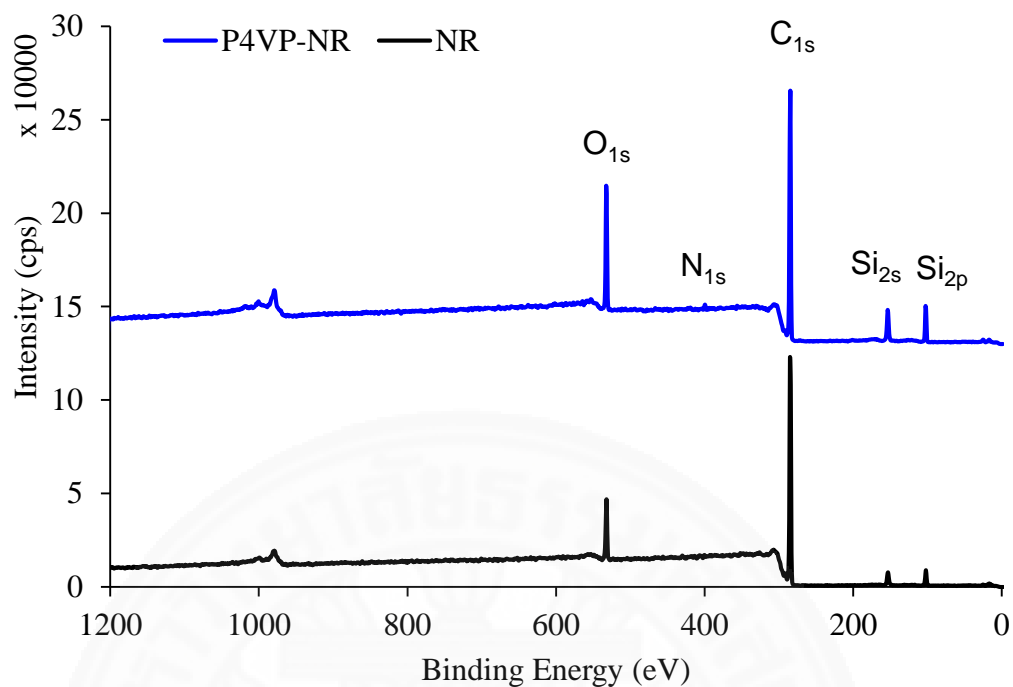
\*N/A means not available

### 4.1.3 XPS characterization of P4VP-NR

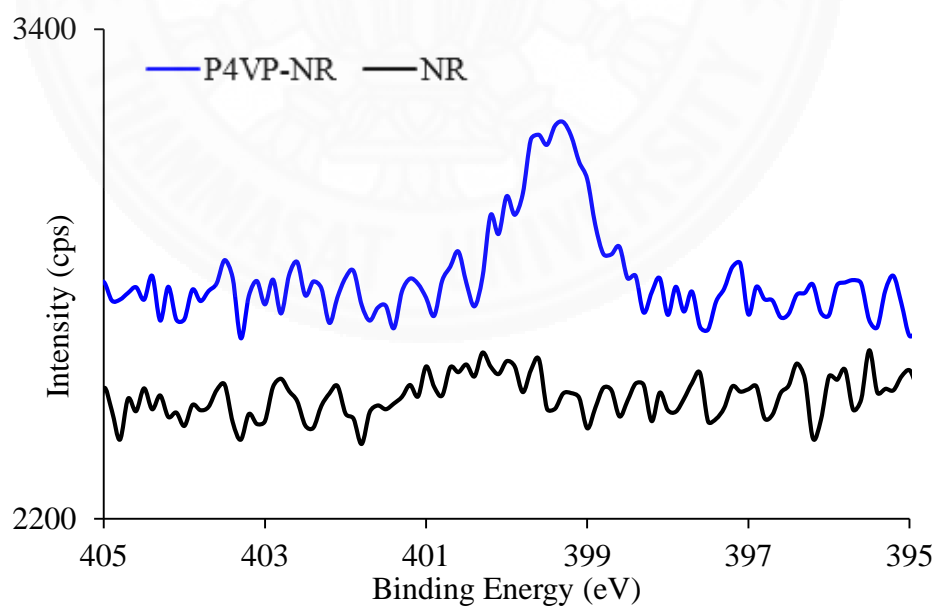
Apart from the FT-IR, the chemical compositions at the surface of P4VP-NR and NR samples were further characterized using X-ray photoelectron spectroscopy (XPS).

From the survey spectra as shown in Figure 37, it was found that most of chemical compositions of the unmodified NR and P4VP-NR samples were carbon atoms which showed up at 284 eV. The reason is due to the intrinsic polymeric hydrocarbon. In addition, the other signals which located at 532 eV, 153 eV, and 102 eV corresponded to O<sub>1s</sub>, Si<sub>2s</sub>, and Si<sub>2p</sub>, respectively. The silicon signals arose from the silicon substrate used for the measurement, and the presence of the small oxygen signal is because the oxygen is always presence on samples that exposed to the atmosphere and silica substrate also contains oxygen [115]. However, only the P4VP-NR sample obviously showed the nitrogen signal at 399 eV, which was clearly observed by the XPS high-resolution in N region as presented in Figure 38. The appearing of N signal in the product after purification resulted from the existence of P4VP in the crosslinked material, as confirmed that the P4VP was crosslinked to NR chains.

Therefore, the results from FT-IR and XPS confirmed the successful crosslinking reaction.



**Figure 37** XPS survey scan spectra of NR and P4VP-NR (gel content = 63%).



**Figure 38** XPS high-resolution spectra of N<sub>1s</sub> region of NR and P4VP -DPNR (gel content = 63%).

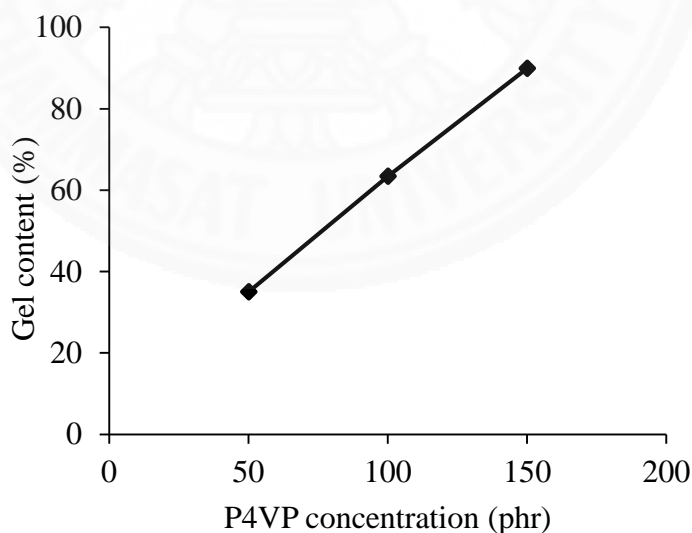
#### 4.1.4 Effect of influential parameters on gel contents

In this study, the effects of reagent concentrations and reaction conditions on gel content were investigated.

##### 4.1.4.1 Effect of P4VP concentration

Firstly, to study the effect of P4VP concentration on the gel content (%) of the crosslinking reaction, the P4VP concentration was varied from 50 to 150 phr with respect to NR. The other reagent concentrations and reaction condition were kept constant in which using a BPO concentration of 10 phr, reaction time of 24 h, and reaction temperature of 90 °C.

In Figure 39, it was found that as the P4VP concentration was increased from 50 to 150 phr, the gel content increased from 35% to 90%. The increase in P4VP concentration led to an increase in the gel content on the crosslinking reaction. From this result, it can be explained that when the concentration of polymer was increased due to the availability of precursors required for the reaction [116].

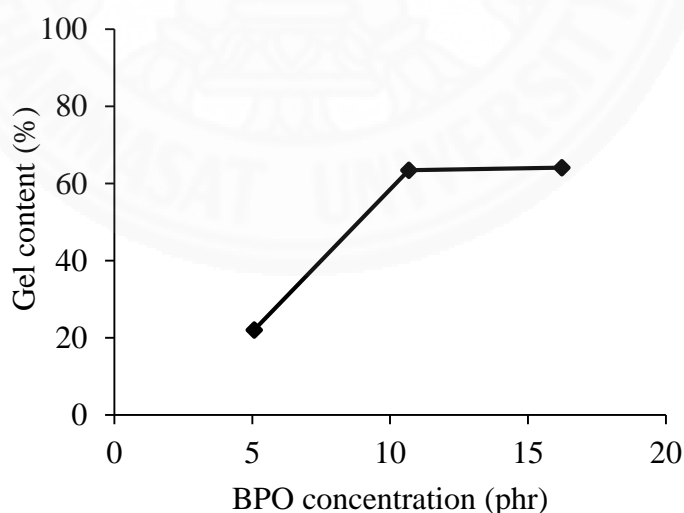


**Figure 39** Gel content as a function of P4VP concentration.

#### 4.1.4.2 Effect of BPO concentration

The effect of BPO concentration on the gel content (%) was also studied. The reaction was carried out by varying the BPO concentration from 5 to 15 phr with respect to NR, while the other reagent concentrations and reaction conditions were fixed constant in which using a P4VP concentration of 100 phr, reaction time of 24 h, and reaction temperature of 90 °C.

It was found that when the BPO concentration was increased from 5 to 15 phr as shown in Figure 40, the gel content increased rapidly from 22% to 63% and then seemed to be unchanged at the highest concentration. First, the initial stage of increasing the BPO concentration increased the gel content, possibly because the higher amount of initiators might promote the formation of free radicals on both P4VP and NR chains, resulting in the effective formation of macroradicals and consequently a gel or network structure between the polymer chains. However, the increasing of BPO concentration above these point (10 phr) can cause a reduction of the free radical concentration possibly due to a termination reaction, and as a result the gel content did not increase further.

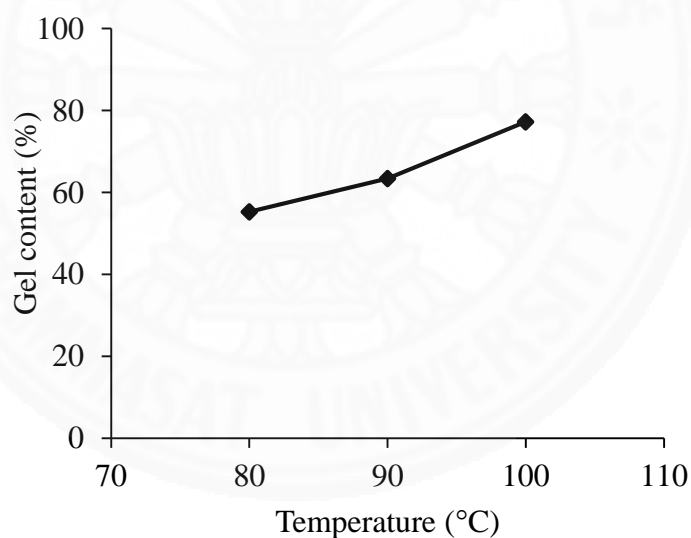


**Figure 40** Gel content as a function of BPO concentration.

#### 4.1.4.3 Effect of reaction temperature

The effect of reaction temperature on the gel content (%) was investigated by varying the reaction temperature in a range of 80 °C – 100 °C, whereas the other reagent concentrations and reaction time were fixed constant in which using a P4VP concentration of 100 phr, BPO concentration of 10 phr, and reaction time of 24 h.

In Figure 41, it was found that when the reaction temperature was increased from 80 to 100 °C, which is an optimum working range for benzoyl peroxide [117], the gel content increased from 55% to 77%. This result indicated that increasing the reaction temperature increased the gel content. It is well known that the reaction temperature is an essential parameter, which directly affects to the rate of decomposition of an initiator and crosslink process, leading to high gel contents.

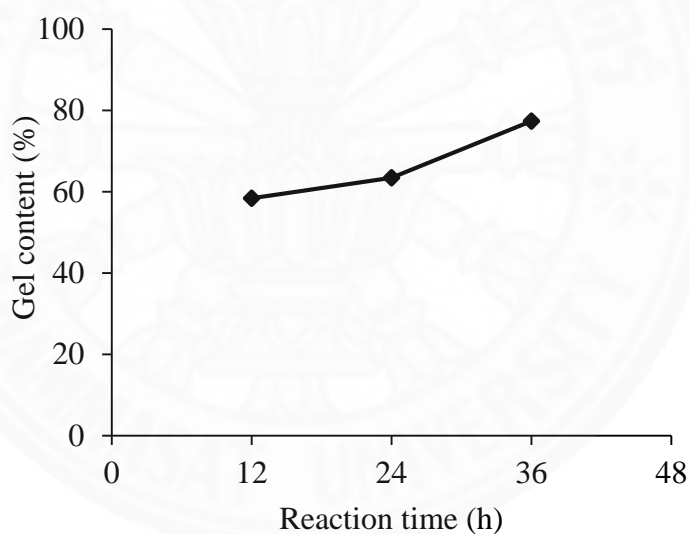


**Figure 41** Gel content as a function of reaction temperature.

#### 4.1.4.4 Effect of reaction time

Lastly, the effect of reaction time on the gel content (%) was also studied. The reaction was carried out by varying the reaction time in a range of 12-36 h. Meanwhile, the other reagent concentrations and reaction temperature were kept constant which used a P4VP concentration of 100 phr, BPO concentration of 10 phr, and reaction temperature of 90 °C.

In Figure 42, it was found that when the reaction time was increased from 12 to 36 h, the gel content increased from 58% to 77%. This result indicated that increasing the reaction time increased the gel content. From the obtained results, it can be explained that a prolonged reaction time is desirable for effective crosslinking reaction, leading to high gel contents [115].



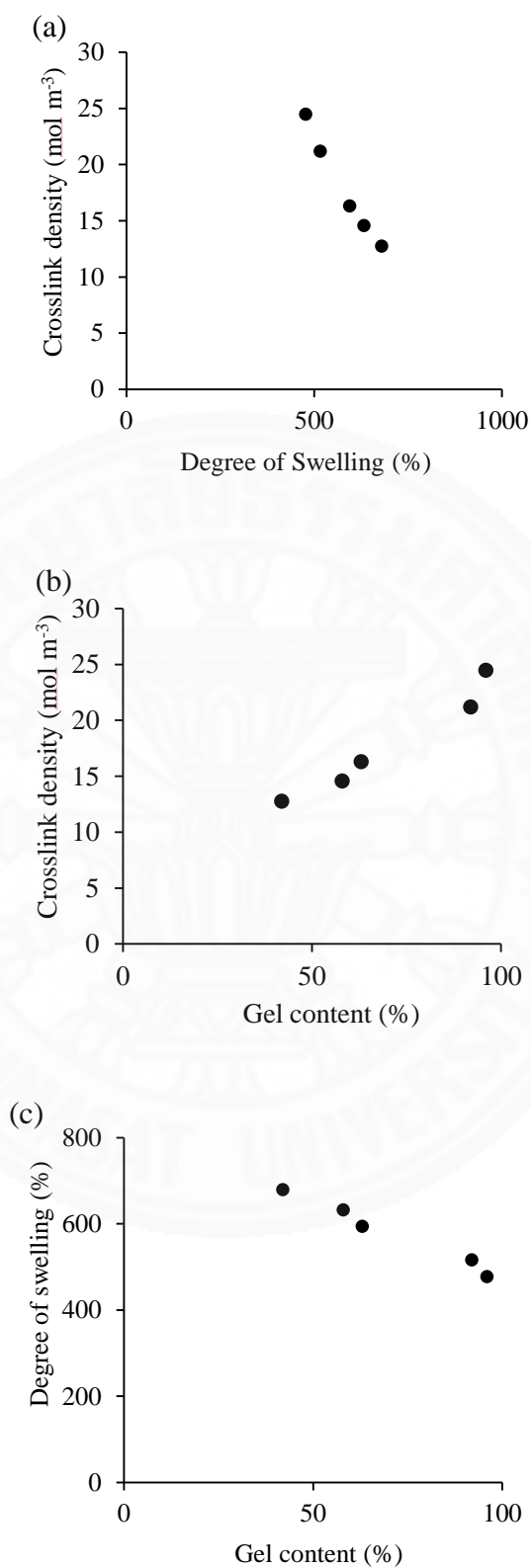
**Figure 42** Gel content as a function of reaction time.

#### 4.1.5 Determination of crosslink density of P4VP-NR

In this experiment, the determination of crosslink density was carried out *via* an equilibrium swelling of the crosslinked product in toluene solvent. The crosslink densities of the P4VP-NR samples were subsequently calculated using the Flory-Rehner equation.

As shown in Figure 43a, it was found that at the higher of the crosslink density, the lower of the solvent swelling of the crosslinked materials was obtained. As expected, the crosslink density is inversely proportional to the swelling behavior, because the increasing crosslink density leads to an increase of the restriction of the polymeric chain mobility [118]. As a result, less amount of solvent can be absorbed by the materials. In addition, the crosslink density was dependent on the gel content as shown in Figure 43b. At a gel content of 42%, the crosslink density was 13%. This increased to 24% at a gel content of 96%. Therefore, a greater amount of P4VP in the crosslinked products led to an increase in crosslink density but a decrease in solvent swelling degree as shown in Figure 43b and c. The higher of gel content means that the greater amounts of P4VP was immobilized to the samples, leading to more chain restriction.





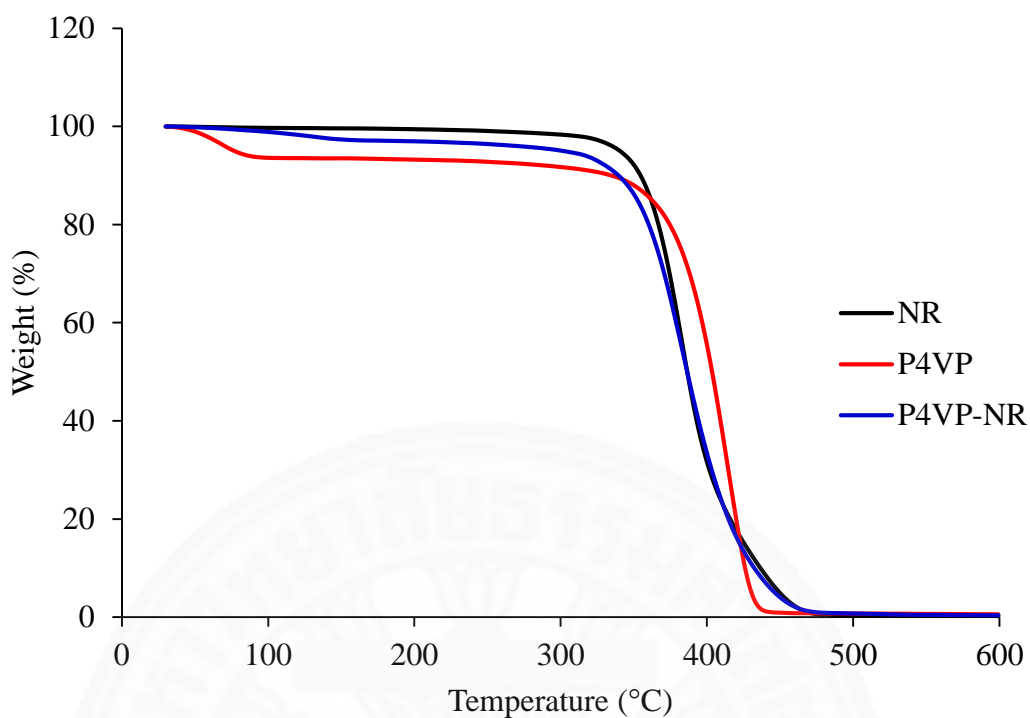
**Figure 43** Crosslink density as a function of (a) degree of swelling in toluene and (b) gel content, and (c) the degree of solvent swelling as a function of gel content.

## 4.1.6 Determination of thermal properties of P4VP-NR

### 4.1.6.1 Thermal Gravimetric Analysis (TGA)

The thermal stability as a decomposition temperature of the materials was measured by thermal gravimetric analyzer. The TGA thermograms of all samples are shown in Figure 44. The initial temperature of weight loss ( $T_i$ ), the final temperature of weight loss ( $T_f$ ), and the decomposition temperatures of the materials ( $T_d$ ) are shown in Table 10.

It was found that P4VP-NR was only slightly more thermally stable than NR, but both of them were obviously less stable than pure P4VP. In addition, the TGA thermogram of pure NR showed a single-step thermal decomposition at a range of 300-480 °C, whereas the P4VP and the P4VP-NR showed two-step thermal decompositions. The first step at below 150°C was attributed to the loss of moisture and possibly the remaining organic solvent. Moreover, the second-step at the higher temperatures, which started to lose weight at about 300 °C, was related to the degradation temperature of natural rubber and P4VP. However, the decomposition temperatures of the polymers, which were determined from the intersection of two tangents at the onset of the decomposition temperatures, were found to be about 386 °C, 403 °C, and 388 °C for the NR, P4VP, and P4VP-NR, respectively. The results of P4VP and NR are corresponded to the previous work [119, 120].



**Figure 44** TGA thermograms of NR, P4VP and P4VP-NR (gel content = 63%).

**Table 10** Decomposition temperatures of P4VP-NR sample, in comparison with those of NR and P4VP.

Samples	Thermal degradation (°C)		
	$T_i^a$	$T_f^b$	$T_d^c$
NR	300	480	386
P4VP (1 <sup>st</sup> step)	50	110	72
(2 <sup>nd</sup> step)	300	460	403
P4VP-NR (1 <sup>st</sup> step)	50	150	110
(2 <sup>nd</sup> step)	300	490	388

<sup>a</sup>  $T_i$ : the initial temperature of weight loss

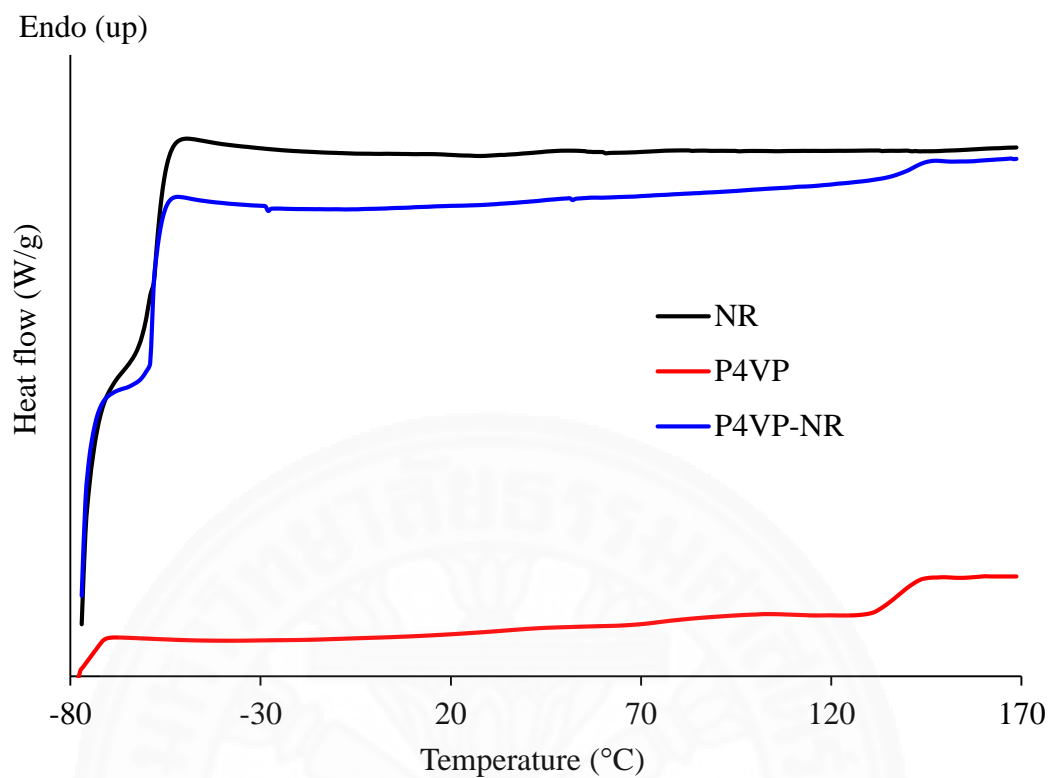
<sup>b</sup>  $T_f$ : the final temperature of weight loss

<sup>c</sup>  $T_d$ : the decomposition temperature, which determined from the intersection of two tangents at the onset of the decomposition temperatures

#### 4.1.6.2 Differential Scanning Calorimetry (DSC)

The glass transition temperature ( $T_g$ ) of the materials was examined by differential scanning calorimeter. The DSC thermograms of all samples are shown in Figure 45, and the  $T_g$ s value are shown in Table 11.

From DSC thermograms, it was found that the NR showed a single glass transition temperature at  $-58.9\text{ }^\circ\text{C}$ , which is higher than those reported in the previous studies. They reported the truly  $T_g$  of NR around  $-65\text{ }^\circ\text{C}$  [18, 116] and  $-70\text{ }^\circ\text{C}$  [17]. These differences of  $T_g$  values might be due to many reasons, including the difference in sample preparation, the molecular weight of measured polymer, the pretreatment, and the measuring conditions used. Meanwhile, the P4VP-NR gave two different  $T_g$  values in which the first at  $-57.8\text{ }^\circ\text{C}$  is related to NR. The other one at  $140.5\text{ }^\circ\text{C}$  corresponded to P4VP, because the pristine P4VP has a  $T_g$  closely located at  $137.2\text{ }^\circ\text{C}$  [121]. This suggested that the obtained material still consists of two phase regions including NR and P4VP phases. However, the higher shift of  $T_g$  values of both NR and P4VP phases in the P4VP-NR sample was possibly due to the crosslinked structure restricting the mobility of polymer chains, so it required the higher temperature to phase transition.



**Figure 45** DSC thermograms of NR, P4VP and P4VP-NR (gel content = 63%).

**Table 11** Glass transition temperatures ( $T_g$ ) of P4VP-NR sample, in comparison with those of NR and P4VP.

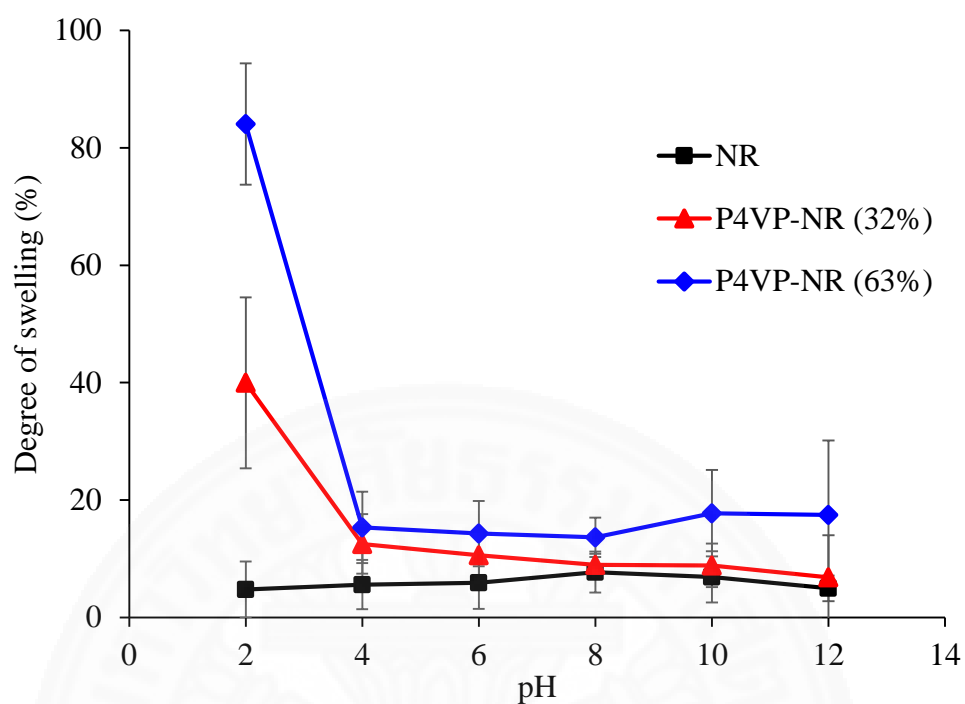
Samples	Transition temperature (°C)	
	1 <sup>st</sup> $T_g$	2 <sup>nd</sup> $T_g$
NR	-58.9	-
P4VP	137.2	-
P4VP-NR	-57.9	140.5

#### 4.1.7 Determination of pH responsiveness of P4VP-NR

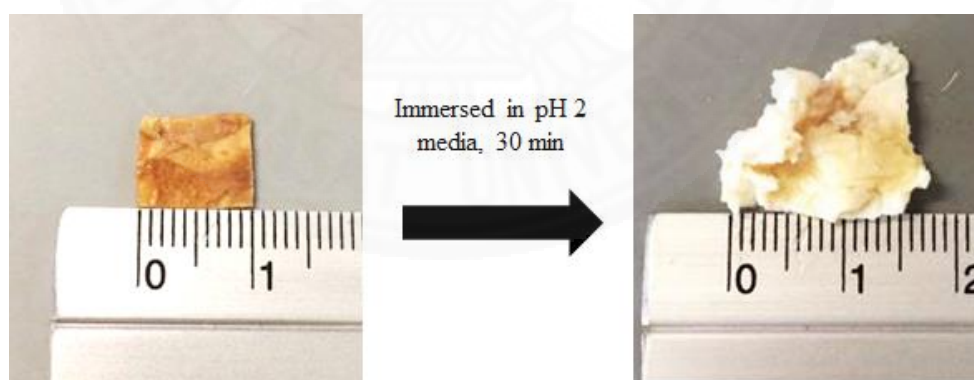
##### 4.1.7.1 The water swelling of P4VP-NR in pH solutions

The pH responsiveness of NR and P4VP-NR were investigated *via* the water swelling experiment. The experiment was carried out by immersing the samples in an aqueous solutions of a pH range from 2 to 12 for 24 h.

As shown in Figure 46, it was found that P4VP-NR became more swollen than the pristine NR due to the presence of hydrophilic 4-vinylpyridine unit. The P4VP-NR samples with highest swelling degree showed the hydrogel-like behavior as shown in Figure 47. By further considering the P4VP-NR samples (both of blue and red lines), it was observed that the degree of swelling obviously increased when the pH of the solution was below 4 whereas that of the NR sample did not change. From the obtained results, it can be explained by the followings. As pyridine is a weak base, in which the  $pK_a$  of its conjugate acid, pyridinium salt, is 4.7 [83]. When the pH of solution is below 4.7, pyridine is protonated and converted into pyridinium salt form, which contains a positive charge representing on their structure. Due to the electrostatic repulsion of their positive charges between the polymer chains, the materials become swollen. Another reason is that the presence of those ions led to an increasing the hydrophilicity of the materials, and as a result the materials could absorb more water. On the other hand, when the pH was increased above 4, the pyridine groups were deprotonated and become neutral, and accordingly the lower of swelling percentage was obtained. In addition, it was also found that the P4VP-NR sample with higher gel content (blue line) was more swollen than the sample with lower gel content (red line) because of the greater amount of P4VP (Figure 46).



**Figure 46** Degree of swelling (%) of NR and P4VP-NR (gel content = 34% and 63%) in aqueous solutions with different pH values.



**Figure 47** Swelling behavior of P4VP-NR (gel content = 63%) in aqueous solutions with pH 2 for 30 min.

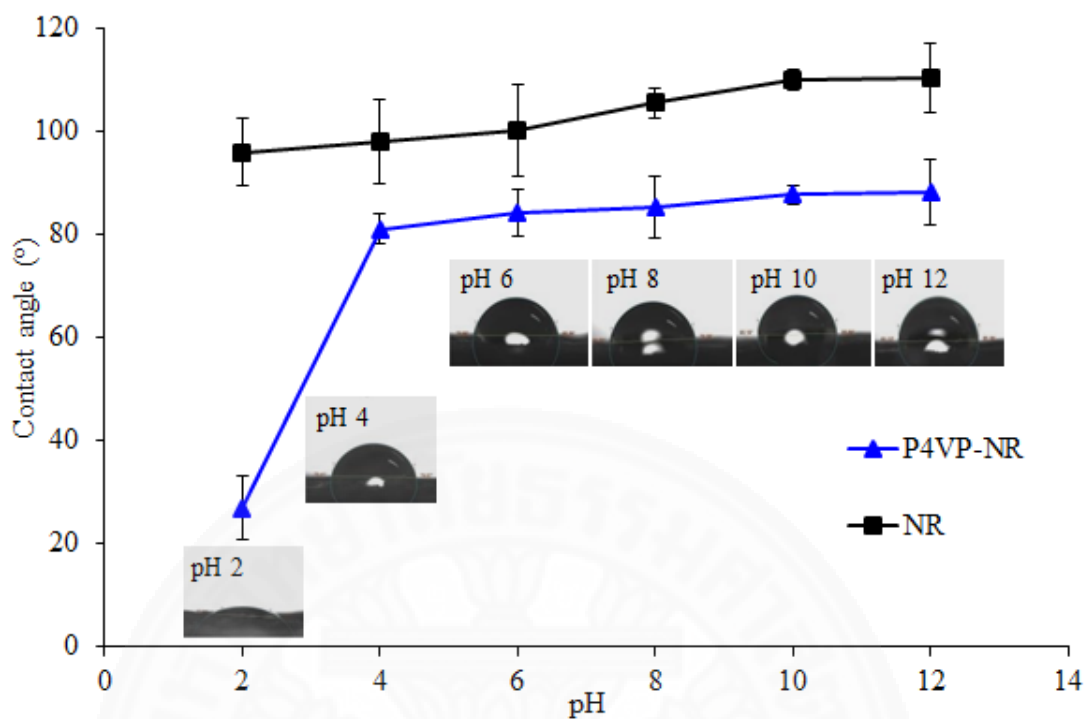
#### 4.1.7.2 The water contact angle of P4VP-NR

To confirm the pH responsiveness of the P4VP-NR, the samples were subsequently investigated by water contact angle measurement. The NR and P4VP-NR samples were immersed in a range of pH aqueous solutions from 2 to 12 for 24 h before measurement.

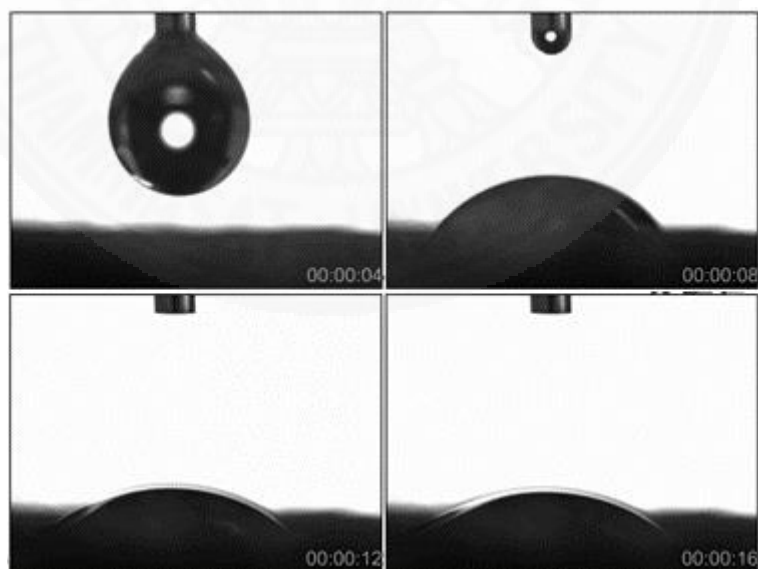
In Figure 48, it was found that the NR sample showed contact angles of around 95-110° through the pH range used in this experiment, consistent with the previous reports [9, 23]. The slight increase in contact angle was possibly due to the interaction with the surface protein or the non-rubber compositions of the latex [122]. In addition, the P4VP-NR samples showed an abrupt increase in contact angle from 28° to 80° when the pH was changed from 2 to 4, and the contact angles remained steady after that point. As mentioned earlier, since the positive charge of pyridine unit was generated when the pH of surroundings was below 4, the surface of the P4VP-NR became more polarity. Due to its high hydrophilicity, the water droplet gradually passed through the materials that wetted with pH 2 as shown in Figure 49. Consequently, a decrease in water contact angle and swelling behavior of P4VP-NR were obtained. Moreover, the affinity of water towards the P4VP-NR also indicated that the P4VP could improve the hydrophilicity of NR.

The result from water swelling experiment and water contact angle measurement confirmed that the obtained P4VP-NR was pH-responsive under acidic conditions in which the pH of surroundings is below 4.





**Figure 48** Water contact angles of NR and P4VP-NR (gel content = 63%) at different pH values.



**Figure 49** Water contact angles of P4VP-NR (gel content = 63%) sample after wetted with pH 2.

## **4.1.8 Demonstration of the pH responsive releasing behavior of P4VP-NR**

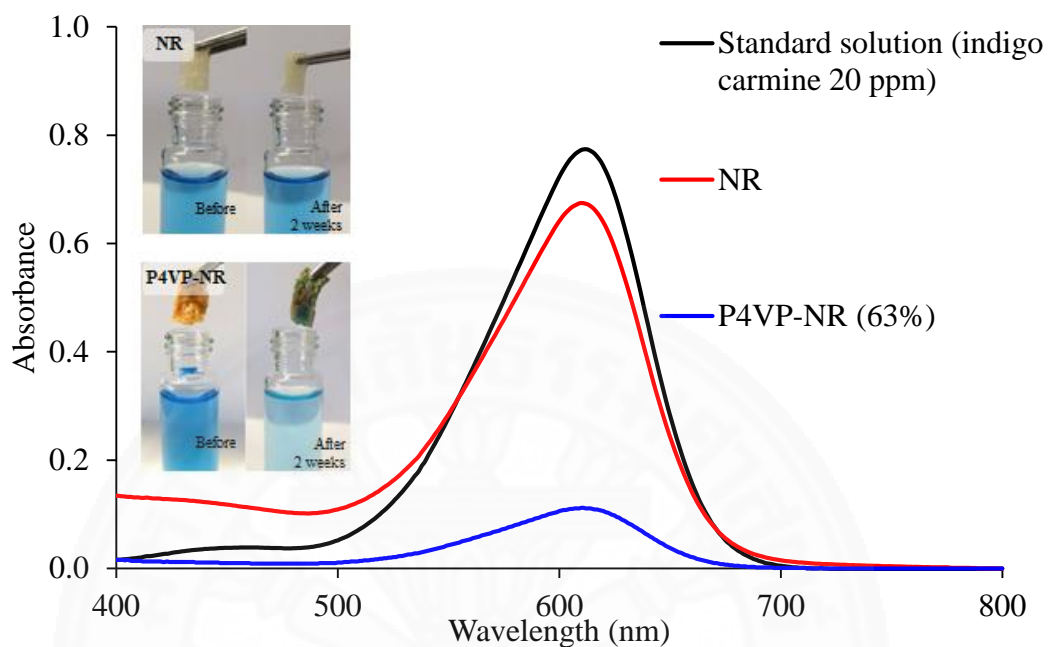
### **4.1.8.1 Study the controlled release of indigo carmine from the resultant products**

In order to demonstrate the pH responsive behavior and as responsive releasing materials, the absorption and desorption of indigo carmine dye from P4VP-NR and NR were studied. Indigo carmine was chosen to represent a water-soluble anionic drug. The samples were incubated in indigo carmine solution for two weeks at room temperature.

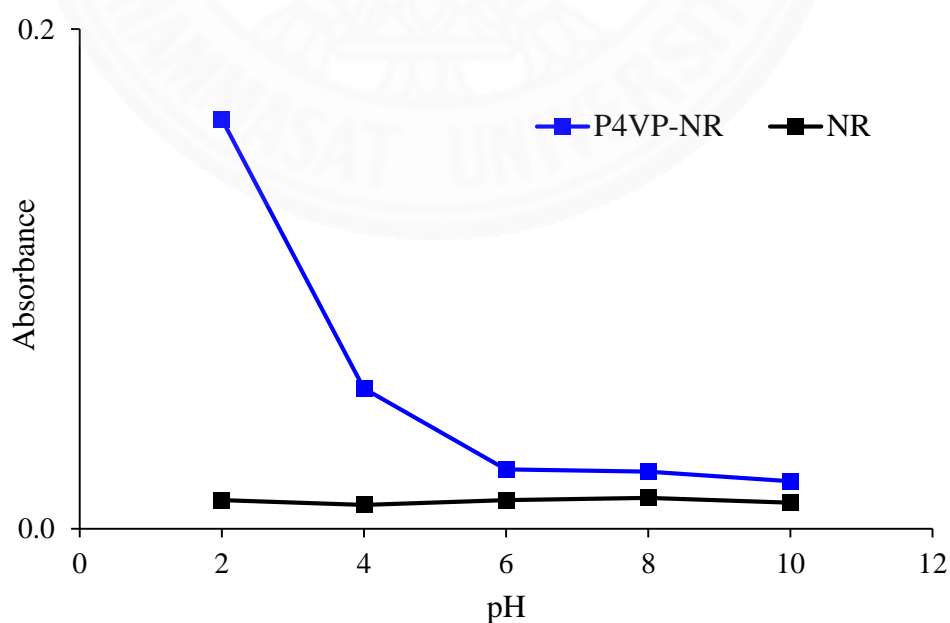
It was found that P4VP-NR could absorb more dye than NR, observing by an obvious reduction of absorbance intensity as shown in Figure 50. Based on this result, it suggested that the P4VP in the crosslinked material play a crucial role which affected the loading and releasing behaviors, because the nitrogen atom of pyridine ring unit interacted with indigo carmine molecules by hydrogen bonding interaction, leading to a greater decreasing of dye concentration.

After dye absorption, the samples were taken out, dried up and then immersed in aqueous solutions with different pH values from 2 to 10. The absorbance was measured to monitor the release of the indigo carmine. As shown in Figure 51, the absorbance of the NR samples did not change significantly as the pH was increased from 2 to 10, indicating that the NR was not pH responsive. For the P4VP-NR samples, more dyes were significantly released when the pH value of the solution were below 6. At a pH below 6 (pH<4.7), the dye release was possibly due to the material becoming highly protonated, leading to the chain elongation and straightening out to expand its polymer size. This event caused the loss of hydrogen bonding interactions of the entrapped indigo carmine at the external surface of P4VP-NR, and then the dye could be released after that [123]. Moreover, a large free volume that occurred from the expansion of the material was thereby allowed the water to diffuse in and out easily, as a result the occupying dye inside could be likewise taken away. At a pH above 6, the small amounts of dye release might result from the release of surface dye. In addition, dye release was also studied as a function of immersion time. As shown in Figure 52, when the immersion time was increased, the relative absorbance

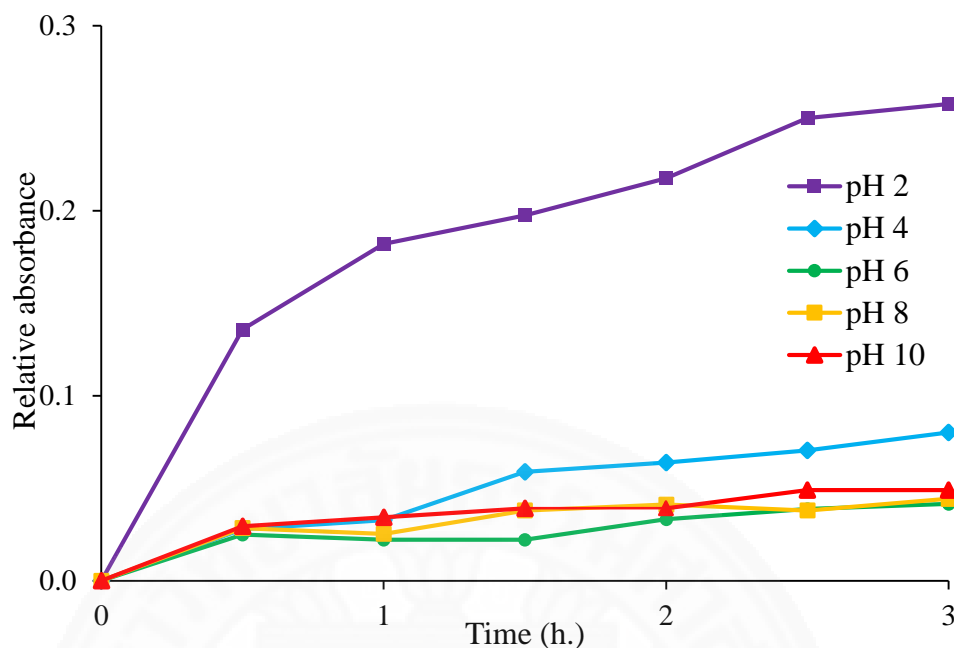
gradually increased. These pH response studies suggested that P4VP-NR material has potential applications in responsive drug release.



**Figure 50** UV-visible spectra of NR and P4VP-NR (gel content = 63%) after immersion in dye solutions compared with standard dye solution.



**Figure 51** Absorbance values of NR and P4VP-NR samples.



**Figure 52** Relative absorbance as a function of immersion time.

#### 4.1.9 Study of adsorption isotherms

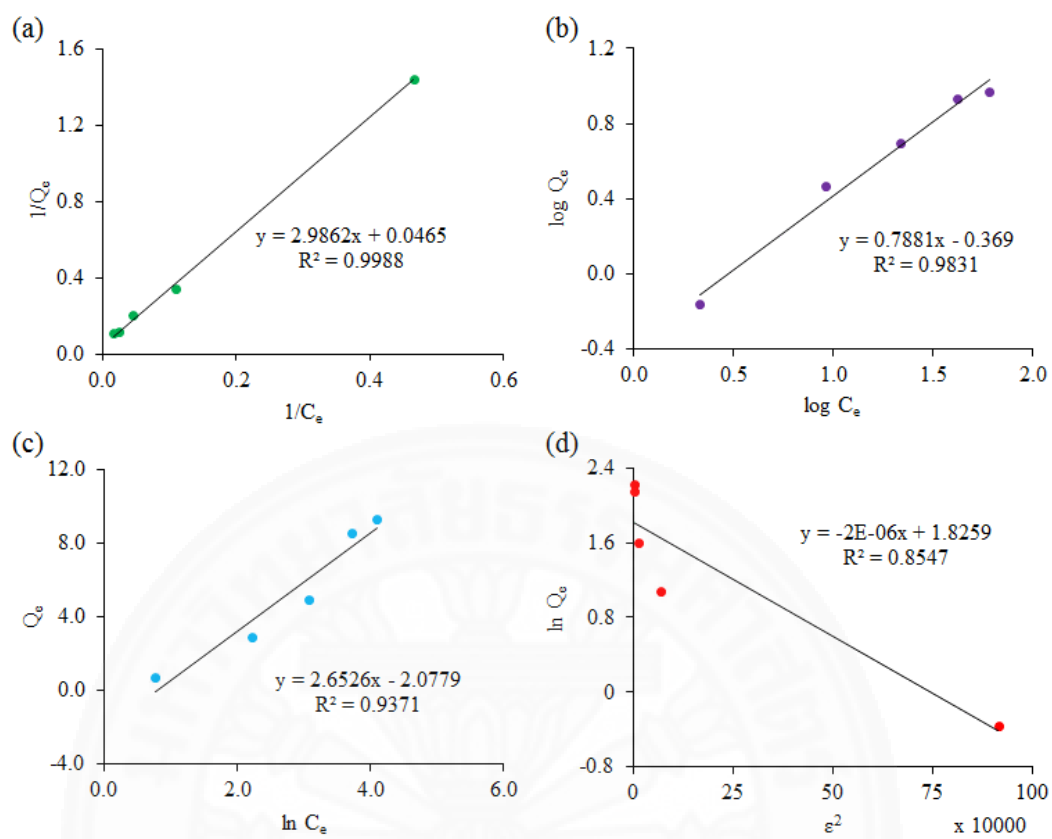
To predict the absorption process of indigo carmine (adsorbate) onto P4VP-NR (adsorbent), the adsorption isotherm was studied. In this work, the experimental data from adsorption study were analyzed using four models of adsorption isotherms which included the Langmuir, Freundlich, Temkin, and Dubinin-Radushkevich isotherms as shown in Figure 53, and the linear regression analysis was employed to determine the best fit of those theoretical models for the experimental data. Moreover, the characteristic parameters of all isotherms were subsequently clarified in Table 12.

From the linear regression analysis (Figure 53), it was found that the Langmuir adsorption isotherm represented the highest linear regression coefficient value ( $R^2=0.9988$ ) and hence the best fit model of experiment. This study indicates that the adsorption process of indigo carmine onto P4VP-NR likely took place as a monolayer adsorption with the maximum monolayer coverage capacity ( $Q_0$ ) of 21.51 mg/g. Since the assumption of Langmuir equation indicates the surface of adsorbent is

a homogeneous surface, so it can be further concluded that the P4VP-NR surface is homogeneously distribution of active sites [124]. In addition, the affinity of adsorption behaviors can be revealed by a dimensionless parameter ( $R_L$ ) that is also an evidence on adsorption mechanism. As presented in Table 12, the  $R_L$  value of this experiment was found to be in a range of 0-1 indicating the favorable adsorption process of the dye and P4VP-NR.

By considering to the other isotherms, it was found that the Freundlich, Temkin, and Dubinin-Radushkevich isotherms did not fit well to the experimental data when compared to the Langmuir isotherm. There were ranked as the second, third, and fourth order with respect to the linear regression coefficient ( $R^2$ ) values, respectively.

However, the characteristic parameters of the Freundlich can also be used to identify the favorability of adsorption process. It was found that the value of adsorption intensity ( $n$ ) from the Freundlich isotherm is larger than 1 (1.27), indicating that the adsorption of dye onto P4VP-NR is favorable. Additionally, the value of mean sorption energy ( $E$ ) from Dubinin-Radushkevich isotherm gives information about chemical and physical adsorption. In Table 12, the  $E$  value (0.5 kJ/mol) is found to be less than 8 kJ/mol, revealing that the type of adsorption of indigo carmine on P4VP-NR was a physical adsorption.



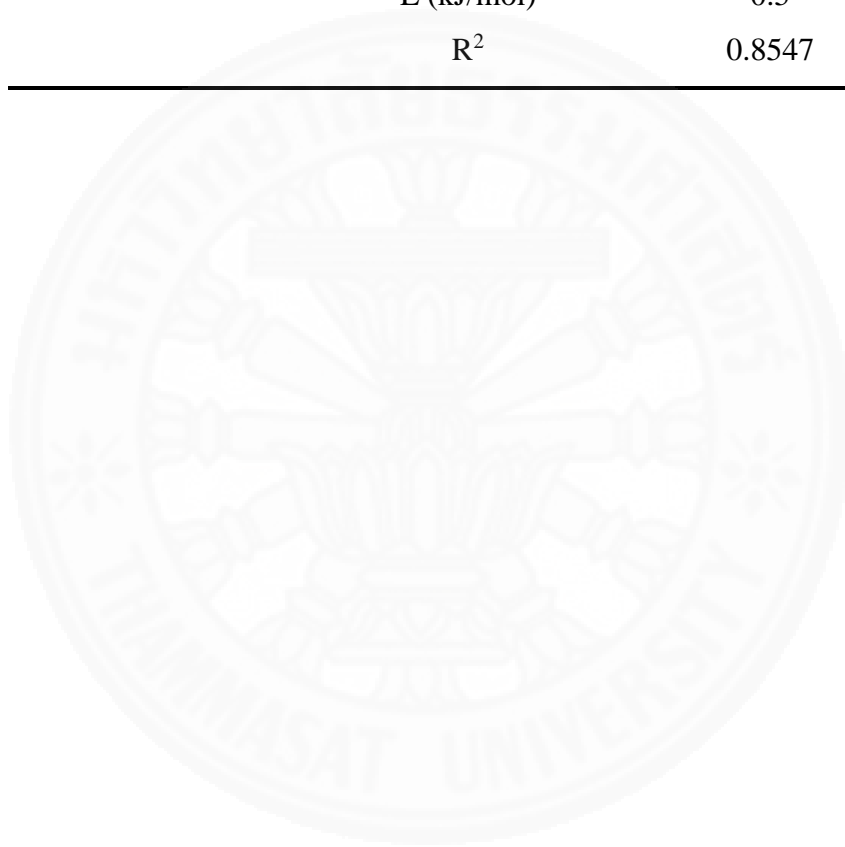
**Figure 53** Linear adsorption isotherms based on (a) Langmuir, (b) Freundlich, (c) Temkin, and (d) Dubinin-Radushkevich models.

**Table 12** Langmuir, Freundlich, Temkin and Dubinin-Radushkevich isotherm constants for the adsorption of indigo carmine onto P4VP-NR.

Adsorption Isotherm Models	Parameters	The constant values from Linear transform
Langmuir	$Q_0$ (mg/g)	21.51
	$K_L$ (L/mg)	0.02
	$R_L$	0.2 - 0.9
	$R^2$	0.9988
Freundlich	$1/n$	0.781
	$n$	1.27
	$K_f$ (mg/g)	0.428

	$R^2$	0.9831
Temkin	$A_T$ (L/mg)	0.457
	$b_T$	943.42
	B	2.653
	$R^2$	0.9371
Dubinin-Radushkevich	$q_s$ (mg/g)	6.208
	$K_{ad}$ (mol <sup>2</sup> /J <sup>2</sup> )	$2 \times 10^{-6}$
	E (kJ/mol)	0.5
	$R^2$	0.8547

---



## 4.2 Synthesis and characterizations of 4VP-grafted DPNR (4VP-g-DPNR)

### 4.2.1 Preparation of deproteinized natural rubber latex

Prior to grafting reaction, the NR latex was deproteinized for removing the surrounding proteins in order to increase grafting efficiency on the reaction. In this work, the DPNR latex was prepared using urea treatment and surfactant washing, respectively. After preparation, the total nitrogen content of the as-prepared DPNR latex was evaluated using the CHN elemental analyzer, and the obtained data have been reported as shown in Table 13.

It was found that total nitrogen content of the DPNR decreased to approximately 50 %, compared with untreated NR. Generally, the urea is often used to denature the proteins by forming interaction such as hydrogen bonding with proteins leading to a changing of their conformation. As expected, if the interaction between the surrounding proteins and the rubber particles are only the physical interaction, it may be possible to remove the proteins from NR latex after denaturation the proteins [44]. From the obtained results, most of surrounding proteins are bound to the rubber particles by a weak attraction force, which can be discharged by denaturation with urea. Moreover, the proteins are also solubilized with SDS from the surfactant washing process [125], as a result the proteins could be effectively separated from the rubber phase after centrifugation. Therefore, it can be noted that the urea and SDS were able to remove protein from fresh NR latex, corresponding to the previous reports [44-45, 58].

**Table 13** The C, H, and N data of NR and DPNR.

Sample Name	Composition (%w/w)		
	Carbon	Hydrogen	Nitrogen
NR	84.79	12.68	0.76
DPNR	84.19	12.88	0.43

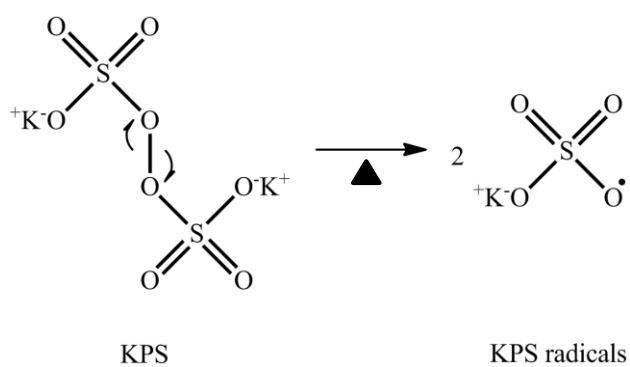


### 4.2.2 Preparation of 4VP-grafted DPNR

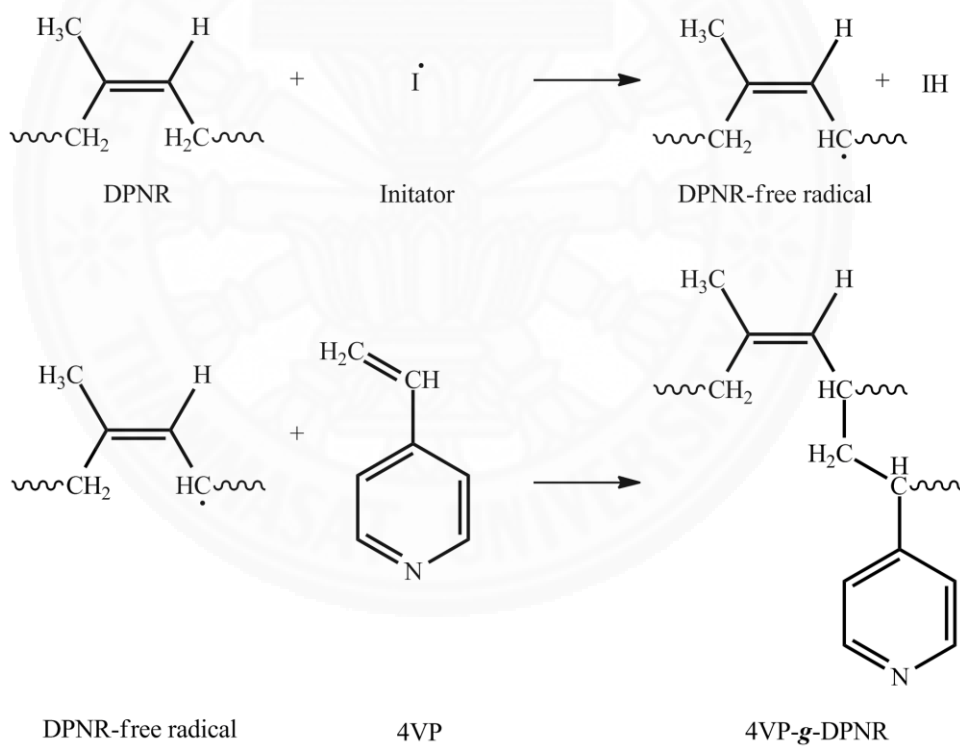
In this approach, the graft copolymerization of 4VP onto natural rubber was performed *via* an emulsion polymerization method which started from the 4VP monomer and DPNR latex. This method was carried out in a latex or water medium in which the potassium persulfate (KPS) and sodium dodecyl sulfate (SDS) were employed as an initiator and emulsifier, respectively.

Although many types of initiators have reported for using in grafting of natural rubber. The KPS is an effective water soluble initiator. We believe that if it can dissolve well in a water medium, it will disperse well in the reaction mixture. As a result, the use of KPS may possibly promote the graft copolymerization between DPNR and 4VP. Moreover, from the experimental, it was found that only KPS has given the successful reaction and higher grafting ratio compared with the other initiators such as couple of CHP/TEPA, AIBN and BPO, which did not dissolve well in water at the same conditions.

Normally, it is commonly known that the KPS thermally dissociates to generate free radicals as shown in Figure 54. Those free-radicals usually reacted with the surface of DPNR particles at the  $\alpha$ -methylenic hydrogen atom *via* hydrogen abstraction processes to give polyisoprene radicals [19, 126]. The polyisoprene radicals then reacted with 4VP monomer during propagation to obtain 4VP-*g*-DPNR. The proposed mechanism is presented in Figure 55. During the reaction, the change of color was observed as the reaction mixture turned from white latex to orange latex due to the color of propagating P4VP.



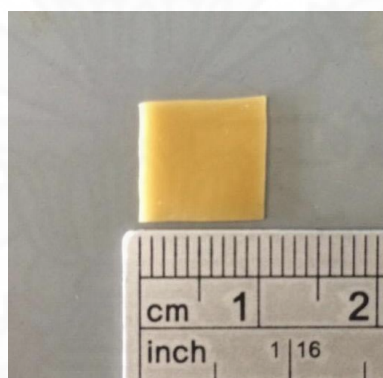
**Figure 54** Thermal decomposition of potassium persulfate.



**Figure 55** The proposed mechanism of the grafting reaction between 4VP and DPNR.

After the reaction, the soxhlet extraction with acetone was chosen to purify the grafted materials because it can remove any residue of ungrafted 4VP monomer or P4VP homopolymer, which could be observed from a decrease in the grafting ratio after extraction. The photograph of the obtained 4VP-*g*-DPNR was taken, presenting a yellowing solid rubber as shown in Figure 56.

In this approach, the use of NR latex and emulsion polymerization method has some advantages. Although it requires many of chemical substances to carry out the reaction, but this reaction proceed in the water medium which is an environmental friendly and low cost solvent. Another advantage is that the water shows an excellent heat transfer that will prevent the problem of heat accumulation in the system, suitable for the industrial scale. The functionalized product was subsequently investigated using FT-IR, XPS, and  $^1\text{H-NMR}$  techniques.



**Figure 56** Photograph of 4VP-*g*-DPNR. Sample size is approximately 1x1 cm<sup>2</sup>.

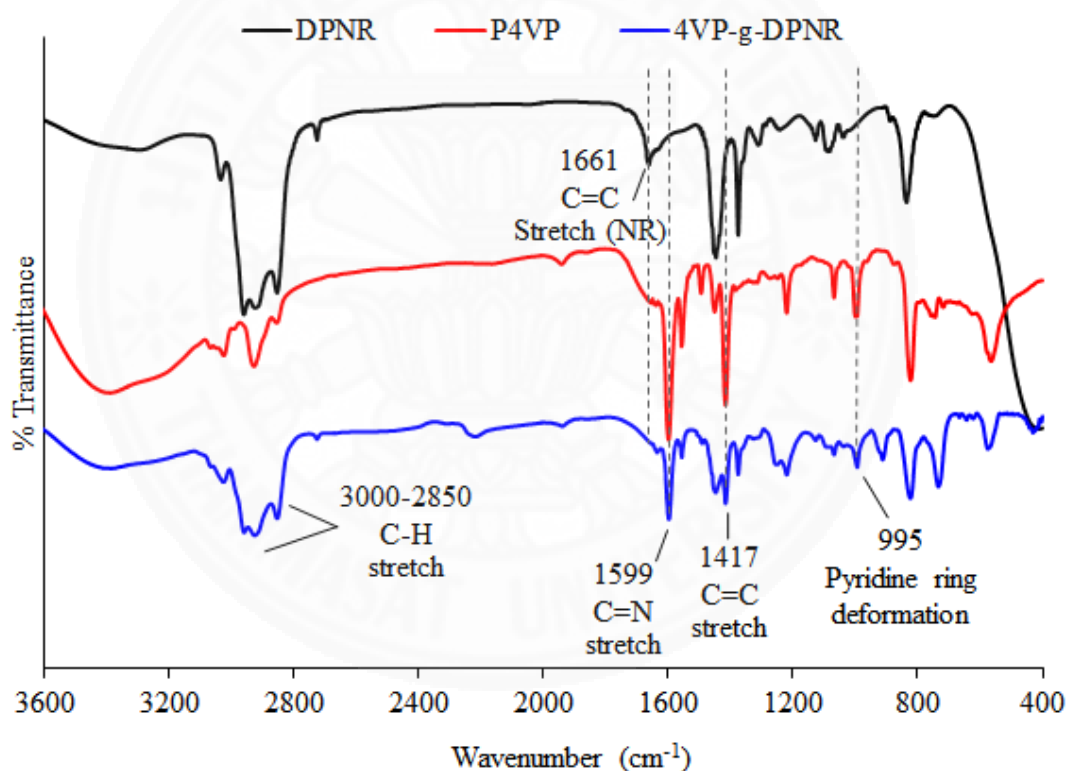
#### 4.2.3 FT-IR characterization of 4VP-*g*-DPNR

The FT-IR technique was used to investigate the functional groups and chemical structure of the grafted materials. The comparison of the characteristic IR absorption bands of all samples at a specific wavenumber (cm<sup>-1</sup>) was shown in Table 14.

In Figure 57, after purification process, the 4VP-*g*-DPNR sample still showed the signatures of both P4VP and DPNR. The important characteristic bands for the grafted material appeared at 1599 cm<sup>-1</sup>, 1417 cm<sup>-1</sup>, and 995 cm<sup>-1</sup>, corresponding to

C=N, C=C, and pyridine ring deformation of 4VP unit, respectively [27]. Meanwhile, the signal at  $3000\text{--}2850\text{ cm}^{-1}$ ,  $1451\text{ cm}^{-1}$ ,  $1377\text{ cm}^{-1}$ , and  $827\text{ cm}^{-1}$  corresponded to  $\text{CH}_3$  stretching,  $\text{CH}_2$  bending,  $\text{CH}_3$  bending, and  $\text{CH}_2$  wagging of the polyisoprene unit, respectively. This result suggested that the grafting process of 4VP onto DPNR was successfully achieved.

Furthermore, the decrease in characteristic band at  $1661\text{ cm}^{-1}$  consistent with C=C stretching of NR after grafting process suggested that this reaction could likely occur *via* the addition reaction at the double bond of the DPNR backbone as well as the abstraction reaction took place.



**Figure 57** FT-IR spectra of DPNR (black line), P4VP (red line), and 4VP-g-DPNR (grafting ratio = 45%) (blue line).

**Table 14** The comparison of the characteristic IR absorption bands of DPNR, P4VP, and 4VP-*g*-DPNR at a specific wavenumber ( $\text{cm}^{-1}$ ).

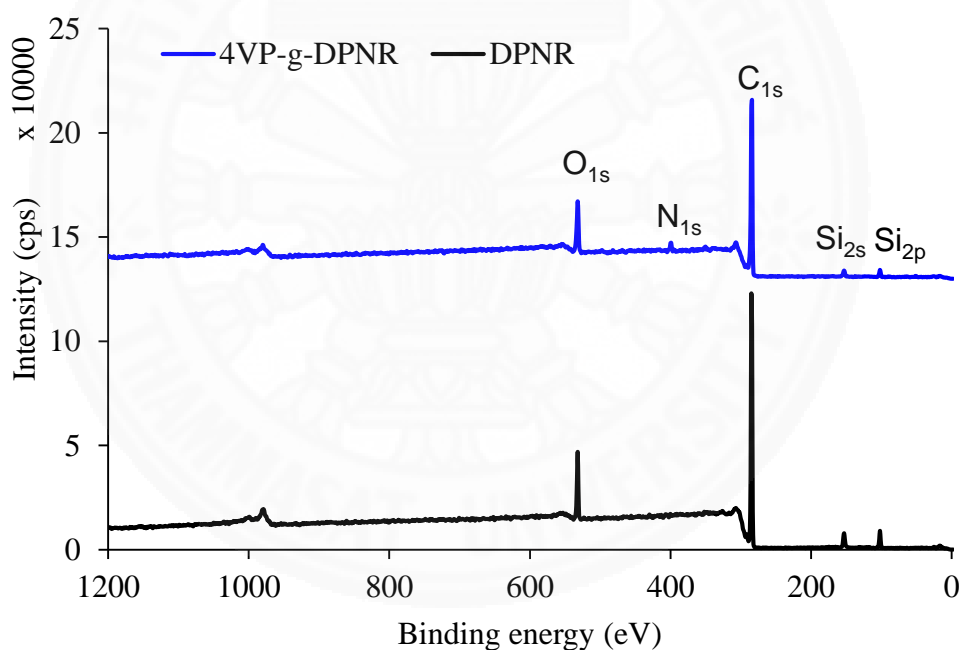
Type of bonds	Wavenumber ( $\text{cm}^{-1}$ )		
	DPNR	P4VP	4VP- <i>g</i> -DPNR
O-H stretching (broad, moisture)	3600-3300	3600-3300	3600-3300
N-H stretching (protein)	3360	-	N/A
=C-H stretching	3037	3034	2995
CH <sub>3</sub> asymmetric stretching	2960	2927	2932
CH <sub>2</sub> asymmetric stretching	1917	N/A	1948
CH <sub>2</sub> symmetric stretching	2851	2854	2851
C=C stretching	1661	-	weak
CH <sub>2</sub> scissoring	1472	1452	1451
CH <sub>3</sub> asymmetric deformation	1376	-	1376
CH <sub>2</sub> wagging	1308	-	1312
CH <sub>2</sub> twisting	1261	N/A	1272
CH <sub>2</sub> wagging	1126	N/A	N/A
C-CH <sub>2</sub> stretching	1093	1069	1070
C-CH <sub>3</sub> stretching	1040	N/A	N/A
CH <sub>3</sub> rocking	927	N/A	924
CH <sub>3</sub> wagging	890	N/A	854
=C-H wagging	838	824	824
CH <sub>2</sub> rocking	745	744	733
C=C stretching of aromatic pyridine ring	-	1604	1599
C=N stretching of aromatic pyridine ring	-	1417	1417
Pyridine ring deformation	-	1000	995

\*N/A means not available

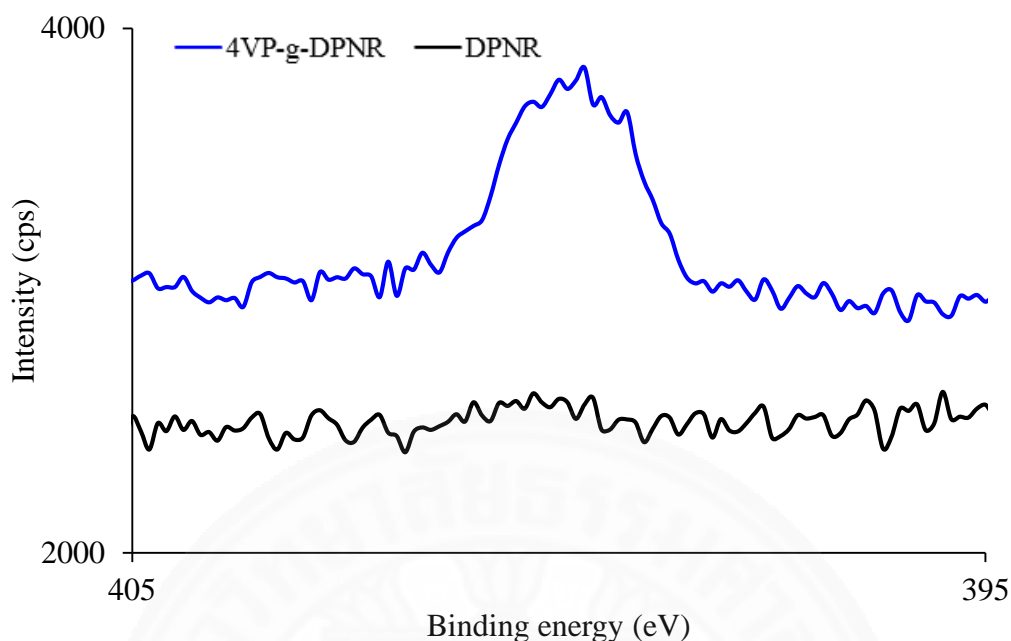
#### 4.2.4 XPS characterization of 4VP-*g*-DPNR

In addition, the elemental compositions at the surface of the grafted material were also evaluated using an XPS technique.

Figure 58 showed the XPS wide scan spectra of all samples. It was found that signals of O<sub>1s</sub>, C<sub>1s</sub>, Si<sub>2s</sub>, and Si<sub>2p</sub> were found in both NR and 4VP-*g*-DPNR. The carbon signal came from the intrinsic hydrocarbon polymeric material, and the silicon signal resulted from the sample preparation for measurement. However, an appearance of a nitrogen signal at 399 eV of the grafted material (Figure 59) suggested that the 4VP had been grafted onto the DPNR [127]. The results both of FTIR and XPS were similar to the as-prepared crosslinked material.



**Figure 58** XPS survey scan spectra of DPNR and 4VP-*g*-DPNR (grafting ratio = 45%).

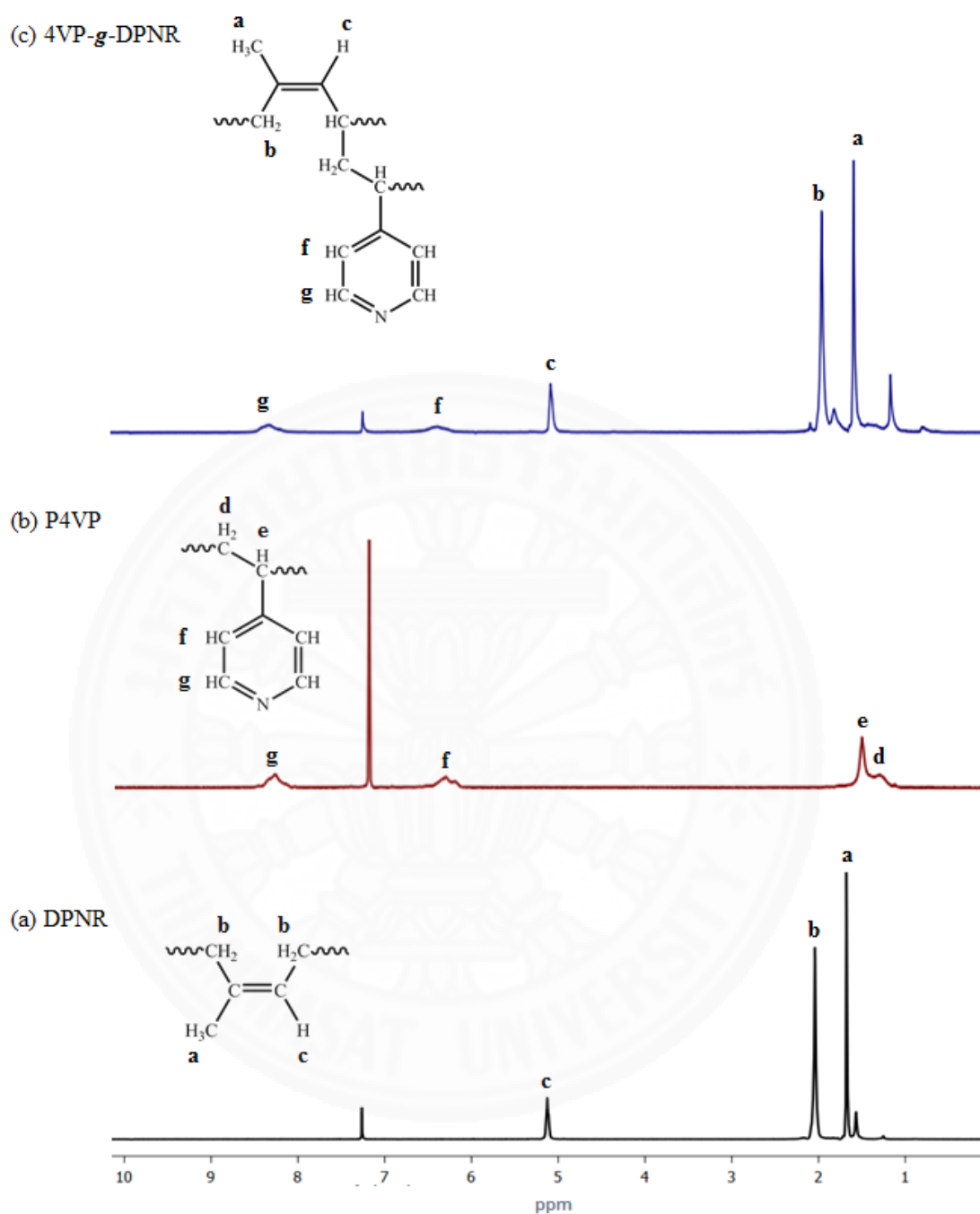


**Figure 59** XPS high-resolution spectra of  $N_{1s}$  region of DPNR and 4VP-*g*-DPNR (grafting ratio = 45%).

#### 4.2.5 $^1\text{H-NMR}$ characterization of 4VP-*g*-DPNR

The  $^1\text{H-NMR}$  technique was used to characterize the graft copolymer and calculate the grafting efficiency. The  $^1\text{H-NMR}$  spectra of DPNR, P4VP, and 4VP-*g*-DPNR are shown in Figure 60. It was found that the characteristic peak of 4VP-*g*-DPNR (Figure 59c) appeared at 1.7, 2.0 and 5.1 ppm, which were assigned to methyl ( $-\text{CH}_3$ ), methylene ( $-\text{CH}_2-$ ), and unsaturated methyne ( $=\text{C-H}$ ) protons of isoprene units, respectively. Moreover, broad signals at around 6.5 and 8.5 ppm were attributed to the aromatic protons of the pyridine ring units [108].

Therefore, the results of FT-IR, XPS, and  $^1\text{H-NMR}$  on 4VP-*g*-DPNR sample indicated that the 4VP was successfully grafted onto the DPNR backbone *via* an emulsion polymerization process.



**Figure 60**  $^1\text{H-NMR}$  spectra of (a) DPNR, (b) P4VP, and (c) 4VP-*g*-DPNR (grafting ratio = 45%)



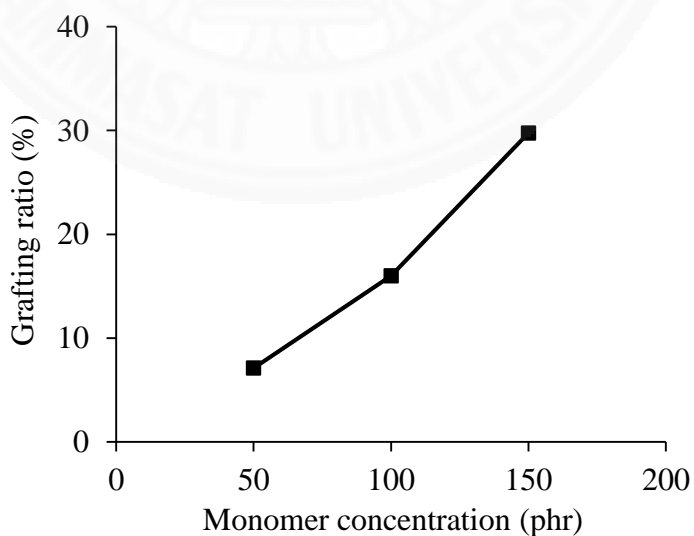
#### 4.2.6 Effect of influential parameters on grafting ratio

In this study, the effects of reagent concentrations and reaction conditions on grafting ratio were evaluated.

##### 4.2.6.1 Effect of 4VP concentration

At first, to study the effect of 4VP concentration on the grafting ratio (%GR) of the grafting reaction, the 4VP monomer concentration was varied from 50 to 150 phr, while the concentration of other reagents and reaction conditions were kept constant in which a 10 phr of KPS concentration, 10 phr of emulsifier concentration, 3 hours of reaction time, and 90 °C of reaction temperature were employed.

Figure 61 showed the grafting ratio as a function of 4VP concentration. It was found that increasing of 4VP concentration led to an increase in the grafting ratio. When the 4VP concentration was increased from 50 to 150 phr, the grafting ratio also increased from 7.11% to 29.76%. From this result, it can be explained that the higher amounts of monomer concentration might increase the probability of reaction with the active sites of the macroradicals of DPNR [20].

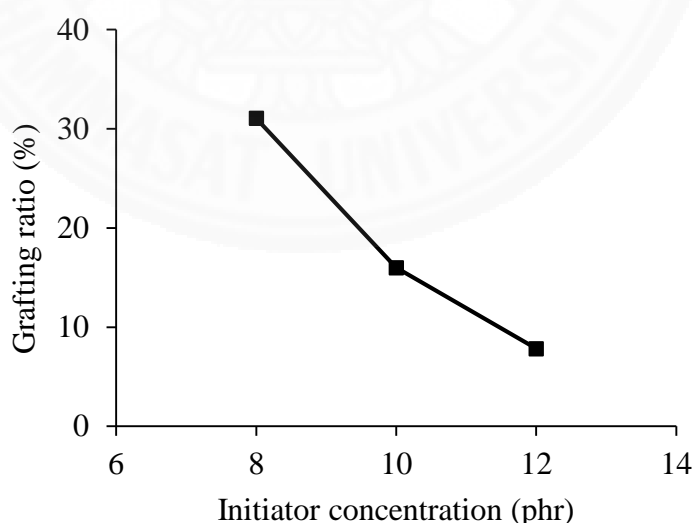


**Figure 61** Grafting ratio as a function of 4VP concentration.

#### 4.2.6.2 Effect of KPS concentration

The effect of KPS or initiator concentration on the grafting ratio (%GR) was also studied. The reaction was carried out by varying the concentration of KPS from 8 to 12 phr. Meanwhile, the concentration of other reagents and reaction conditions were kept constant in which a 100 phr of 4VP concentration, 10 phr of emulsifier concentration, 90 °C of reaction temperature and 3 hours of reaction time were used.

From Figure 62, it was observed that when the KPS concentration was increased from 8 to 12 phr, the grafting ratio substantially decrease from 31.05% to 7.84%. As expected, at the higher concentration of initiator, a plenty of active sites on DPNR could be generated as well as in the 4VP monomer, due to the higher level of produced free radicals. However, it is possible that only 4VP free radicals preferentially reacted with themselves and produce an only free homopolymer rather than grafting onto DPNR backbone [128]. Moreover, the excess amount of free radical concentration can cause a termination reaction which led to the depletion of active species, and hence the grafting ratio did not increase at the higher of initiator concentration [20].

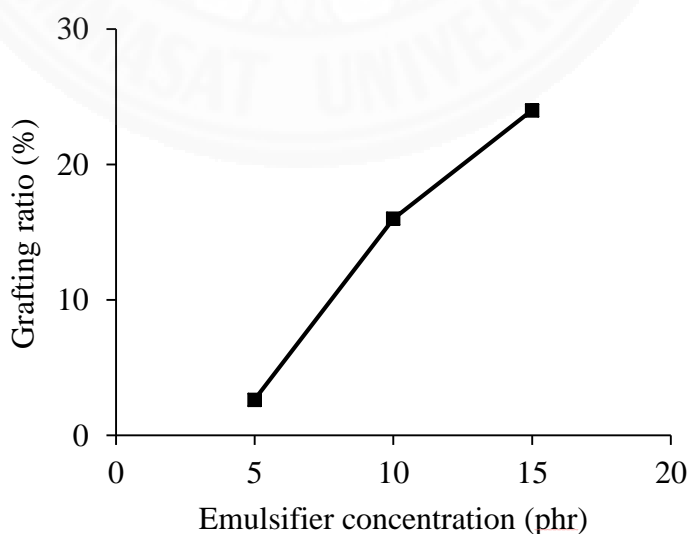


**Figure 62** Grafting ratio as a function of KPS concentration.

#### 4.2.6.3 Effect of emulsifier concentration

It is well known that the emulsifier is an essential parameter in an emulsion polymerization method, so the effect of emulsifier concentration, SDS, on the grafting ratio (%GR) was then investigated. The reaction was carried out by varying the concentration of SDS from 5 to 15 phr, while the concentration of other reagents and reaction conditions were kept constant in which a 100 phr of 4VP concentration, 10 phr of KPS concentration, 90 °C of reaction temperature and 3 hours of reaction time were used.

Figure 63 presented the grafting ratio as a function of emulsifier concentration. It was found that increasing emulsifier concentration resulted in an increase in the grafting ratio. As the emulsifier concentration was increased from 5 to 15 phr, the grafting ratio continually increased from 2.63% to 24.01%. From this result, it can be indicated that the adding of SDS to the system is not only to maintain the colloidal stability of the rubber particles for preventing the early event of coagulation during the reaction, but also to increase a possibility to form micelles. Thus, a poor water-soluble monomer such a 4VP can be dispersed well in water phase in the presence of emulsifier, and they will reach extensively to the active sites on the DPNR backbone, leading to higher grafting ratio.

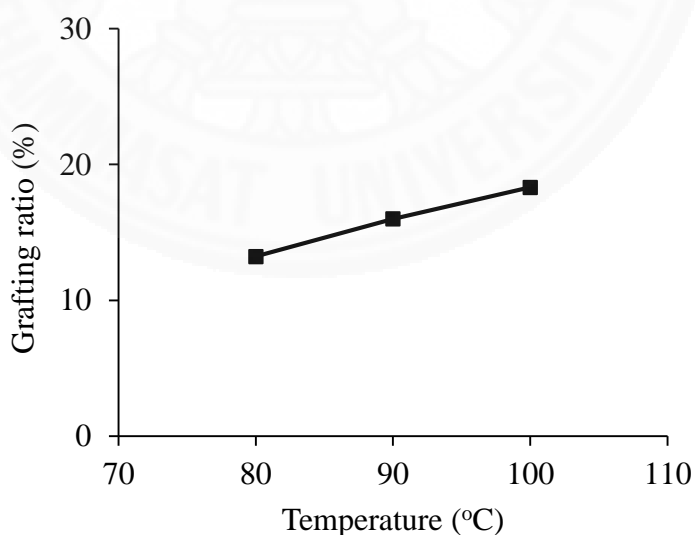


**Figure 63** Grafting ratio as a function of emulsifier concentration.

#### 4.2.6.4 Effect of reaction temperature

The effect of reaction temperature on the grafting ratio (%GR) was subsequently studied. The reaction was carried out by varying the temperature in a range of 80-100 °C. Meanwhile the reagent concentrations and reaction time were kept constant in which a 100 phr of 4VP concentration, 10 phr of KPS concentration, 10 phr of emulsifier concentration, and 24 hours of reaction time were employed.

As shown in Figure 64, it was found that when the reaction temperature was increased from 80 to 100 °C, which is an optimum working range for potassium persulfate (KPS), the grafting ratio increased from 13.22% to 18.32%. This result indicated that increasing the reaction temperature increased the grafting ratio. In fact, the reaction temperature is an essential parameter which significantly affects the rate of decomposition of an initiator. At higher reaction temperatures, more free radicals were produced, and those of produced free radicals could transfer to react with 4VP monomer and DPNR backbone to generate active sites or macroradicals. As a result, there was a greater possibility to proceed a graft copolymerization of 4VP onto DPNR backbone.

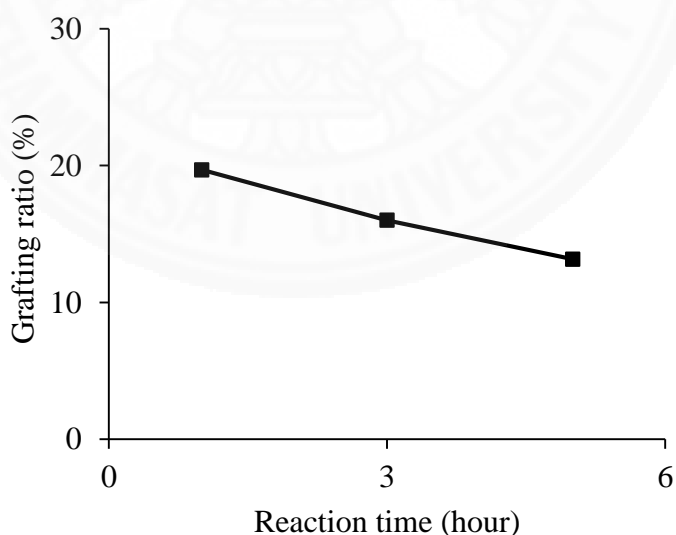


**Figure 64** Grafting ratio as a function of reaction temperature.

#### 4.2.6.5 Effect of reaction time

Finally, the effect of reaction time on the grafting ratio (%GR) was evaluated. The reaction was carried out by varying the reaction time in a range of 1-5 h. Meanwhile, the reagent concentrations and reaction temperature were fixed constant in which a 100 phr of 4VP concentration, 10 phr of KPS concentration, 10 phr of emulsifier concentration, and 90 °C of reaction temperature were employed.

It was found that when the reaction time was increased from 1 to 5 h, the grafting ratio gradually decreased from 19.69% to 13.16% as shown in Figure 65. For a prolonged reaction time, the competition between the polymerization of only 4VP and the grafting of 4VP onto DPNR backbone occurred in the system. Based on this result, the decrease in grafting ratio suggested that the free P4VP homopolymer was readily formed rather than grafting onto DPNR backbone. The reasons are possibly due to the limited active sites available on the DPNR backbone as well as the recombination of 4VP radical under the longer reaction time [19]. Furthermore, the use of high temperature (90 °C) and longer time for the reaction might lead to the degradation of the grafted product.



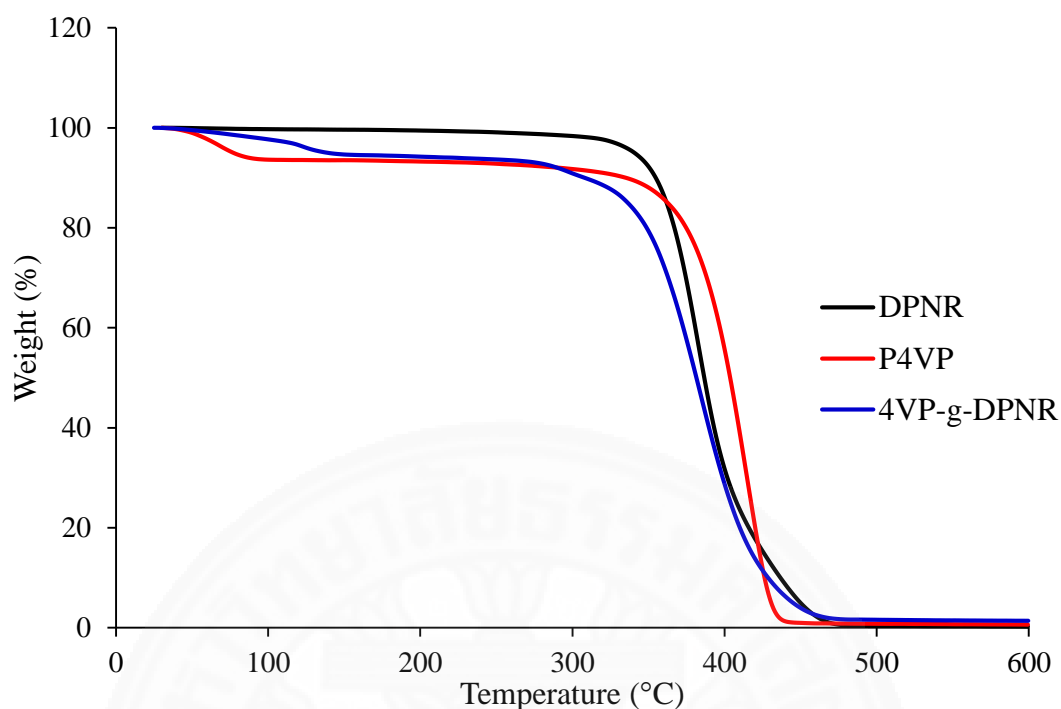
**Figure 65** Grafting ratio as a function of reaction time.

## 4.2.7 Determination of thermal properties of 4VP-*g*-DPNR

### 4.2.7.1 Thermal Gravimetric Analysis (TGA)

The thermal stability of the materials was measured to determine the decomposition temperature by using thermal gravimetric analyzer. The TGA thermograms of all samples are shown in Figure 66. The values of the initial temperature of weight loss ( $T_i$ ), the final temperature of weight loss ( $T_f$ ), and the decomposition temperatures of the materials ( $T_d$ ) are shown in Table 15.

It was found that 4VP-*g*-DPNR was slightly less thermally stable than DPNR. A single-step thermal decomposition at a range of temperature of 300-480 °C was observed in NR, whereas both the P4VP and the 4VP-*g*-DPNR showed several steps of thermal decompositions. For the P4VP, it has two-step thermal decompositions, resulting from the removal of moisture, remaining organic solvent and its polymer structure. For the grafted material, it has a three-step thermal decomposition in which the first step at below 160 °C was attributed to the loss of moisture and other impurities. Additionally, the second step and third step at the higher temperatures, which started to lose weight at about 300 °C, were expectedly due to the degradation of natural rubber and P4VP. However, the decomposition temperatures of the polymers, which were determined from the intersection of two tangents at the onset of the decomposition temperatures, were found to be about 385 °C, 403 °C, and 384 °C for the DPNR, P4VP, and 4VP-*g*-DPNR, respectively.



**Figure 66** TGA thermograms of DPNR, P4VP and 4VP-*g*-DPNR (grafting ratio = 45%).

**Table 15** Degradation temperatures of 4VP-*g*-DPNR sample, in comparison with those of DPNR and P4VP.

Samples	Thermal degradation (°C)		
	$T_i^a$	$T_f^b$	$T_d^c$
DPNR	300	490	385
P4VP (1 <sup>st</sup> step)	50	110	72
(2 <sup>nd</sup> step)	300	460	403
4VP- <i>g</i> -DPNR (1 <sup>st</sup> step)	100	160	130
(2 <sup>nd</sup> step)	256	318	304
(3 <sup>rd</sup> step)	318	490	386

<sup>a</sup>  $T_i$ : the initial temperature of weight loss

<sup>b</sup>  $T_f$ : the final temperature of weight loss

<sup>c</sup>  $T_d$ : the decomposition temperature, which determined from the intersection of two tangents at the onset of the decomposition temperatures

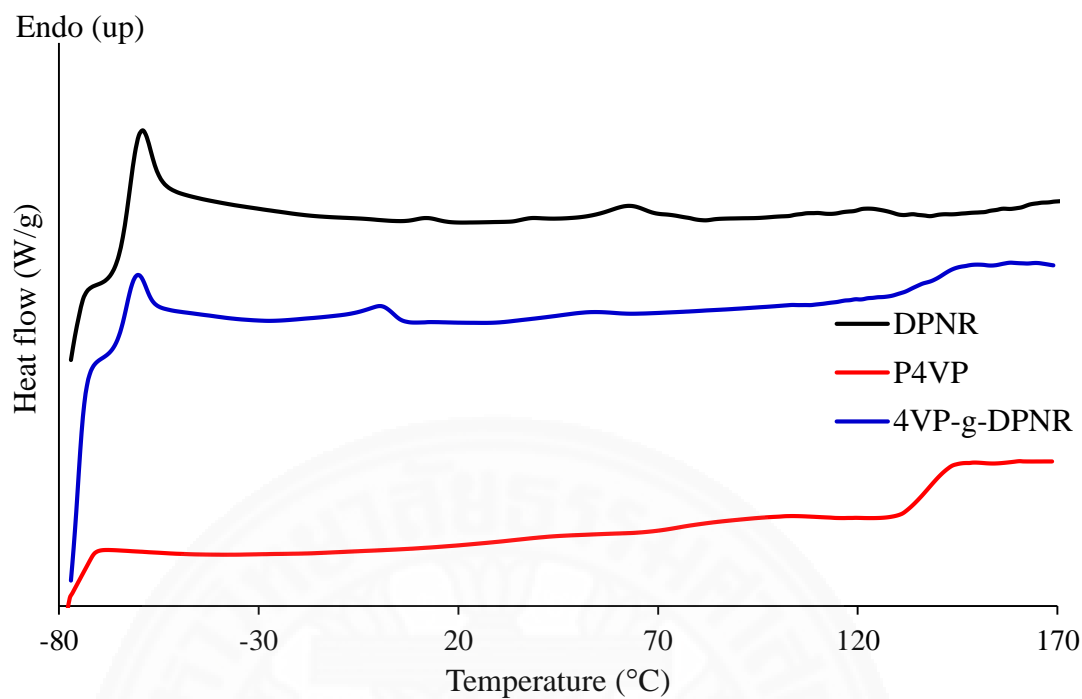
#### 4.2.7.2 Differential Scanning Calorimetry (DSC)

The glass transition temperature ( $T_g$ ) of the materials was examined by differential scanning calorimeter. The DSC thermograms of all samples are shown in Figure 67, and the  $T_g$  values are presented in Table 16.

From DSC thermograms, it was found that the pure DPNR and P4VP showed single glass transition temperatures at  $-63\text{ }^\circ\text{C}$  and  $137.2\text{ }^\circ\text{C}$ , respectively, which is slightly different from the previous reports. From those studies, they reported that the  $T_g$  of DPNR were around  $-61.8\text{ }^\circ\text{C}$  and  $-65\text{ }^\circ\text{C}$  [18, 116], and that of P4VP was around  $\sim 140\text{ }^\circ\text{C}$  [121]. The differences of  $T_g$  values might be caused by the different sample preparation methods, the molecular weight of polymer, the pretreatment before measurement, and the measurement conditions used. On the contrary, the 4VP-*g*-DPNR provided two different  $T_g$  values in which the first at  $-64.1\text{ }^\circ\text{C}$  was related to DPNR, and the other one at  $139.5\text{ }^\circ\text{C}$  expectedly corresponded to P4VP. This suggested that the grafted material consisted of two phase regions including DPNR and P4VP.

Although it is commonly known that the  $T_g$  of copolymer would be located between  $T_g$  values of both constituent homopolymers. However, some reports stated that the block or graft copolymers, which have an adequately long chain portion of their homopolymers, can possibly show their characteristic  $T_g$  for each polymers instead of exhibiting a new single value at the intermediate value [129]. Moreover, from the obtained result, the shift of the first  $T_g$  in the grafted material to the lower temperature indicated that the grafting of 4VP onto DPNR backbone may increase the free volume of the material, owing to the steric effect from the structure of P4VP unit.





**Figure 67** DSC thermograms of DPNR, P4VP and 4VP-*g*-DPNR (grafting ratio = 45%).

**Table 16** Glass transition temperature ( $T_g$ ) of 4VP-*g*-DPNR sample, in comparison with those of NR and P4VP.

Samples	Transition temperature (°C)	
	1 <sup>st</sup> $T_g$	2 <sup>nd</sup> $T_g$
DPNR	-63	-
P4VP	137.2	-
4VP- <i>g</i> -DPNR	-64.1	139.5

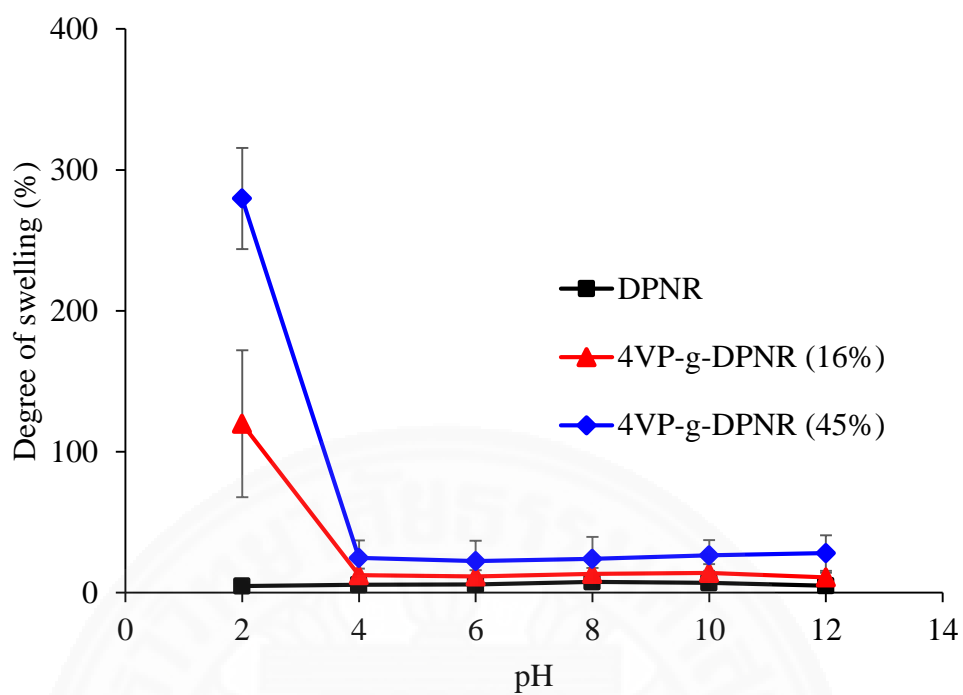
## 4.2.8 Determination of pH responsiveness of 4VP-*g*-DPNR

### 4.2.8.1 The water swelling of 4VP-*g*-DPNR in pH solutions

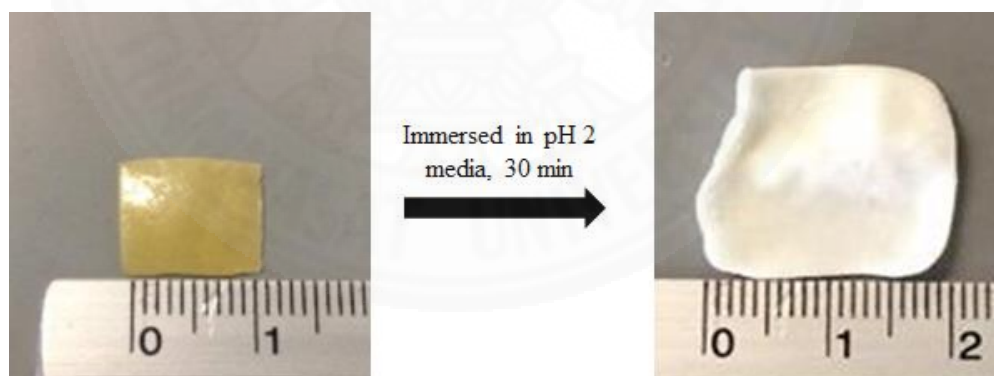
After the characterization parts, the pH responsiveness of DPNR and 4VP-*g*-DPNR with different grafting ratios were investigated *via* the water swelling experiment. The experiment was carried out by immersing the samples in an aqueous solutions of a pH range from 2 to 12 for 24 h.

In Figure 68, it was found that 4VP-*g*-DPNR became more swollen than the DPNR due to the presence of hydrophilic portion of 4-vinylpyridine unit as expected. In addition, the 4VP-*g*-DPNR sample with a higher grafting ratio (blue line) was found to be more swollen than the sample with a lower grafting ratio (red line). By further considering to the 4VP-*g*-DPNR samples (both of blue and red lines), it is noted that the degree of swelling (%) explicitly increased when the pH of the solution was below 4 while that of the DPNR sample did not change in any pH solutions. When the pH of solution was below 4.7, pyridine is protonated generating positive charges on their structure, resulting in the formation of electrostatic repulsion between the polymer chains. Hence, the materials became swollen, and also the increase in the hydrophilicity due to the presence of positive charges led to more water absorption of the materials. The swelling behavior of the 4VP-*g*-DPNR sample with a grafting ratio of 45% in a pH 2 solution was also observed by taking a photograph as shown in Figure 69.

Furthermore, when compared to the P4VP-NR sample, the 4VP-*g*-DPNR was found to be more swollen than that crosslinked product, even if the P4VP ratio with respect to NR is smaller than P4VP-NR. The reason is mainly due to the difference in their structures. The P4VP-NR is a crosslinked material which has a restriction between the polymer chains due to the network structure. Meanwhile, the polymer chains of grafted product is more flexible and freely to accommodate water molecules.



**Figure 68** Degree of swelling (%) of DPNR and 4VP-g-DPNR (grafting ratio = 16% and 45%) in aqueous solutions with different pH values.

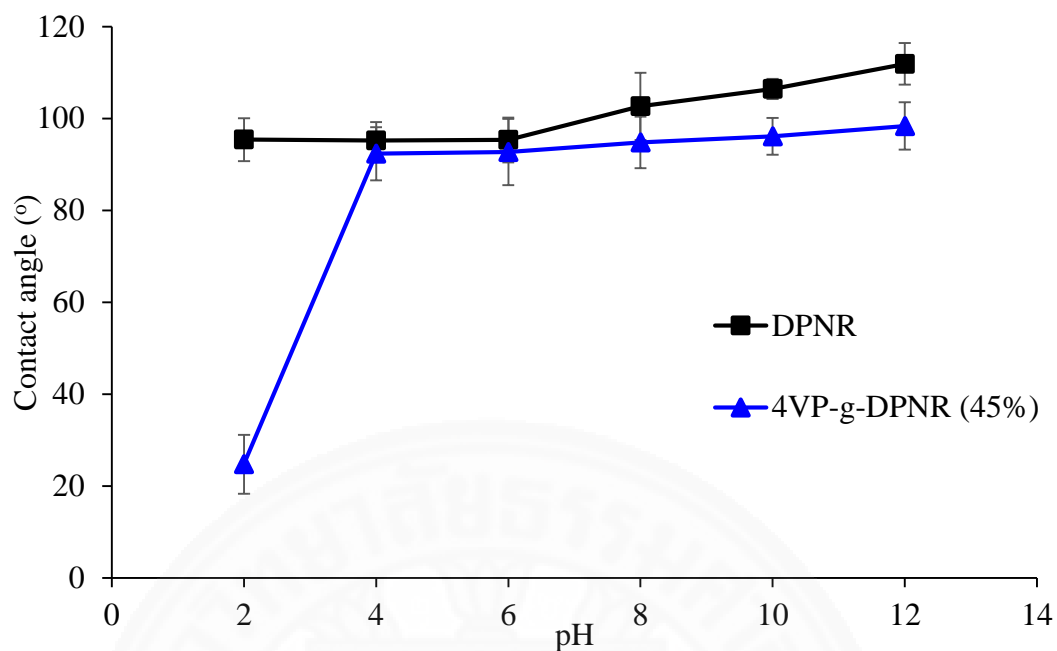


**Figure 69** Swelling behavior of 4VP-g-DPNR (grafting ratio = 45%) in aqueous solutions with pH 2 for 30 min.

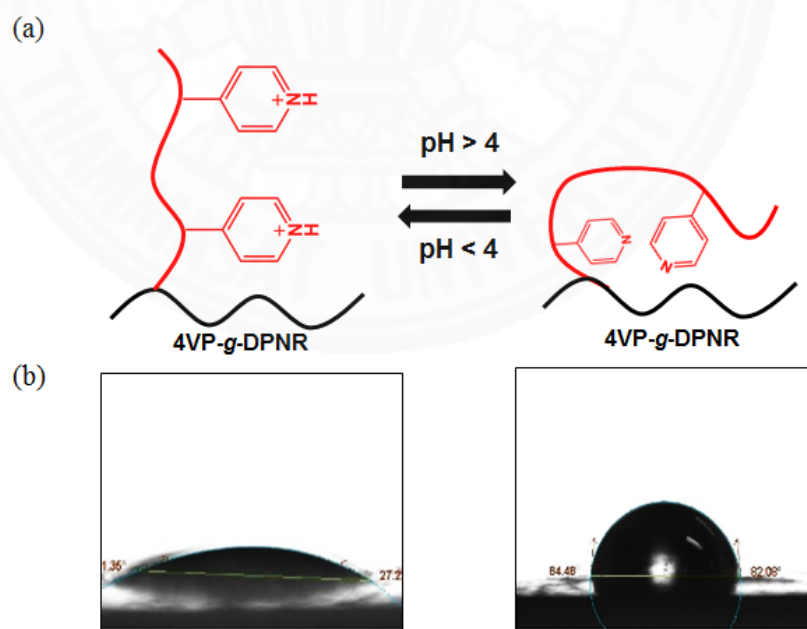
#### 4.2.8.2 The water contact angle of 4VP-*g*-DPNR

To further confirm the pH responsiveness of the grafted material, the samples were subsequently examined by water contact angle measurement. The DPNR and 4VP-*g*-DPNR samples were wetted with different pH aqueous solutions before measurement.

As shown in Figure 70, it was found that the DPNR sample showed contact angles of around 95-110° through the pH range used in this experiment. The negligible increase in contact angle was possibly due to the interaction with the surface of non-rubber compositions of the latex. On the other hand, the 4VP-*g*-DPNR samples showed an instantaneous increase in contact angle from 24° to 90° when the pH was changed from 2 to 4. After that point, the contact angles seemingly remained steady. As mentioned in the water swelling experiment, when the pH of the surroundings was below 4, the protonation or positive charges of pyridine unit in the sample were produced. As a result, the surface of the materials became more hydrophilic. Therefore, the water can be absorbed towards the materials, exhibiting a decrease in water contact angle (Figure 71). This result definitely confirms that the 4VP-*g*-DPNR is pH-responsive under acidic conditions in which the pH of solution was below 4, similar to the crosslinked sample.



**Figure 70** Water contact angles of DPNR and 4VP-*g*-DPNR (grafting ratio = 45%) at different pH values.



**Figure 71** (a) An image representation of protonated and deprotonated pyridyl groups on 4VP-*g*-DPNR and (b) water contact angles of 4VP-*g*-DPNR (grafting ratio = 45%) at pH 2 and 4.

#### **4.2.9 Demonstration of the pH-responsive releasing behavior of 4VP-*g*-DPNR**

To display the pH responsive behavior of pH responsive releasing materials, the release of indigo carmine dye and carbon quantum dots of 4VP-*g*-DPNR and DPNR were studied.

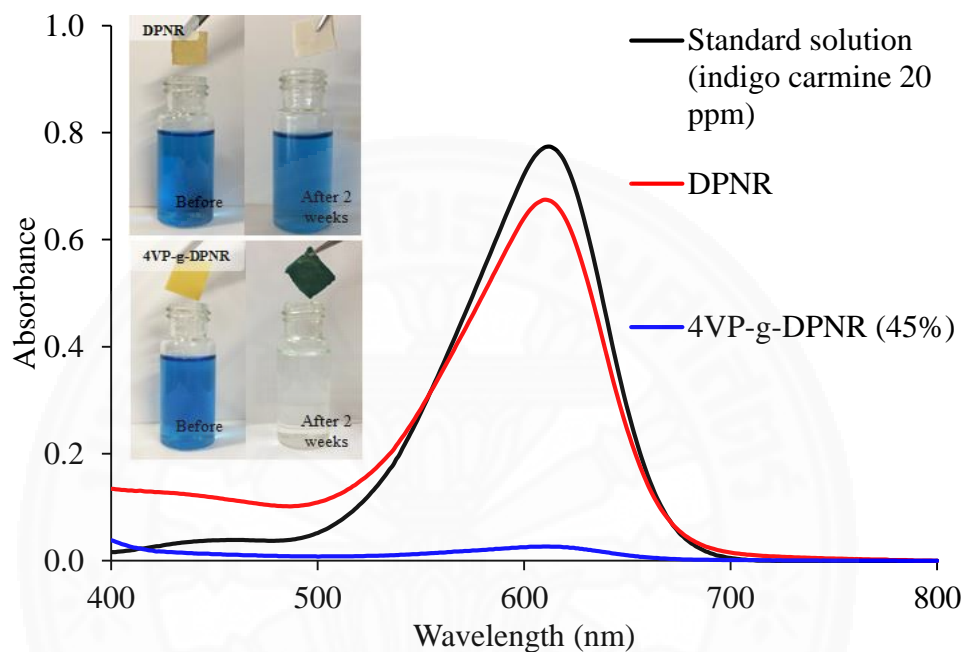
##### **4.2.9.1 Study the controlled release of indigo carmine from the resultant products**

In this study, the absorption and desorption of indigo carmine dye from 4VP-*g*-DPNR and DPNR were analyzed. Indigo carmine was chosen to represent a water-soluble anionic drug. The samples were immersed in indigo carmine solution (20 ppm) for two weeks at room temperature.

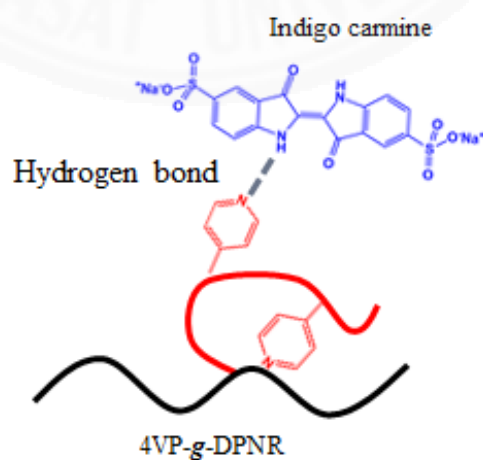
It was found that the 4VP-*g*-DPNR could absorb more dye than the pure DPNR, as shown by a greater reduction of absorbance intensity in Figure 72. Based on this result, it suggested that the 4VP in the grafted material may involve in the loading and releasing behaviors. Since the nitrogen atom of pyridine ring unit can interact with indigo carmine molecules by hydrogen bonding interaction (Figure 73), and therefore the dye concentration obviously decreased after immersion as also mentioned in P4VP-NR.

After dye absorption, the samples were withdrawn, dried up and then immersed in aqueous solutions with different pH values, and the absorbance was subsequently measured to monitor the release of the indigo carmine. As shown in Figure 74, the absorbance of the DPNR samples did not change significantly as the pH was increased from 2 to 10, indicating that the DPNR was not pH responsive. In contrast, the 4VP-*g*-DPNR samples showed that the dye could be released when the pH value of the solution were below 6. The reason is possibly due to the 4VP-*g*-DPNR becoming swollen when the pH below 4.7. Moreover, a large free volume inside that came from the swollen of the material was thus allowed the water to diffuse in and out easily, and as a result the dye inside could also be allowed to diffuse out. Apart from that, the dye release as a function of immersion time was further studied (Figure 75).

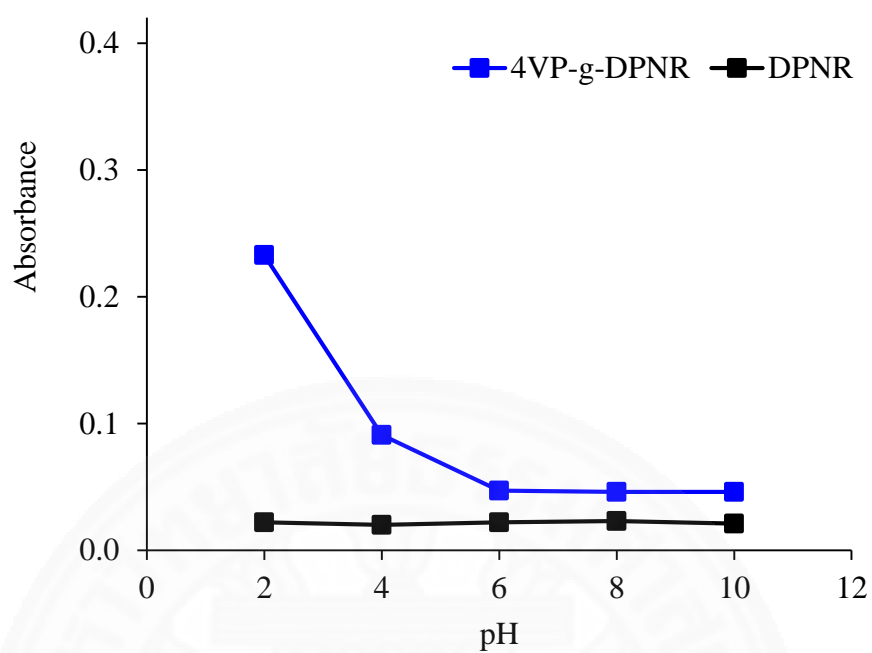
As the immersion time was increased, the relative absorbance gradually increased in any of pH solutions at a period of 0.5-3 h and remained steady after that. However, the release of indigo carmine at pH 2 was found to be the highest, similar to the crosslinked material.



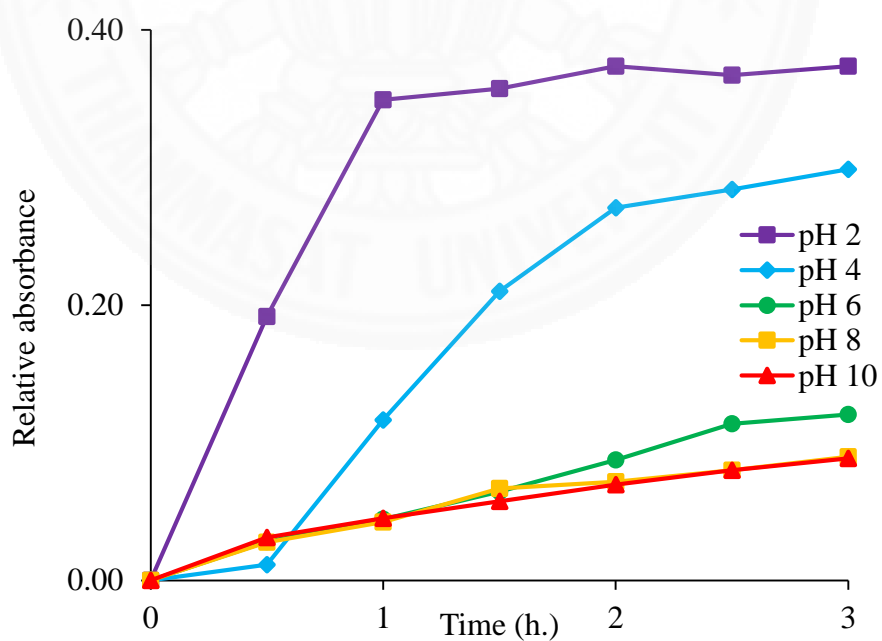
**Figure 72** UV-visible spectra of DPNR and 4VP-g-DPNR (grafting ratio = 45%) after immersion with dye solution compared with standard dye solution.



**Figure 73** Interaction between 4VP-g-DPNR and indigo carmine molecule.



**Figure 74** Absorbance values of DPNR and 4VP-g-DPNR samples.



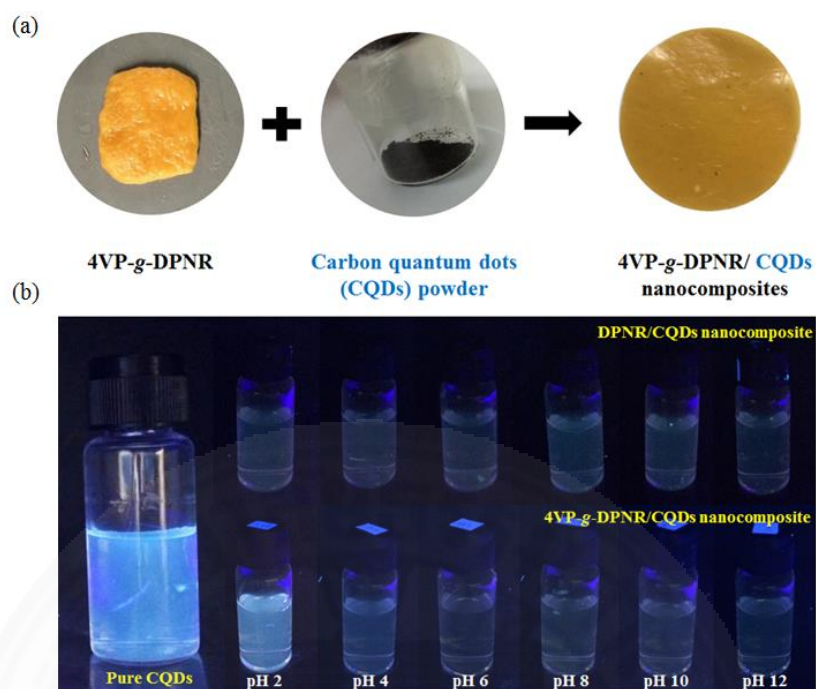
**Figure 75** Relative absorbance as a function of immersion time.



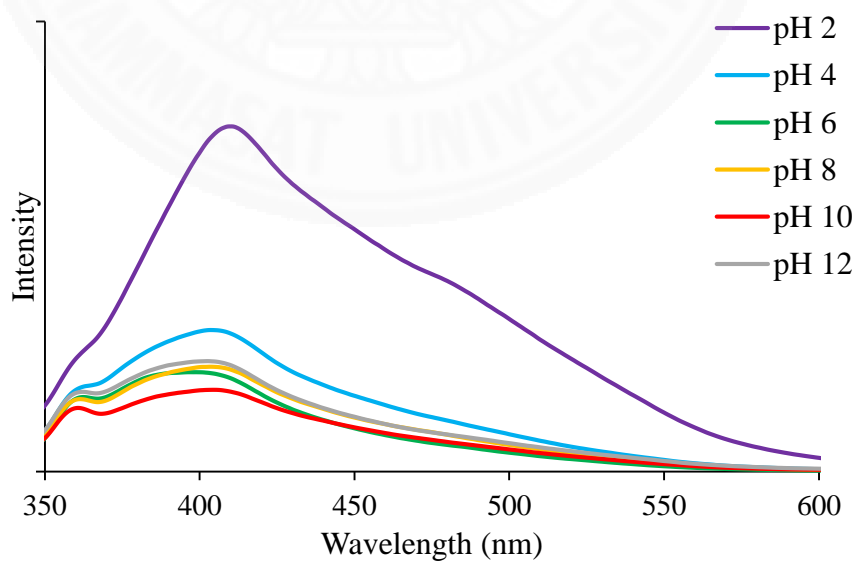
#### 4.2.9.2 Study the controlled release of carbon quantum dots from the resultant nanocomposites

In order to further confirm the pH responsive releasing behavior of the 4VP-*g*-DPNR, the release of carbon quantum dots (CQDs) from DPNR/CQDs and 4VP-*g*-DPNR/CQDs nanocomposites were also analyzed. The CQDs, a type of carbon nanoparticles, was used because it is a fluorescent material.

Prior to the study of the releasing behavior, the CQDs were embedded in the 4VP-*g*-DPNR and DPNR samples *via* polymer nanocomposite method (Figure 76a). The nanocomposite samples were subsequently immersed in different pH solutions from 2 to 12. From Figure 76b, it was found that the pH 2 solution that contained 4VP-*g*-DPNR/CQD nanocomposite showed the highest fluorescence intensity under the UV light when compared to other pH solutions. Meanwhile, the DPNR/CQD nanocomposite did not significantly display the difference in fluorescent intensity in any of pH solutions. As expected, the fluorescence intensity came from the release of CQDs. In acidic solution (pH < 4), it is already known that the protonation of pyridine ring unit led to the straightening up of the polymer chains due to the repulsive interaction between the same charges. As a result, the water can diffuse into the materials and dissolve the embedded CQDs particles out from the swollen material. Therefore, the CQD particles, which has an excellent water solubility, could be released from the materials to the solution and the solution displayed the fluorescence. In addition, the release of CQDs of 4VP-*g*-DPNR/CQD nanocomposite was subsequently confirmed using fluorescence spectroscopy. It was found that the pH 2 solution used to immerse the 4VP-*g*-DPNR/CQD nanocomposite exhibited the highest fluorescent intensity in a region of blue wavelength (400-450 nm) as shown in Figure 77. This result corresponded to the solution observed under UV light. However, the small amount of fluorescence intensity that presented in other pH solutions might results from the trace amount of remaining CQDs on the surface of the samples, which did not embed in the materials. Consequently, these pH responsive studies suggested that 4VP-*g*-DPNR material can potentially be used as a pH responsive releasing materials in the field of releasing applications, including drug delivery.



**Figure 76** (a) A schematic of preparation of 4VP-g-DPNR/CQDs nanocomposite, and (b) a photograph of fluorescence intensity of DPNR/CQDs and 4VP-g-DPNR/CQDs nanocomposites after immersion in aqueous solutions at a range of pH 2-12 under the UV light.



**Figure 77** Fluorescence spectra of the pH solutions from 2-12 after immersion with 4VP-g-DPNR/CQDs nanocomposite samples.

#### 4.2.10 Study of adsorption isotherms

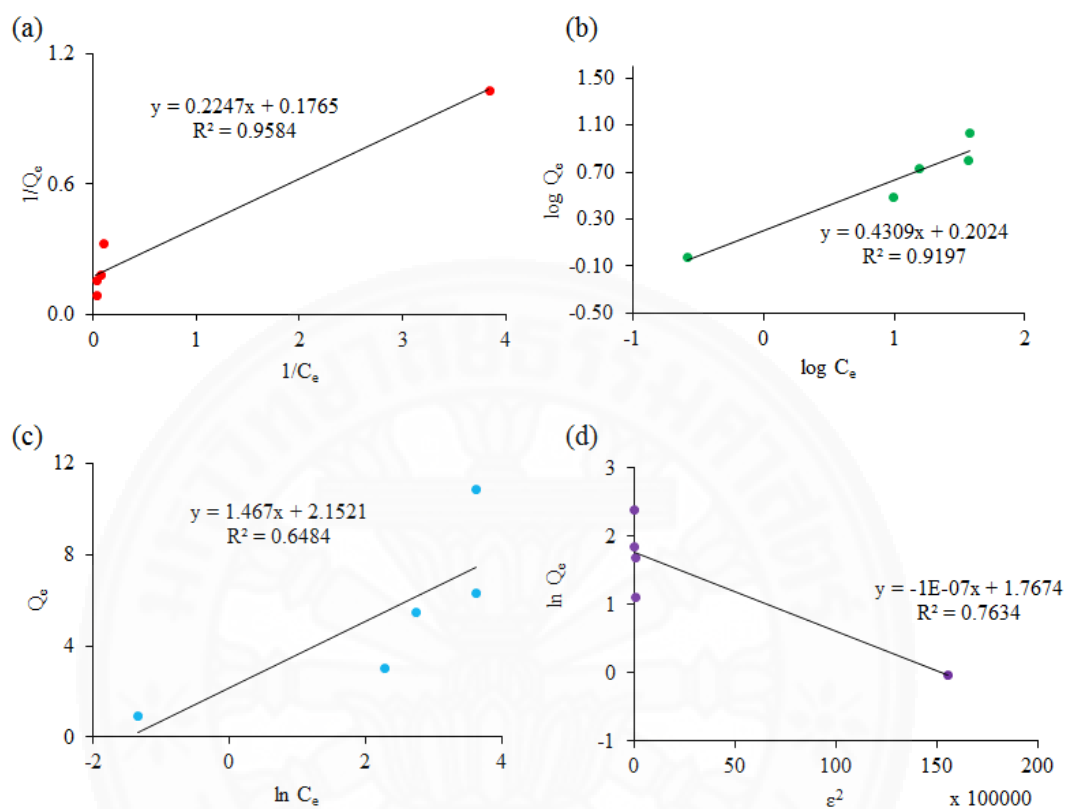
Finally, to determine the adsorption process of indigo carmine (adsorbate) onto 4VP-*g*-DPNR (adsorbent), the adsorption isotherm was studied. In this study, the experimental data from adsorption studies were computed using four models of adsorption isotherms which included the Langmuir, Freundlich, Temkin, and Dubinin-Radushkevich isotherms as shown in Figure 78. The linear regression analysis was employed to determine the best fit of those theoretical models with respective the regression coefficient ( $R^2$ ) that should be close to unity ( $R^2=1$ ). Moreover, the characteristic parameters of these isotherms were subsequently enumerated as presented in Table 17.

It was found that the Langmuir adsorption isotherm represented the highest linear regression coefficient value ( $R^2=0.9584$ ) and therefore the best fit model of experiment for the 4VP-*g*-DPNR sample. This study indicated that the uptake process of indigo carmine onto the 4VP-*g*-DPNR likely took place as a monolayer adsorption, and also suggested that the 4VP-*g*-DPNR is a homogeneous surface. The maximum monolayer coverage capacity ( $Q_0$ ) of dye onto the functionalized material is 5.67 mg/g. In addition, the affinity of adsorption behaviors can be revealed by a dimensionless parameter ( $R_L$ ). As presented in Table 17, the  $R_L$  value of this experiment was found to be in a range of 0-1, indicating the favorable adsorption of the dye onto 4VP-*g*-DPNR.

By considering to the other isotherms, it was found that the Freundlich, Temkin, and Dubinin-Radushkevich isotherms did not fit well to the experimental data when compared to that of the Langmuir isotherm, due to lower  $R^2$  values. There were ranked as the second, fourth, and third with respect to the linear regression coefficient ( $R^2$ ) values, respectively.

However, the characteristic parameters of the Freundlich isotherm can also be used to identify the favorability of adsorption process. It was found that the value of adsorption intensity ( $n$ ) from the Freundlich isotherm is larger than 1 ( $n = 2.321$ ), indicating that the adsorption of dye onto 4VP-*g*-DPNR is favorable. Additionally, the value of mean sorption energy ( $E$ ) from the Dubinin-Radushkevich isotherm gives information about chemical and physical adsorption. In Table 17, the  $E$  value (2.236

kJ/mol) is found to be less than 8 kJ/mol, revealing that the type of adsorption of indigo carmine onto 4VP-*g*-DPNR is a physical adsorption.



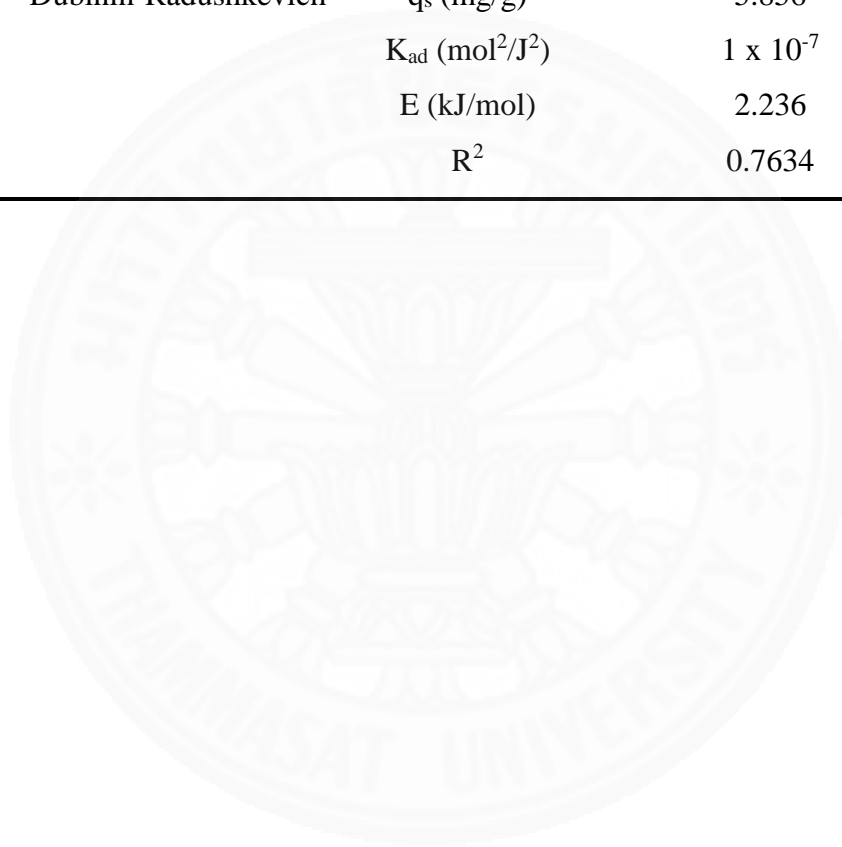
**Figure 78** Linear adsorption isotherms based on (a) Langmuir, (b) Freundlich, (c) Temkin, and (d) Dubinin-Radushkevich models.

**Table 17** Langmuir, Freundlich, Temkin and Dubinin-Radushkevich isotherm constants for the adsorption of indigo carmine onto 4VP-*g*-DPNR.

Adsorption Isotherm Models	Parameters	The constant values from Linear transform
Langmuir	$Q_0$ (mg/g)	5.666
	$K_L$ (L/mg)	0.785
	$R_L$	0.01 - 0.1
	$R^2$	0.9584
Freundlich	$1/n$	0.431

	n	2.321
	$K_f$ (mg/g)	1.594
	$R^2$	0.9197
Temkin	$A_T$ (L/mg)	4.336
	$b_T$	1705.87
	B	1.467
	$R^2$	0.6484
Dubinin-Radushkevich	$q_s$ (mg/g)	5.856
	$K_{ad}$ (mol <sup>2</sup> /J <sup>2</sup> )	$1 \times 10^{-7}$
	E (kJ/mol)	2.236
	$R^2$	0.7634

---



## CHAPTER 5

### CONCLUSIONS AND RECOMMENDATIONS

#### 5.1 Conclusions

In this thesis research, the 4-vinylpyridine-functionalized natural rubbers as pH responsive materials were prepared *via* two chemical-based methods: crosslinking and graft copolymerization methods.

##### 5.1.1 Synthesis and characterization of P4VP-crosslinked NR (P4VP-NR)

In this approach, the crosslinking reaction between P4VP and NR was carried out *via* solution polymerization method using BPO as an initiator for crosslinking. The obtained product was characterized by FT-IR and XPS techniques, in which the results showed the existence of P4VP in the materials after purification, confirming the success of this crosslinking reaction. After that, the determination of crosslink density showed that the presence of P4VP increase the crosslink density of the materials observed from the increase in the crosslink density as the gel content increased. In addition, the P4VP concentration, BPO concentration, reaction temperature, and reaction time all affected the reaction efficiency or the gel content, which the increase in P4VP concentration, reaction temperature, and reaction time increased the gel content. In contrast, the higher amount of initiator concentration did not provide an advantage for this reaction. The highest gel content from this study was found to be around 90 % when using a P4VP concentration of 150 phr and a BPO concentration of 10 phr at 90 °C for 24 h. For the thermal properties, the P4VP-NR was slightly more thermally stable than pure NR, and had a two differences of  $T_g$  values which indicated the P4VP and NR portions were present in the material.

As anticipated, the resultant product was a pH responsive material in acidic solution at pH below 4, compared to the pristine NR, which had been confirmed by the water swelling experiment and water contact angle measurement. Moreover, it showed a pH responsive releasing behavior that the absorbed indigo carmine on the

surface could be released in acidic condition ( $\text{pH} < 4$ ). Finally, the adsorption isotherm study indicated that the Langmuir isotherm was the best fit for describing the adsorption process of dye onto the P4VP-NR, in which the process took place *via* a monolayer adsorption.

### 5.1.2 Synthesis and characterization of 4VP-grafted DPNR (4VP-g-DP NR)

In this approach, the graft copolymerization of 4VP onto DPNR was carried out *via* an emulsion polymerization method using KPS as an initiator and SDS as an emulsifier. The deproteinization of NR latex was carried out to increase the grafting efficiency. It was found that the urea treatment and surfactant washing processes effectively removed the surface proteins from the rubber particles, confirmed by the decrease in nitrogen content. After the grafting reaction, the resultant product were characterized by FT-IR, XPS, and  $^1\text{H-NMR}$  techniques, in which the characteristic signal of 4VP after purification was still observed, confirming the success of this reaction. Furthermore, the 4VP concentration, KPS concentration, SDS concentration, reaction temperature, and reaction time all influenced the reaction efficiency or the grafting ratio, in which the increasing 4VP concentration, SDS concentration, and reaction time increased the grafting ratio. Meanwhile, the increase in KPS concentration and reaction time were found to reduce the grafting ratio. The highest grafting ratio of this study was found to be around 31 % when using a 4VP concentration of 100 phr and a KPS concentration of 8 phr for 3 h at 90 °C. For the thermal properties, the 4VP-g-DP NR was slightly less thermally stable than pure DPNR, and had two different  $T_g$  values which indicated the presence of P4VP and NR segments in the material.

Also, the resultant product was a pH responsive materials similar to the product obtained from the crosslinked reaction. When the pH of the environment was below 4, the resultant product became swollen and decreased the water contact angle (more hydrophilicity), which was confirmed by the water swelling experiment and water contact angle measurement. Additionally, the graft copolymer showed its potentials to be used as a pH responsive releasing material because it could release the absorbed dye and embedded CQDs in only acidic condition ( $\text{pH} < 4$ ). Lastly, the

Langmuir isotherm was found to be the best fit of this experimental data, indicating the monolayer adsorption process of dye onto 4VP-*g*-DPNR.

Based on this thesis research, the prepared pH-responsive materials, including the P4VP-NR and 4VP-*g*-DPNR, will potentially be useful for a variety of biomedical applications such a drug delivery system in a certain area, i.e. stomach. Other potential applications are consumer products, such as smart bandages that can release a loaded drug during a bacterial infection because of the acidic surroundings. Moreover, the method developed in this work can be applied to other types of stimuli-responsive rubbers, which will not only extend the properties of the NR, but also add a value to NR and expand the range of applications of the rubber-based materials.

## **5.2 Recommendations**

5.2.1 Other crosslinkers and initiators can be used to increase the crosslinking and grafting efficiencies, respectively.

5.2.2 The study of pore volume, pore size and surface area should be considered, because these affects the absorption process. This can be done using Brunauer–Emmett–Teller (BET) analysis.

5.2.3 In order to further apply in biomedical applications, the resultant products including P4VP-NR and 4VP-*g*-DPNR should be tested for their toxicity using bacteria dish method, for example.



## REFERENCES

1. Kohjiya, S. and Y. Ikeda, *Introduction*, in *Chemistry, Manufacture and Applications of Natural Rubber*. 2014, Woodhead Publishing. p. xvii-xxvi.
2. Saengruksawong, C., et al., *Growths and Carbon Stocks of Para Rubber Plantations on Phonpisai Soil Series in Northeastern Thailand*. RUBBER THAI JOURNAL, 2012. **1**: p. 1-18.
3. Budiman, A.F.S. *Recent Developments in Natural Rubber Prices*. [cited 2017 15/04]; Available from: <http://www.fao.org/docrep/006/Y4344E/y4344e0d.htm>.
4. Ltd, T.R.E. *Problems with NR prices*. Available from: [http://www.therubbereconomist.com/Problem\\_with\\_NR\\_prices.html](http://www.therubbereconomist.com/Problem_with_NR_prices.html).
5. *Thailand rubber production: High production vs low prices*. [cited 2017 14/04]; Available from: <https://www.emis.com/insight/thailand-rubber-production-high-production-vs-low-prices>.
6. Hinchiranan, N., et al., *Hydrogenation of Synthetic cis-1,4-Polyisoprene and Natural Rubber Catalyzed by [Ir(COD)py(PCy<sub>3</sub>)]PF<sub>6</sub>*. Journal of Applied Polymer Science, 2006. **100**: p. 4219-4233.
7. Kookarinrat, C. and P. Paoprasert, *Versatile one-pot synthesis of grafted-hydrogenated natural rubber*. Iranian Polymer Journal, 2015. **24**(2): p. 123–133.
8. ZHONG, J.-P., et al., *Study on Preparation of Chlorinated Natural Rubber from Latex and Its Thermal Stability*. Journal of Applied Polymer Science, 1999. **73**: p. 2863-2867.
9. Chanroj, T. and P. Paoprasert, *CHLOROHYDRINATION OF NR LATEX BY USING SODIUM HYPOCHLORITE FOR FUEL-RESISTANT MATERIALS*. Rubber Chemistry and Technology, 2016. **89**(2): p. 251-261.
10. Phinyocheep, P., et al., *Chemical Degradation of Epoxidized Natural Rubber Using Periodic Acid: Preparation of Epoxidized Liquid Natural Rubber*. Journal of Applied Polymer Science, 2005. **95**: p. 6-15.

11. Chuayjuljit, S., et al., *Oil Resistance and Physical Properties of In Situ Epoxidized Natural Rubber from High Ammonia Concentrated Latex*. Journal of Applied Polymer Science, 2006. **100**: p. 3948-3955.
12. Xue, X., et al., *Preparation and Thermal Stability of Brominated Natural Rubber from Latex*. Journal of Applied Polymer Science, 2010. **118**: p. 25-29.
13. XAVIER, T., et al., *New Ionic Polymer: Synthesis and Properties of ‘Zinc Sulfonated Natural Rubber’*. Journal of Elastomers and Plastics, 2002. **34**: p. 91-101.
14. Turner, D.T., *Document Radiation crosslinking of rubber: Yields of hydrogen and crosslinks*. Polymer, 1960: p. 27-40.
15. Lewis, P.M., *Vulcanizate structure and its effects on properties*. NR technology, 1986. **17**(4): p. 57-65.
16. Suksawad, P., Y. Yamamoto, and S. Kawahara, *Preparation of thermoplastic elastomer from natural rubber grafted with polystyrene*. European Polymer Journal, 2011. **47**: p. 330-337.
17. Nakason, C., A. Kaesaman, and P. Supasanthitikul, *The grafting of maleic anhydride onto natural rubber*. Polymer Testing, 2004. **23**: p. 35-41.
18. Kangwansupamonkon, W., R.G. Gilbert, and S. Kiatkamjornwong, *Modification of Natural Rubber by Grafting with Hydrophilic Vinyl Monomers*. Macromolecular Chemistry and Physics, 2005. **206**: p. 2450-2460.
19. Kochthongrasamee, T., P. Prasassarakich, and S. Kiatkamjornwong, *Effects of Redox Initiator on Graft Copolymerization of Methyl Methacrylate onto Natural Rubber*. Journal of Applied Polymer Science, 2006. **101**: p. 2587-2601.
20. Amnuaypanich, S. and P. Ratpolsan, *Pervaporation Membranes from Natural Rubber Latex Grafted with Poly(2-hydroxyethyl methacrylate) (NR-g-PHEMA) for the Separation of Water–Acetone Mixtures*. Journal of Applied Polymer Science, 2009. **113**: p. 3313-3321.
21. Juntuek, P., et al., *Glycidyl Methacrylate Grafted Natural Rubber: Synthesis, Characterization, and Mechanical Property*. Journal of Applied Polymer Science, 2011. **122**: p. 3152-3159.
22. Pisuttisap, A., et al., *ABS Modified with Hydrogenated Polystyrene-grafted-Natural Rubber*. Journal of Applied Polymer Science, 2013. **129**: p. 94-104.

23. Nuntahirun, P., O. Yamamoto, and P. Paoprasert, *Preparation and Temperature-Responsive Behavior of Crosslinked Polymers Between Poly(N-Isopropylacrylamide) and Natural Rubber*. *Macromolecular Research*, 2016. **24**(9): p. 816-823.
24. Chen, J.-K. and C.-J. Chang, *Fabrications and Applications of Stimulus-Responsive Polymer Films and Patterns on Surfaces: A Review*. *Materials*, 2014. **7**: p. 805-875.
25. Yoshida, T., et al., *pH- and ion-sensitive polymers for drug delivery*. *Expert Opinion on Drug Delivery*, 2013. **10**(11).
26. Almeida, H., M.H. Amaral, and P. Lobão, *Temperature and pH stimuli-responsive polymers and their applications in controlled and self-regulated drug delivery*. *Journal of Applied Pharmaceutical Science*, 2012. **02**(06): p. 01-10.
27. Kavitha, T., I.-K. Kang, and S.-Y. Park, *Poly(4-vinyl pyridine)-grafted graphene oxide for drug delivery and antimicrobial applications*. *Polymer International*, 2015. **64**: p. 1660-1666.
28. Ozaya, O., et al., *P(4-vinyl pyridine) hydrogel use for the removal of  $UO_2^{2+}$  and  $Th^{4+}$  from aqueous environments*. *Journal of Environmental Management*, 2011. **92**: p. 3121-3129.
29. El-Hamshary, H., et al., *Synthesis of Poly(acrylamide-co-4-vinylpyridine) Hydrogels and Their Application in Heavy Metal Removal*. *Journal of Applied Polymer Science*, 2003. **89**: p. 2522-2526.
30. Viela, P., et al., *Electropolymerized poly-4-vinylpyridine for removal of copper from wastewater*. *Applied Surface Science* 2003. **212-213**: p. 792-796.
31. Cao, L., et al., *Synthesis of cross-linked poly(4-vinylpyridine) and its copolymer microgels using supercritical carbon dioxide: Application in the adsorption of copper(II)*. *Journal of Supercritical Fluids*, 2011. **58**: p. 233- 238.
32. Borah, K.J., P. Dutta, and R. Borah, *Synthesis, Characterization and Application of Poly(4-vinylpyridine)-Supported Brønsted Acid as Reusable Catalyst for Acetylation Reaction*. *Bulletin of the Korean Chemical Society*, 2011. **32**(1): p. 225-228.

33. Pardey, A.J., et al., *Spectroscopic characterization of coordination complexes based on dichlorocopper(II) and poly(4-vinylpyridine): Application in catalysis*. *Polyhedron*, 2005. **24**(4): p. 511-519.
34. Cornish, K., *Biochemistry of natural rubber, a vital raw material, emphasizing biosynthetic rate, molecular weight and compartmentalization, in evolutionarily divergent plant species* *Natural Products Report*, 2001. **18**(2): p. 182-189.
35. *Tire*. [cited 2017 25/04]; Available from: <http://www.explainthatstuff.com/rubber.html>.
36. *Gloves*. [cited 2017 25/04]; Available from: <https://www.b4brands.com/blog/latex-vs-nitrile-vs-vinyl-gloves-which-to-choose/>.
37. *Rubber toys*. [cited 2017 25/04]; Available from: <https://www.imprintitems.com/blog/6846/rubber-toy-smiling-frog/>.
38. *Rubber boots*. [cited 2017 25/04]; Available from: <https://www.lowes.com/pl/Rubber-boots-Clothing-apparel-Safety/4294644911>.
39. CORNISH, K., et al., *Fundamental Similarities in Rubber Particle Architecture and Function in Three Evolutionarily Divergent Plant Species*. *Journal of Natural Rubber Research*, 1993. **8**(4): p. 275-285.
40. Venkatachalam, P., et al., *Natural rubber producing plants: An overview*. *African Journal of Biotechnology*, 2013. **12**(12): p. 1297-1310.
41. *Rubber Plantation Guide*. [cited 2017 27/04]; Available from: <http://www.agrifarming.in/rubber-plantation/>.
42. Anuntathanawanich, S., *Natural Rubber-Polystyrene Interpenetrating Polymer Networks as Impact Modifier*, in *Petrochemistry and Polymer Science*. 1999, Chulalongkorn University.
43. Ferreira, M., *Angiogenic Properties of Natural Rubber Latex Biomembranes and The Serum Fraction of Hevea brasiliensis*. *Brazilian Journal of Physics*, 2009. **39**(3): p. 564-569.

44. Yamamoto, Y., et al., *Removal of Proteins from Natural Rubber with Urea and Its Application to Continuous Processes*. Journal of Applied Polymer Science, 2008. **107**: p. 2329-2332
45. Pukkate, N., et al., *Nano-matrix structure formed by graft-copolymerization of styrene onto natural rubber*. European Polymer Journal, 2007. **43**: p. 3208-3214.
46. Kawahara, S., et al., *Preparation and characterization of natural rubber dispersed in nano-matrix*. Polymer, 2003. **44**: p. 4527-4531.
47. Ho, C.C., et al., *Surface Structure of Natural Rubber Latex Particles from Electrophoretic Mobility Data*. Journal of Colloid and Interface Science, 1996. **178**(2): p. 442-445.
48. Thomas, S., et al., *Natural Rubber Materials : Volume 2: Composites and Nanocomposites* Vol. 2. 2013.
49. Chaikumpollerta, O., et al., *Low temperature degradation and characterization of natural rubber*. Polymer Degradation and Stability, 2011. **96**: p. 1989-1995.
50. Santos, K.A.M.d., P.A.Z. Suarez, and J.C. Rubim, *Photo-degradation of synthetic and natural polyisoprenes at specific UV radiations*. Polymer Degradation and Stability 2005. **90**: p. 34-43.
51. Chaikumpollert, O., et al., *Low temperature degradation and characterization of natural rubber*. Polym. Degrad. Stabil., 2011. **96**(11): p. 1989-1995.
52. S. Kohjiya, Y.I., *Chemistry, Manufacture and Applications of Natural Rubber*. 2014: Woodhead publishing.
53. Yeganeh-Ghotbi, M. and V. Haddadi-Asl, *Surface Modification of SBR and NR by Hydrophilic Monomers (I): Effect of Structural Parameters and Inhibitors(\$)*. Iranian Polymer Journal, 1999. **9**: p. 183-189.
54. s.r.o., M.R., *RUBBER CHEMISTRY*, in *VERT (Virtual Education in Rubber Technology)*. 2007.
55. Doylea, M.W., et al., *The Non Enzymatic Deproteinization of Natural Rubber Latex (DPNRL) Enabling the Greater Versatility in End Product Applications*.
56. Nawamawat, K., et al., *Surface nanostructure of Hevea brasiliensis natural rubber latex particles*. Colloids and Surfaces A: Physicochemical and Engineering Aspects, 2011. **390**(1-3): p. 157–166.

57. Wren, W.G., *Rubber Chem. Technol.*, 1942. **15**(1): p. 107.
58. Nawamawat, K., J.T. Sakdapipanich, and C.C. Ho, *Effect of Deproteinized Methods on the Proteins and Properties of Natural Rubber Latex during Storage*. *Macromolecular Symposia*, 2010. **288**: p. 95–103.
59. Pukkate, N., et al., *Nano-matrix structure formed by graft-copolymerization of styrene onto natural rubber*. *European Polymer Journal*, 2007. **43**(8): p. 3208–3214.
60. Kawahara, S., et al., *Preparation and characterization of natural rubber dispersed in nano-matrix*. *Polymer*, 2003. **44**(16): p. 4527–4531.
61. Nakason, C., A. Kaesaman, and N. Yimwan, *Preparation of graft copolymers from deproteinized and high ammonia concentrated natural rubber latices with methyl methacrylate*. *Journal of Applied Polymer Science*, 2003. **87**: p. 68-75.
62. Kreua-ongarjnukool, N., P. Pittayavinai, and S. Tuampoemsab, *Grafted Deproteinized Natural Rubber as an Impact Modifier in Styrene-Methyl Methacrylate Copolymer Sheet* *J. Chem. Chem. Eng.*, 2012. **6**: p. 698-707.
63. Arayapranee, W. and G.L. Rempel, *Morphology and Mechanical Properties of Natural Rubber and Styrene-Grafted Natural Rubber Latex Compounds*. *Journal of Applied Polymer Science*, 2008. **109**: p. 1395-1402.
64. Oliveira, P.C., et al., *Poly(dimethylaminoethyl methacrylate) grafted natural rubber from seeded emulsion polymerization*. *Polymer*, 2005. **46**(4): p. 1105-1111.
65. Promdum, Y., P. Klinpituksa, and J. Ruamcharoen, *Grafting copolymerization of natural rubber with 2-hydroxyethyl methacrylate for plywood adhesion improvement*. *Songklanakarin J. Sci. Technol.*, 2009. **31**(4): p. 453-457.
66. Zhang, S., et al., *Grafting of methyl methacrylate onto natural rubber in supercritical carbon dioxide*. *POLYMERS FOR ADVANCED TECHNOLOGIES*, 2008. **19**: p. 54-59.
67. Aprem, A.S., K. Joseph, and S. Thomas, *RECENT DEVELOPMENTS IN CROSSLINKING OF ELASTOMERS*. *Rubber Chemistry and Technology*, 2005. **78**(3): p. 458-488.



68. KAMPOURIS, E.M. and A.G. ANDREOPOULOS, *Benzoyl Peroxide as a Crosslinking Agent for Polyethylene*. Journal of Applied Polymer Science, 1987. **34**: p. 1209-1216.
69. LOAN, L.D., *PEROXIDE CROSSLINKING REACTIONS OF POLYMERS*. Pure and Applied Chemistry, 2009. **30**(1-2): p. 173-180.
70. Mathew, A.P., et al., *Effect of initiating system, blend ratio and crosslink density on the mechanical properties and failure topography of nano-structured full-interpenetrating polymer networks from natural rubber and polystyrene*. European Polymer Journal 2001. **37**: p. 1921-1934.
71. John, J., et al., *Relaxations and chain dynamics of sequential full interpenetrating polymer networks based on natural rubber and poly(methyl methacrylate)*. Polym International, 2014. **63**: p. 1427 - 1438.
72. Nie, Y., et al., *Cure Kinetics and Morphology of Natural Rubber Reinforced by the In Situ Polymerization of Zinc Dimethacrylate*. Journal of Applied Polymer Science, 2010. **115**: p. 99-106.
73. Johns, J. and C. Nakason, *Novel Interpenetrating Polymer Networks Based on Natural Rubber/Poly(vinyl alcohol)*. Polymer-Plastics Technology and Engineering, 2012. **51**: p. 1046-1053.
74. Amnuaypanich, S. and N. Kongchana, *Natural Rubber/Poly(acrylic acid) Semi-Interpenetrating Polymer Network Membranes for the Pervaporation of Water–Ethanol Mixtures*. Journal of Applied Polymer Science, 2009. **114**: p. 3501-3509.
75. Myer, Y.P., Z.J. Chen, and H.L. Frisch, *Resonance Raman spectroscopic study of an iodine-doped pseudo-interpenetrating polymer network of natural rubber-poly(carbonate urethane)*. Polymer, 1997. **38**(3): p. 729-731.
76. Thitithammawong, A., et al., *Effect of different types of peroxides on rheological, mechanical, and morphological properties of thermoplastic vulcanizates based on natural rubber/polypropylene blends*. Polymer Testing 2007. **26**: p. 537-546.
77. Phinyocheep, P., *Chemical modification of natural rubber (NR) for improved performance*. Chemistry, Manufacture and Applications of Natural Rubber, 2014: p. 68-118.

78. M, Y.G. and H. V, *Surface Modification of SBR and NR by hydrophilic monomers (I): effect of structural parameters and inhibitors (§)*. IRANIAN POLYMER JOURNAL, 2000. **9**: p. 183-189.
79. Satraphan, P., et al., *Effects of methyl methacrylate grafting and in situ silica particle formation on the morphology and mechanical properties of natural rubber composite films*. Polym. Adv. Technol, 2009. **20**: p. 473-486.
80. Almeida, H., M.H. Amaral, and P. Lobão, *Temperature and pH stimuli-responsive polymers and their applications in controlled and selfregulated drug delivery*. Journal of Applied Pharmaceutical Science, 2012. **2**(6): p. 01-10.
81. Dai, S., P. Ravi, and K.C. Tam, *pH-Responsive polymers: synthesis, properties and applications*. Soft Matter, 2008. **4**: p. 435-449.
82. Weaver, J.V.M. and D.J. Adamsa, *Synthesis and application of pH-responsive branched copolymer nanoparticles (PRBNs): a comparison with pH-responsive shell cross-linked micelles*. Soft Matter, 2010. **6**: p. 2575-2582.
83. Arizaga, A., et al., *Encapsulation of magnetic nanoparticles in a pH-sensitive poly(4-vinyl pyridine) polymer: a step forward to a multi-responsive system*. Journal of Experimental Nanoscience, 2014. **9**(6): p. 561-569.
84. Kavitha, T., I.-K. Kang, and S.-Y. Park, *Poly(4-vinyl pyridine)-grafted graphene oxide for drug delivery and antimicrobial applications*. Polym. Int., 2015. **64**(11): p. 1660-1666.
85. Ozgur Ozay, S.E., Nahit Aktas, Nurettin Sahiner, *P(4-vinyl pyridine) hydrogel use for the removal of  $UO_2^{2+}$  and  $Th^{4+}$  from aqueous environments*. Journal of Environmental Management, 2011. **92**: p. 3121-3129.
86. El-Hamshary, H., et al., *Synthesis of Poly(acrylamide-co-4-vinylpyridine) Hydrogels and Their Application in Heavy Metal Removal*. J. Appl. Polym. Sci., 2003. **89**: p. 2522-2526.
87. Viela, P., et al., *Electropolymerized poly-4-vinylpyridine for removal of copper from wastewater*. Appl. Surf. Sci., 2003. **212-213**: p. 792-796.
88. Cao, L., et al., *Synthesis of cross-linked poly(4-vinylpyridine) and its copolymer microgels using supercritical carbon dioxide: Application in the adsorption of copper(II)*. J. Supercrit. Fluids, 2011. **58**: p. 233-238.



89. Borah, K.J. and P.D. Borah, *Synthesis, Characterization and Application of Poly(4-vinylpyridine)-Supported Brønsted Acid as Reusable Catalyst for Acetylation Reaction*. Bull. Korean Chem. Soc., 2011. **32**(1): p. 225-228.
90. Pardey, A.J., et al., *Spectroscopic characterization of coordination complexes based on dichlorocopper(II) and poly(4-vinylpyridine): Application in catalysis*. Polyhedron, 2005. **24**: p. 511-519.
91. KH, K., et al., *Polymer-grafted cellulose nanocrystals as pH-responsive reversible flocculants*. Biomacromolecules, 2013. **14**(9): p. 3130-3139.
92. Wen, X., L. Tang, and L. Qiang, *Stimuli-responsive one-dimensional copolymer nanostructures fabricated by metallogel template polymerization and their adsorption of aspirin*. Soft Matter, 2014. **10**: p. 3960-3969.
93. Gonzalez, L., et al., *Conventional and Efficient Crosslinking of Natural Rubber: Effect of Heterogeneities on the Physical Properties*. KGK Kautschuk Gummi Kunststoffe, 2005. **58**(12): p. 638-643.
94. Department, C.U.E., *Materials Data Book*. 2003.
95. Birkner, N. and Q. Wang. *How an FTIR Spectrometer Operates*. 2015 [cited 2017 21/04]; Available from: [https://chem.libretexts.org/Core/Physical\\_and\\_Theoretical\\_Chemistry/Spectroscopy/Vibrational\\_Spectroscopy/Infrared\\_Spectroscopy/How\\_an\\_FTIR\\_Spectrometer\\_Operates](https://chem.libretexts.org/Core/Physical_and_Theoretical_Chemistry/Spectroscopy/Vibrational_Spectroscopy/Infrared_Spectroscopy/How_an_FTIR_Spectrometer_Operates).
96. Clark, J. *WHAT IS NUCLEAR MAGNETIC RESONANCE (NMR)?* 2014 [cited 2017 21/04]; Available from: <http://www.chemguide.co.uk/analysis/nmr/background.html>.
97. *X-ray photoelectron spectroscopy*. [cited 2017 22/04]; Available from: [https://en.wikipedia.org/wiki/X-ray\\_photoelectron\\_spectroscopy](https://en.wikipedia.org/wiki/X-ray_photoelectron_spectroscopy).
98. *CHN analyzer*. [cited 2017 22/04]; Available from: [https://en.wikipedia.org/wiki/CHN\\_analyzer](https://en.wikipedia.org/wiki/CHN_analyzer).
99. Fungaro, D.A., S.I. Borrely, and T.E.M. Carvalho, *Surfactant Modified Zeolite from Cyclone Ash as Adsorbent for Removal of Reactive Orange 16 from Aqueous Solution*. American Journal of Environmental Protection, 2013. **1**(1): p. 1-9.

100. Dada, A.O., et al., *Langmuir, Freundlich, Temkin and Dubinin–Radushkevich Isotherms Studies of Equilibrium Sorption of Zn<sup>2+</sup> Unto Phosphoric Acid Modified Rice Husk*. Journal of Applied Chemistry, 2012. **3**(1): p. 38-45.
101. Chen, X., *Modeling of Experimental Adsorption Isotherm Data*. Information, 2015. **4**: p. 14-22.
102. Zheng, H., et al., *Sorption isotherm and kinetic modeling of aniline on Cr-bentonite*. J. Hazard Mater., 2009. **167**: p. 141-147.
103. McKAY, G., H.S. BLAIR, and J.R. GARDNER, *Adsorption of dyes on chitin. I. Equilibrium studies*. Journal of Applied Polymer Science, 1982. **27**: p. 3043-3057.
104. Gamal, A.M., et al., *Kinetic Study and Equilibrium Isotherm Analysis of Reactive Dyes Adsorption onto Cotton Fiber*. Nature and Science, 2010. **8**(11): p. 95-110.
105. Ismail, M.G.B.H., et al., *Freundlich Isotherm Equilibrium Equations in Determining Effectiveness a Low Cost Absorbent to Heavy Metal Removal In Wastewater (Leachate) At Teluk Kitang Landfill, Pengkalan Chepa, Kelantan, Malaysia*. Journal of Geography and Earth Science 2013. **1**(1): p. 01-08.
106. Ibrahim, M.B. and S. Sani, *Comparative Isotherms Studies on Adsorptive Removal of Congo Red from Wastewater by Watermelon Rinds and Neem-Tree Leaves*. Open Journal of Physical Chemistry, 2014. **4**: p. 139-146.
107. A.U., I. and I. H.U, *Sorption Energies Estimation Using Dubinin-Radushkevich and Temkin Adsorption Isotherms*. Life Science Journal 2010. **7**(4): p. 31-39.
108. Yuan, J.-J., et al., *Synthesis and Characterization of Polystyrene/Poly(4-vinylpyridine) Triblock Copolymers by Reversible Addition–Fragmentation Chain Transfer Polymerization and Their Self-Assembled Aggregates in Water*. Journal of Applied Polymer Science, 2003. **89**: p. 1017-1025.
109. Maitra, J. and V.K. Shukla, *Cross-linking in Hydrogels - A Review*. American Journal of Polymer Science, 2014. **4**(2): p. 25-31.
110. Manaila, E., et al., Polym. Bull., 2014. **71**: p. 2001.
111. Halimatuddahlia, H. Ismaila, and H.M. Akil, Int. J. Polym. Mater., 2005. **54**: p. 1169.

112. Liu, H., et al., *J. Appl. Polym. Sci.*, 2011. **122**: p. 973.
113. Tamboli, S.M., S.T. Mhaske, and I.F.A.o.P.b.C. D. D. Kale, 853 (2004). *Improving Foam Ability of Polypropylene by Crosslinking*. *J. Appl. Polym. Sci.*, 2011. **122**(2): p. 973-980.
114. Santos, K.A.M.d., P.A.Z. Suarez, and J.C. Rubim, *Photo-degradation of synthetic and natural polyisoprenes at specific UV radiations*. *Polymer Degradation and Stability*, 2005. **90**: p. 34-43.
115. Wongthong, P., et al., *Modification of deproteinized natural rubber via grafting polymerization with maleic anhydride*. *European Polymer Journal*, 2013. **49**(12): p. 4035-4046.
116. Arayapranee, W., P. Prasassarakich, and G.L. Rempel, *Process variables and their effects on grafting reactions of styrene and methyl methacrylate onto natural rubber*. *Journal of Applied Polymer Science*, 2003. **89**: p. 63-74.
117. Paoprasert, P., S. Moonrinta, and S. Kanokul, *Highly efficient interpenetrating polymerization of styrene and 4-vinylpyridine with poly(ethylene terephthalate) using benzoyl peroxid*. *Polym. Int.*, 2014. **63**(6): p. 1041-1046.
118. RS, W., A. M, and D. K, *Effect of Crosslinking Agent Concentration on the Properties of Unmedicated Hydrogels*. *Pharmaceutics*, 2015. **7**(3): p. 305-319.
119. Huang, C.-F., et al., *Synthesis and Characterization of Polystyrene-b-Poly(4-vinyl pyridine) Block Copolymers by Atom Transfer Radical Polymerization*. *Journal of Polymer Research* 2005. **12**: p. 449-456.
120. Wongthong, P., et al., *Styrene-Assisted Grafting of Maleic Anhydride onto Deproteinized Natural Rubber*. *European Polymer Journal*, 2014. **59**: p. 144-155.
121. Kuo, S.-W., C.-H. Wu, and F.-C. Chang, *Thermal Properties, Interactions, Morphologies, and Conductivity Behavior in Blends of Poly(vinylpyridine)s and Zinc Perchlorate*. *Macromolecules*, 2004. **37**(1): p. 192-200.
122. Ho, C.C. and M.C. Khew, *Surface Free Energy Analysis of Natural and Modified Natural Rubber Latex Films by Contact Angle Method*. *Langmuir*, 2000. **16**(3): p. 1407-1414.

123. Samart, C., et al., *Preparation of poly acrylic acid grafted-mesoporous silica as pH responsive releasing material*. Journal of Industrial and Engineering Chemistry 2014. **20**: p. 2153-2158.
124. Meroufel, B., et al., *Adsorptive removal of anionic dye from aqueous solutions by Algerian kaolin: Characteristics, isotherm, kinetic and thermodynamic studies*. Journal of Materials and Environmental Science 2013. **4**(3): p. 482-491.
125. Pichayakorn, W., et al., *Preparation of Deproteinized Natural Rubber Latex and Properties of Films Formed by Itself and Several Adhesive Polymer Blends*. Ind. Eng. Chem. Res, 2012. **51**(41): p. 13393-13404.
126. Pukkate, N., Y. Yamamoto, and S. Kawahara, *Mechanism of graft copolymerization of styrene onto deproteinized natural rubber*. Colloid and Polymer Science, 2008. **286**(4): p. 411-416.
127. Goh, S.H., et al., *X-ray Photoelectron Spectroscopic Studies of Interactions between Poly(4-vinylpyridine) and Poly(styrenesulfonate) Salts*. Macromolecules, 1998. **31**(13): p. 4260-4264.
128. Angnanon, S., P. Prasassarakich, and N. Hinchiranan, *Styrene/Acrylonitrile Graft Natural Rubber as Compatibilizer in Rubber Blends*. Polymer-Plastics Technology and Engineering, 2011. **50**: p. 1170-1178.
129. YAMASHITA, K., et al., *Graft Copolymerization by Iniferter Method; Structural Analyses of Graft Copolymer by Glass Transition Temperature*. Journal of Applied Polymer Science, 1990. **40**: p. 1445-1452.



## APPENDIX A

### PREPARATION OF CROSSLINKED MATERIALS (P4VP-NR)

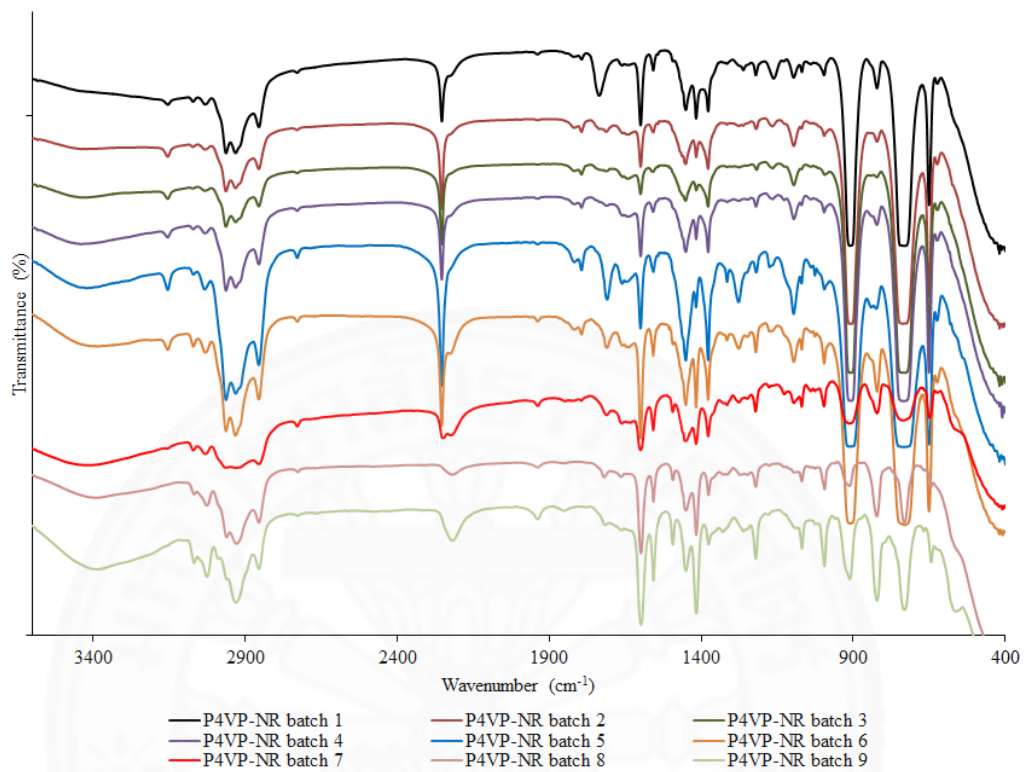
The effect of influential parameters on the gel content (%)

Batch No.	NR (g)	P4VP (phr)	BPO (phr)	Temperature (°C)	Time (h)	Gel content (%)
1	1	50	10	90	24	35.03
2	1	100	10	90	24	63.39
3	1	150	10	90	24	89.93
4	1	100	5	90	24	22.04
5	1	100	15	90	24	64.98
6	1	100	10	80	24	55.31
7	1	100	10	100	24	63.39
8	1	100	10	90	12	58.35
9	1	100	10	90	36	77.36

Determination of crosslink density

Gel content (%)	crosslink density (mol m <sup>-3</sup> )	Degree of swelling (%)
42	12.76	679.63
58	14.57	632.21
63	16.32	594.53
92	21.19	516.37
96	24.49	477.71

## FT-IR characterization



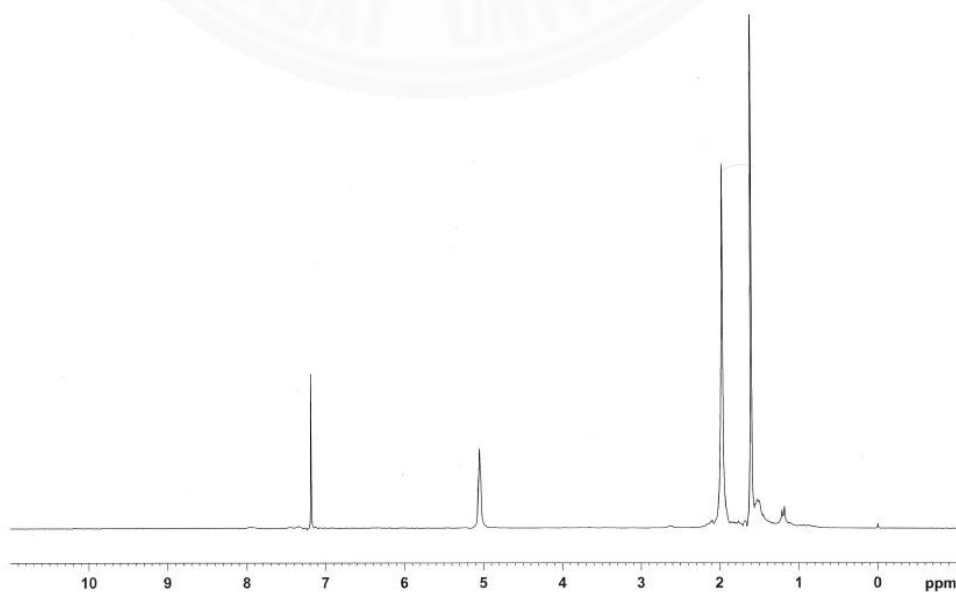
## APPENDIX B

### PREPARATION OF GRAFTED MATERIALS (4VP-g-DPNR)

The effect of influential parameters on the grafting ratio (%)

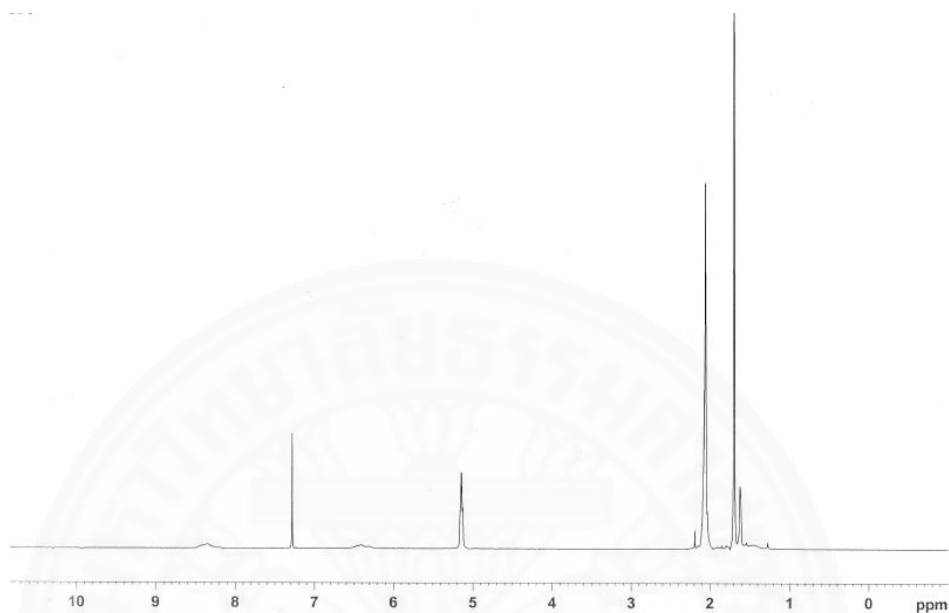
Batch no.	DPNR (g)	4VP (phr)	KPS (phr)	SDS (phr)	Temperature (°C)	Time (h)	Grafting ratio (%)
1	5	50	10	10	90	3	7.1
2	5	100	10	10	90	3	16.0
3	5	150	10	10	90	3	29.76
4	5	100	8	10	90	3	31.1
5	5	100	12	10	90	3	7.8
6	5	100	10	5	90	3	2.6
7	5	100	10	15	90	3	24.0
8	5	100	10	10	80	3	13.2
9	5	100	10	10	100	3	18.3
10	5	100	10	10	90	1	19.7
11	5	100	10	10	90	5	13.2

The  $^1\text{H-NMR}$  of 4VP-g-HANR (4VP 100 phr, KPS 10 phr, SDS 10 phr, 90 °C, 3 h.)

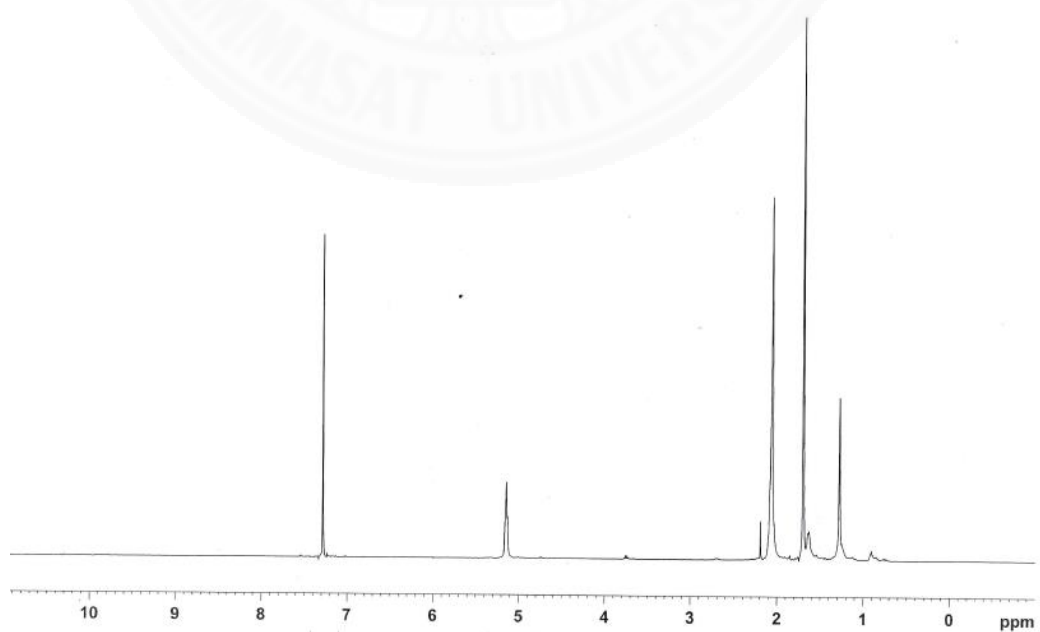




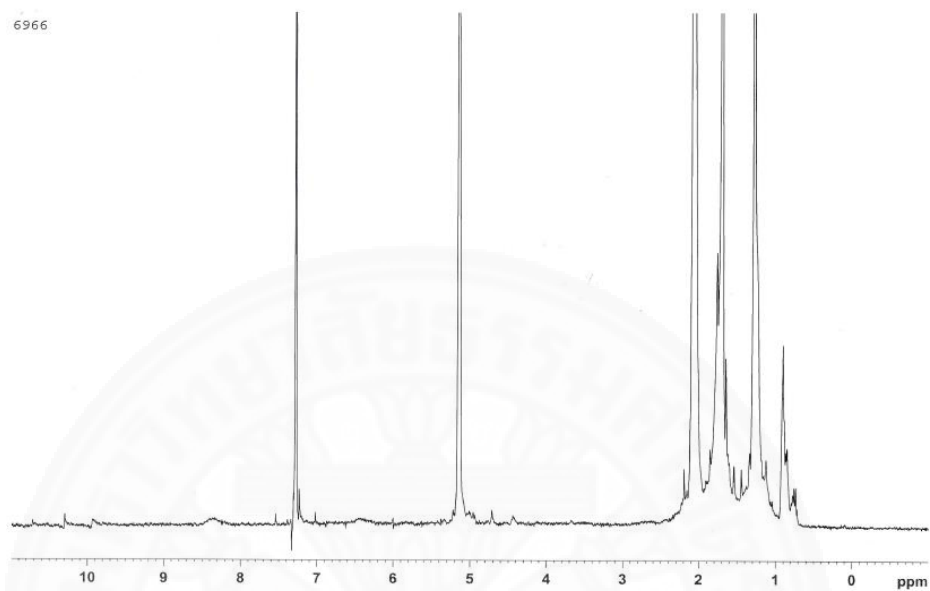
The  $^1\text{H-NMR}$  of 4VP-*g*-DPNR (4VP 100 phr, CHP/TEPA 10 phr, SDS 10 phr, 90 °C, 3 h.)



The  $^1\text{H-NMR}$  of 4VP-*g*-DPNR (4VP 100 phr, BPO 10 phr, SDS 10 phr, 90 °C, 3 h.)



The  $^1\text{H-NMR}$  of 4VP-*g*-DPNR (4VP 100 phr, AIBN 10 phr, SDS 10 phr, 90 °C, 3 h.)



**APPENDIX C**  
**DETERMINATION OF PH RESPONSIVENESS OF THE**  
**MATERIALS**

The water swelling experiments

NR											
pH	1			2			3			AVG	SD
	w <sub>1</sub>	w <sub>2</sub>	%S	w <sub>1</sub>	w <sub>2</sub>	%S	w <sub>1</sub>	w <sub>2</sub>	%S		
2	0.0966	0.0984	<b>1.86</b>	0.0245	0.025	<b>2.04</b>	0.0545	0.0601	<b>10.28</b>	<b>4.73</b>	<b>4.81</b>
4	0.1040	0.1078	<b>3.65</b>	0.0261	0.0268	<b>2.68</b>	0.0529	0.0584	<b>10.40</b>	<b>5.58</b>	<b>4.20</b>
6	0.0886	0.0920	<b>3.84</b>	0.0313	0.0322	<b>2.88</b>	0.0715	0.0794	<b>11.05</b>	<b>5.92</b>	<b>4.47</b>
8	0.0974	0.1014	<b>4.11</b>	0.0214	0.0231	<b>7.94</b>	0.0730	0.0811	<b>11.10</b>	<b>7.72</b>	<b>3.50</b>
10	0.0769	0.0850	<b>10.53</b>	0.0292	0.0298	<b>2.05</b>	0.0592	0.0640	<b>8.11</b>	<b>6.90</b>	<b>4.37</b>
12	0.0795	0.0830	<b>4.40</b>	0.0288	0.0297	<b>3.13</b>	0.0380	0.0408	<b>7.37</b>	<b>4.97</b>	<b>2.18</b>

DPNR											
pH	1			2			3			AVG	SD
	w <sub>1</sub>	w <sub>2</sub>	%S	w <sub>1</sub>	w <sub>2</sub>	%S	w <sub>1</sub>	w <sub>2</sub>	%S		
2	0.0966	0.0974	<b>0.83</b>	0.0909	0.098	<b>7.81</b>	0.0969	0.0987	<b>1.86</b>	<b>3.50</b>	<b>3.77</b>
4	0.1040	0.1088	<b>4.62</b>	0.0979	0.0992	<b>1.33</b>	0.0974	0.1055	<b>8.32</b>	<b>4.75</b>	<b>3.50</b>
6	0.0886	0.1000	<b>12.87</b>	0.0839	0.0902	<b>7.51</b>	0.0834	0.0898	<b>7.67</b>	<b>9.35</b>	<b>3.05</b>
8	0.0974	0.1114	<b>14.37</b>	0.0924	0.0978	<b>5.84</b>	0.0938	0.1002	<b>6.82</b>	<b>9.01</b>	<b>4.67</b>
10	0.0769	0.0890	<b>15.73</b>	0.0740	0.0785	<b>6.08</b>	0.0745	0.0796	<b>6.85</b>	<b>9.55</b>	<b>5.37</b>
12	0.0795	0.0899	<b>13.08</b>	0.0753	0.0806	<b>7.04</b>	0.0753	0.0796	<b>5.71</b>	<b>8.61</b>	<b>3.93</b>

P4VP-NR (34%)											
pH	1			2			3			AVG	SD
	w <sub>1</sub>	w <sub>2</sub>	%S	w <sub>1</sub>	w <sub>2</sub>	%S	w <sub>1</sub>	w <sub>2</sub>	%S		
2	0.1786	0.2788	<b>56.10</b>	0.1050	0.1392	<b>32.57</b>	0.1866	0.2449	<b>31.24</b>	<b>39.97</b>	<b>13.99</b>
4	0.1367	0.1595	<b>16.68</b>	0.1334	0.1487	<b>11.47</b>	0.1353	0.1480	<b>9.39</b>	<b>12.51</b>	<b>3.76</b>
6	0.1586	0.1848	<b>16.52</b>	0.1569	0.1725	<b>9.94</b>	0.1594	0.1678	<b>5.27</b>	<b>10.58</b>	<b>5.65</b>
8	0.1197	0.1368	<b>14.29</b>	0.1183	0.1295	<b>9.47</b>	0.1195	0.1232	<b>3.10</b>	<b>8.95</b>	<b>5.61</b>
10	0.1722	0.1942	<b>12.78</b>	0.1716	0.1883	<b>9.73</b>	0.1735	0.1806	<b>4.09</b>	<b>8.87</b>	<b>4.41</b>
12	0.1150	0.1243	<b>8.09</b>	0.1723	0.1823	<b>5.80</b>	0.1165	0.1241	<b>6.52</b>	<b>6.80</b>	<b>1.17</b>

P4VP-NR (63%)											
pH	1			2			3			Avg	SD
	w <sub>1</sub>	w <sub>2</sub>	%S	w <sub>1</sub>	w <sub>2</sub>	%S	w <sub>1</sub>	w <sub>2</sub>	%S		
2	0.1375	0.2531	<b>84.07</b>	0.1369	0.2378	<b>73.70</b>	0.137	0.2663	<b>94.38</b>	<b>84.05</b>	<b>10.34</b>
4	0.1263	0.1536	<b>21.62</b>	0.1292	0.1484	<b>14.86</b>	0.1294	0.1417	<b>9.51</b>	<b>15.33</b>	<b>6.07</b>
6	0.0839	0.0984	<b>17.28</b>	0.0835	0.0983	<b>17.72</b>	0.0813	0.0877	<b>7.87</b>	<b>14.29</b>	<b>5.57</b>
8	0.1068	0.1241	<b>16.20</b>	0.1071	0.1231	<b>14.94</b>	0.1066	0.1171	<b>9.85</b>	<b>13.66</b>	<b>3.36</b>
10	0.0718	0.0894	<b>24.51</b>	0.0760	0.0903	<b>18.82</b>	0.0738	0.0811	<b>9.89</b>	<b>17.74</b>	<b>7.37</b>
12	0.0747	0.0876	<b>17.27</b>	0.0731	0.0952	<b>30.23</b>	0.0755	0.0792	<b>4.90</b>	<b>17.47</b>	<b>12.67</b>

4VP-g-DPNR (16%)											
pH	1			2			3			AVG	SD
	w <sub>1</sub>	w <sub>2</sub>	%S	w <sub>1</sub>	w <sub>2</sub>	%S	w <sub>1</sub>	w <sub>2</sub>	%S		
2	0.0921	0.2211	<b>140.07</b>	0.0788	0.2039	<b>158.76</b>	0.0792	0.1273	<b>60.73</b>	<b>119.85</b>	<b>52.04</b>
4	0.0858	0.0993	<b>15.73</b>	0.0843	0.0965	<b>14.47</b>	0.0867	0.0931	<b>7.38</b>	<b>12.53</b>	<b>4.5</b>
6	0.0833	0.0964	<b>15.73</b>	0.0826	0.0923	<b>11.74</b>	0.0825	0.0882	<b>6.91</b>	<b>11.46</b>	<b>4.42</b>
8	0.0844	0.0983	<b>16.47</b>	0.0831	0.0956	<b>15.04</b>	0.0836	0.0909	<b>8.73</b>	<b>13.41</b>	<b>4.12</b>
10	0.0784	0.0925	<b>17.98</b>	0.0774	0.0908	<b>17.31</b>	0.079	0.0845	<b>6.96</b>	<b>14.09</b>	<b>6.18</b>
12	0.0773	0.0864	<b>11.77</b>	0.0762	0.0865	<b>13.52</b>	0.0775	0.0831	<b>7.23</b>	<b>10.84</b>	<b>3.25</b>

4VP-g-DPNR (45%)											
pH	1			2			3			AVG	SD
	w <sub>1</sub>	w <sub>2</sub>	%S	w <sub>1</sub>	w <sub>2</sub>	%S	w <sub>1</sub>	w <sub>2</sub>	%S		
2	0.0587	0.2164	<b>268.65</b>	0.0588	0.2469	<b>319.9</b>	0.1119	0.3923	<b>250.58</b>	<b>279.71</b>	<b>35.96</b>
4	0.0565	0.0663	<b>17.35</b>	0.0587	0.069	<b>17.55</b>	0.1413	0.1963	<b>38.92</b>	<b>24.61</b>	<b>12.4</b>
6	0.0609	0.0692	<b>13.63</b>	0.0611	0.0703	<b>15.06</b>	0.14	0.1945	<b>38.93</b>	<b>22.54</b>	<b>14.21</b>
8	0.0588	0.0673	<b>14.46</b>	0.0596	0.0691	<b>15.94</b>	0.1393	0.1976	<b>41.85</b>	<b>24.08</b>	<b>15.41</b>
10	0.0515	0.0613	<b>19.03</b>	0.0526	0.0638	<b>21.29</b>	0.1319	0.1834	<b>39.04</b>	<b>26.46</b>	<b>10.96</b>
12	0.0459	0.0555	<b>20.92</b>	0.046	0.0556	<b>20.87</b>	0.1248	0.1779	<b>42.55</b>	<b>28.11</b>	<b>12.5</b>

## The water contact angle measurement

pH	WCA of NR (°)					AVG	SD
2	101.19	98.69	88.03	101.59	89.52	<b>95.804</b>	<b>6.5334</b>
4	103.55	103.57	84.03	97.02	101.41	<b>97.916</b>	<b>8.2089</b>
6	108.20	97.57	99.42	108.25	86.69	<b>100.026</b>	<b>8.9260</b>
8	110.35	103.25	104.62	103.28	105.54	<b>105.408</b>	<b>2.9261</b>
10	112.86	108.85	108.45	110.89	108.49	<b>109.908</b>	<b>1.9323</b>
12	110.18	105.17	117.40	101.71	116.15	<b>110.122</b>	<b>6.7933</b>

pH	WCA of DPNR (°)					AVG	SD
2	97.99	98.86	88.10	98.68	93.27	<b>95.38</b>	<b>4.6707</b>
4	98.39	94.19	88.67	96.88	97.99	<b>95.224</b>	<b>4.0137</b>
6	91.07	98.39	100.39	97.57	89.15	<b>95.314</b>	<b>4.9072</b>
8	95.74	98.38	110.77	110.35	97.93	<b>102.634</b>	<b>7.3055</b>
10	106.13	103.11	105.99	108.00	108.85	<b>106.416</b>	<b>2.2151</b>
12	110.44	109.50	119.83	108.71	110.89	<b>111.874</b>	<b>4.5268</b>

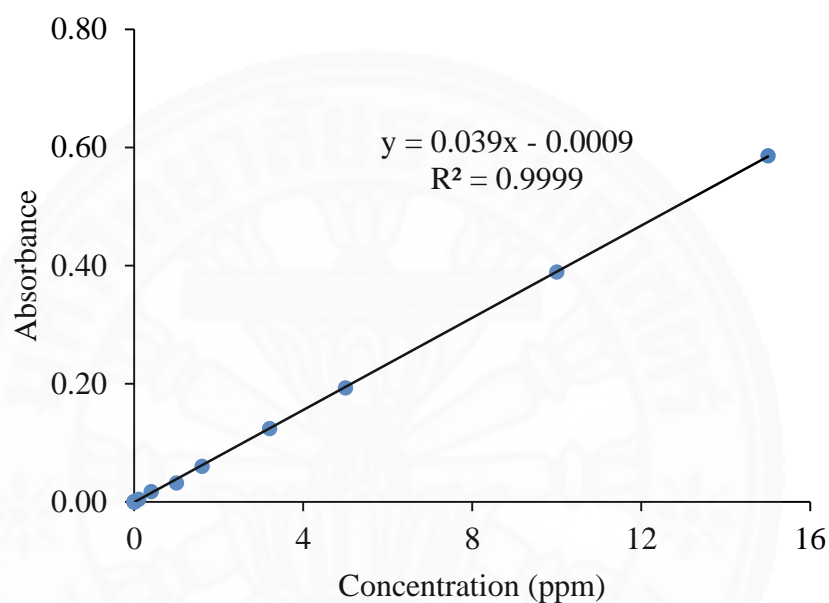
pH	WCA of P4VP-NR (°)					AVG	SD
2	15.99	31.74	28.43	28.46	29.53	<b>26.83</b>	<b>6.2073</b>
4	86.05	79.92	79.95	79.49	79.08	<b>80.898</b>	<b>2.9020</b>
6	80.11	90.09	81.91	87.85	80.88	<b>84.168</b>	<b>4.5001</b>
8	79.79	92.66	81.27	81.21	90.71	<b>85.128</b>	<b>6.0543</b>
10	87.86	88.59	89.18	84.52	87.56	<b>87.542</b>	<b>1.8038</b>
12	90.64	92.12	90.60	90.20	76.87	<b>88.086</b>	<b>6.3124</b>

pH	WCA of 4VP-g-DPNR (°)					AVG	SD
2	33.49	24.59	25.91	15.45	24.28	<b>24.74</b>	<b>6.412284</b>
4	90.77	94.68	98.61	94.30	83.28	<b>92.33</b>	<b>5.770136</b>
6	97.96	80.26	95.45	96.92	92.81	<b>92.68</b>	<b>7.207673</b>
8	89.20	91.39	92.64	103.31	97.29	<b>94.77</b>	<b>5.618454</b>
10	90.39	97.00	99.26	93.84	100.01	<b>96.10</b>	<b>3.993601</b>
12	92.57	105.20	94.20	101.24	98.64	<b>98.37</b>	<b>5.147514</b>



**APPENDIX D**  
**THE STUDY OF CONTROLLED RELEASE OF INDIGO**  
**CARMINE**

Calibration curve for calculating the amount of release indigo carmine



For the P4VP-NR sample

pH	Loaded (ppm)	Released (ppm)					
		0.5 h	1 h	1.5 h	2 h	2.5 h	3 h
2	10.10	2.95	5.48	5.61	5.88	5.77	5.88
4	10.12	0.04	1.73	3.24	4.21	4.42	4.66
6	9.53	0.31	0.57	0.89	1.26	1.68	1.79
8	8.34	0.31	0.55	0.94	1.02	1.15	1.31
10	9.98	0.34	0.55	0.73	0.92	1.07	1.21



For the 4VP-*g*-DPNR sample

pH	Loaded (ppm)	Released (ppm)					
		0.5 h	1 h	1.5 h	2 h	2.5 h	3 h
2	16.09	4.92	9.07	9.29	9.72	9.55	9.72
4	16.07	0.16	2.94	5.41	7.01	7.36	7.75
6	15.99	0.60	1.04	1.56	2.17	2.86	3.04
8	16.17	0.59	0.98	1.62	1.75	1.97	2.23
10	15.17	0.69	1.05	1.37	1.70	1.97	2.20

Calculation of relative absorbance

$$\text{Relative absorbance} = \frac{A_R}{A_0 - A_L}$$

where;  $A_R$  = the absorbance of release indigo carmine

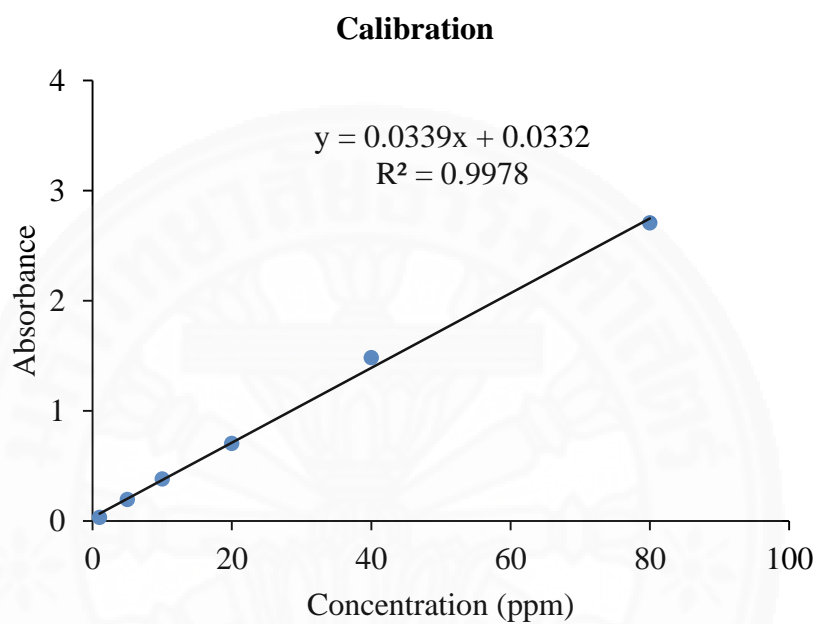
$A_0$  = the absorbance of 20 ppm indigo carmine

$A_L$  = the absorbance of loaded indigo carmine

## APPENDIX E

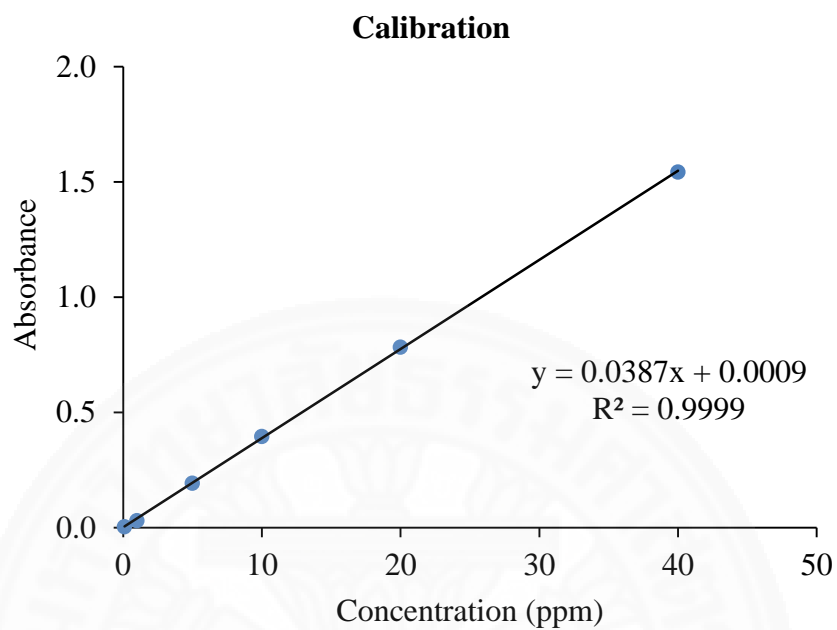
### THE STUDY OF ADSORPTION ISOTHERMS

For the adsorption of indigo carmine onto P4VP-NR



S/N	Conc. (mg/L)	V (ml)	C <sub>i</sub> (mg/L)	C <sub>e</sub> (mg/L)	W (g)	Q (mg/g)
1	10	10	10	2.147	0.1133	0.693
2	50	10	50	9.139	0.1389	2.942
3	100	10	100	21.646	0.1584	4.947
4	150	10	150	41.351	0.1272	8.542
5	200	10	200	60.260	0.1505	9.285

For the adsorption of indigo carmine onto 4VP-g-DPNR



S/N	Conc. (mg/L)	V (ml)	C <sub>i</sub> (mg/L)	C <sub>e</sub> (mg/L)	W (g)	Q (mg/g)
1	10	10	10.0	0.261	0.1008	0.966
2	50	10	50.0	9.693	0.1316	3.063
3	100	10	100.0	15.326	0.1544	5.484
4	150	10	150.0	36.876	0.178	6.355
5	200	10	200.0	37.522	0.1495	10.868

## APPENDIX F PUBLICATION

### Research Article



Received: 5 November 2016 | Revised: 16 December 2016 | Accepted article published: 23 December 2016 | Published online in Wiley Online Library: 8 February 2017

(wileyonlinelibrary.com) DOI 10.1002/pl.5316

# Preparation of pH-responsive crosslinked materials from natural rubber and poly(4-vinylpyridine)

Chanon Sansuk, Sopitcha Phetrong and Peerasak Paoprasert\*

### Abstract

Stimuli-responsive elastomers are smart materials for sensing applications. Natural rubber (NR) is a renewable elastomer with excellent elasticity and fatigue resistance. In this work, a straightforward method for the preparation of pH-responsive crosslinked materials from NR and poly(4-vinylpyridine) (P4VP) via free radical crosslinking reaction using benzoyl peroxide (BPO) as an initiator is described. The effects of P4VP and BPO concentrations, reaction time and reaction temperature on immobilization percentage were investigated. It was found that the immobilization percentage reached 90% when using a P4VP concentration of 150 phr and a BPO concentration of 10 phr for 24 h at 90 °C. The pH responsiveness of the crosslinked materials was studied via water swelling, water contact angle and dye release measurements. Unlike unmodified rubber, the P4VP-crosslinked NR was found to be pH-responsive in acidic solution. Indigo carmine adsorption studies showed the Langmuir isotherm suggesting monolayer coverage of dye on the rubber surface. The dye could also be released upon increasing the pH of solution above 4. Based on these results, the introduction of pH responsiveness to NR will lead to novel responsive rubber-based materials that can be used in biomedical and sensing applications.  
© 2016 Society of Chemical Industry

**Keywords:** natural rubber; poly(4-vinylpyridine); pH-responsive material; crosslinking

### INTRODUCTION

Natural rubber (NR) from *Hevea brasiliensis* is one of the most valuable renewable materials due to its outstanding elasticity and good mechanical properties.<sup>1</sup> However, NR is prone to degradation upon exposure to heat, light, oxygen, ozone and hydrophobic solvents, because it consists of *cis*-polyisoprene.<sup>2,3</sup> Upon exposure to these stimuli, undesirable reactions such as crosslinking and chain scission occur to the double bonds of *cis*-polyisoprene.<sup>4</sup> Many chemical-based methods for improving the properties of NR have been reported, such as hydrogenation,<sup>5,6</sup> chlorination,<sup>7,8</sup> epoxidation,<sup>9,10</sup> bromination,<sup>11</sup> sulfonation,<sup>12,13</sup> grafting<sup>14–19</sup> and crosslinking,<sup>20,21</sup> producing a range of novel rubber-based materials. However, among these materials, NR with responsive functions is rare.

Stimuli-responsive materials are unique because they can sense and respond to changes in ambient conditions, such as pH, temperature, light, ionic strength, electric field and magnetic field.<sup>22–24</sup> Changes in environmental conditions can trigger a change in the physical and chemical properties of stimuli-responsive materials, such as their size, shape, hydrophobicity, hydrophilicity and degradation rate. The Tiller group found that the shape-memory properties of crosslinked NR can be triggered using solvent vapour, temperature or mechanical force.<sup>25,26</sup> Recently, our group reported the preparation of temperature-responsive NR via crosslinking reaction between poly(*N*-isopropylacrylamide) and NR.<sup>27</sup> These stimuli-responsive materials can be used in numerous potential applications, for example in biomedical and sensing devices. Nonetheless, to the best of our knowledge, pH-responsive NR materials have never been reported.

In the work reported here, pH-responsive crosslinked materials were prepared from poly(4-vinylpyridine) (P4VP) and NR. P4VP-based polymers are known as pH-responsive materials that have been used in many sensing and biomedical applications, such as in drug delivery and biosensors.<sup>28</sup> The pendant pyridine groups are protonated in acidic conditions and their electrostatic repulsion affects the physical properties of the polymer. For example, P4VP-based materials have been used for taste-masking and achieving high bioavailability of drugs because of their low water solubility in the oral cavity and high solubility in the stomach. This can mask the unpleasant taste of drugs (pH of the oral cavity is 5.8–7.4).<sup>29</sup> Furthermore, 4-vinylpyridine is a good ligand that can form complexes with various metal ions, thereby allowing P4VP-based polymers to be used as metal absorbents<sup>29–32</sup> and catalyst ligands.<sup>33,34</sup> Despite these attractive properties of P4VP-based materials, to the best of our knowledge, no research to date has been carried out on functionalizing P4VP onto NR.

Herein, crosslinked materials were prepared from P4VP and NR using free radical crosslinking reaction in the presence of benzoyl peroxide (BPO). The crosslinking strategy was chosen because it produces a stable structure and the resulting polymer does not collapse in solution. The immobilization percentage was studied as a function of BPO concentration, P4VP concentration, reaction

\* Correspondence to: P. Paoprasert, Department of Chemistry, Faculty of Science and Technology, Thammasat University, Pathumthani 12120, Thailand. E-mail: peerasak@tu.ac.th

Department of Chemistry, Faculty of Science and Technology, Thammasat University, Pathumthani, Thailand

temperature and reaction time. The P4VP-crosslinked NR was characterized using Fourier transform infrared (FTIR) spectroscopy, NMR spectroscopy, X-ray photoelectron spectroscopy (XPS), DSC and TGA. The pH responsiveness of the material was characterized via water swelling, water contact angle and dye release measurements. Dye adsorption experiments were carried out and four adsorption isotherms, the Langmuir, Freundlich, Temkin and Dubinin–Radushkevich Isotherm models, were used to investigate the adsorption characteristics of the dye onto the modified NR materials. Based on these results, crosslinked polymers based on P4VP and rubber elastomers have a great potential in many applications such as sensing devices, drug delivery, ion exchange resins, gas separation membranes and catalyst supports.

## EXPERIMENTAL

### Materials

High ammonia preserved NR latex with 60% dry rubber content was obtained from the Department of Agriculture, Thailand. 4-Vinylpyridine monomer (95%, Acros) was purified by passing through silica gel columns prior to use. BPO (75%, Acros) was recrystallized using methanol. Formic acid, chloroform, acetone, diethyl ether, toluene and indigo carmine (Sigma-Aldrich) were used as received.

### Preparation of solid NR

NR latex was coagulated in formic acid solution (5% v/v). The coagulated rubber was washed several times with deionized water, and then dried in an oven at 60 °C for 24 h. Then, the dried yellowish rubber was purified by Soxhlet extraction using acetone for 24 h and dried again at 60 °C for 24 h.

### Synthesis of P4VP

4-Vinylpyridine (10 g) and BPO (0.1 g) were placed in a 100 mL round-bottom flask. The reaction mixture was placed in a domestic microwave oven (Electrolux EMS23275) at 800 W for 8 min. The solution was then precipitated in diethyl ether, and the polymer was filtered and dried in vacuum at 55 °C overnight to yield a yellow solid (4.5 g). <sup>1</sup>H NMR (CDCl<sub>3</sub>, 400 MHz; δ, ppm): 8.5 (aromatic CH), 6.5 (aromatic CH), 1.3 (CH<sub>2</sub>).

### Synthesis of crosslinked material from P4VP and NR (P4VP–NR)

Solid NR (1 g) was dissolved in chloroform (30 mL) followed by the addition of P4VP (50–100 phr) and BPO (5–10 phr). The reaction mixture was heated to a predetermined temperature (80–100 °C) for a specified amount of time (12–36 h). The reaction mixture was then cooled to room temperature and filtered. The solid polymer product was washed with chloroform and dried under vacuum at 60 °C for 24 h. The resulting polymer was subsequently purified by Soxhlet extraction in acetone for 24 h and dried overnight at 60 °C.

Immobilization percentage is used to determine the ratio between P4VP and NR in the crosslinked material. The immobilization percentage was calculated from the following equation:

$$\text{Immobilization (\%)} = \frac{W_2 - W_1}{W_1} \times 100$$

where  $W_1$  and  $W_2$  are the weights of the unmodified and modified rubbers, respectively.

### Determination of crosslink density

Thin P4VP–NR samples (0.75 × 0.75 cm<sup>2</sup>) were prepared. The rubber samples were then immersed in toluene at room temperature for one week. The crosslink density was calculated using the Flory–Rehner equation:<sup>35–38</sup>

$$p_c = -\frac{1}{2V_s} \frac{\ln(1 - V_r^0) + V_r^0 + \chi(V_r^0)^2}{(V_r^0)^{1/3} - (V_r^0/2)}$$

where  $p_c$  is the crosslink density (mol m<sup>-3</sup>),  $V_s$  is the molar volume of toluene (1.069 × 10<sup>-4</sup> m<sup>3</sup> mol<sup>-1</sup>) at 25 °C,  $\chi$  is the interaction parameter (0.44 + 0.18V<sub>r</sub><sup>0</sup>) and  $V_r^0$  is the fraction of rubber in the swollen gel, which can be calculated as follows:

$$V_r^0 = \frac{1}{1 + (\rho_s/\rho_r) [(W_2 - W_0)/W_0]}$$

where  $\rho_s$  and  $\rho_r$  are the densities of toluene (0.87 g mL<sup>-1</sup>) and rubber (0.92 g mL<sup>-1</sup>), respectively, and  $W_2$  and  $W_0$  are the weights of swollen and dried rubbers, respectively.<sup>39</sup>

### Determination of degree of swelling

Thin P4VP–NR samples (0.75 × 0.75 cm<sup>2</sup>) were immersed in aqueous solutions with pH values ranging from 2 to 12 at room temperature for 24 h. After removing the surface liquid gently with tissue paper, the weight of materials was measured and the degree of swelling was calculated using the following equation:

$$\text{Degree of swelling (\%)} = \frac{W_2 - W_1}{W_1} \times 100$$

where  $W_1$  and  $W_2$  are the weights of the materials before and after immersion.

### Dye adsorption and desorption studies

A thin rubber sample (0.75 × 0.75 cm<sup>2</sup>) was immersed in an aqueous solution of indigo carmine (20 ppm), a model water-soluble anionic drug, at 30 °C for one week. The rubber sample was then placed in aqueous solution (pH = 2–10) for 24 h. Aliquots were withdrawn for absorbance measurement using UV-visible spectroscopy.

### Adsorption isotherm studies

Five indigo carmine solutions (10, 20, 30, 40 and 50 ppm) were prepared using deionized water. The absorbance of these solutions was measured using a UV-visible spectrophotometer and a calibration curve was constructed. The P4VP–NR samples (0.25 g) were immersed in the indigo carmine solutions (10 mL), which were then placed on a shaker for one week. The rubber samples were removed and the absorbance of solutions was measured. Concentration of indigo carmine remaining in the solution was then calculated from the absorbance using the calibration curve.

The amount of indigo carmine adsorbed on P4VP–NR sample was calculated using the following equation:

$$Q_e = \frac{(C_0 - C_e)V}{W}$$

where  $Q_e$  (mg g<sup>-1</sup>) is the adsorption capacity of the rubber,  $C_0$  (mg L<sup>-1</sup>) is the initial concentration of indigo carmine in the solution,  $C_e$  (mg L<sup>-1</sup>) is the concentration of indigo carmine remaining in the solution,  $V$  (L) is the volume of the solution and  $W$  (g) is the dry weight of rubber sample.



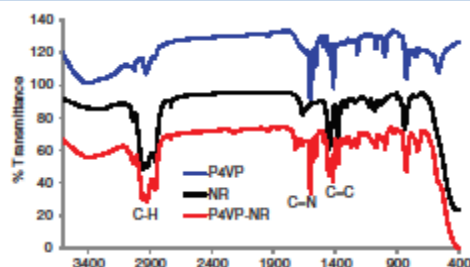


Figure 1. FTIR spectra of P4VP, NR and P4VP-NR.

### Characterization

$^1\text{H}$  NMR (400 MHz) spectra were obtained using a Bruker AVANCE NMR spectrometer with chloroform- $d$  as solvent. FTIR spectra were obtained using a PerkinElmer FTIR spectrometer (Spectrum GX model) and NaCl salt windows. TGA of the polymers was carried out using a Mettler Toledo SDTA851e analyser. The samples were heated at a rate of  $10\text{ }^\circ\text{C min}^{-1}$  under a nitrogen atmosphere. The glass transition temperatures ( $T_g$ ) of the polymers were obtained using a Mettler Toledo DSC822e differential scanning calorimeter. The samples were heated at a rate of  $10\text{ }^\circ\text{C min}^{-1}$  under a nitrogen atmosphere. The surface elements of samples were investigated using XPS (AXIS ULTRA<sup>LD</sup>, Kratos Analytical, Manchester, UK). The samples were excited using X-ray hybrid mode at a  $700 \times 300\text{ }\mu\text{m}$  spot area with monochromatic Al  $K_{\alpha 1,2}$  radiation at 1.4 keV. UV-visible spectra were obtained using a UV-1700 PharmaSpec UV-visible spectrometer. The water contact angle was measured using a TL100 Theta Lite tensiometer. The size of each water droplet was  $8\text{ }\mu\text{L}$ .

## RESULTS AND DISCUSSION

### Analysis of crosslinked material

Crosslinked polymer (P4VP-NR) was prepared from crosslinking reaction between P4VP and NR. First, P4VP was prepared by solution polymerization of 4-vinylpyridine in the presence of BPO as initiator. The P4VP was characterized using NMR and FTIR spectroscopies. NMR signals of P4VP at 6.5 and 8.5 ppm are

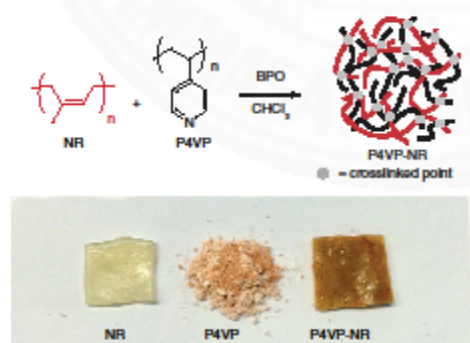


Figure 2. Schematic representation of crosslinking reaction and photographic images of NR, P4VP and P4VP-NR. Sample size is approximately  $1 \times 1\text{ cm}^2$ .

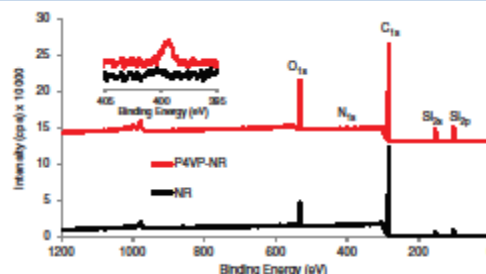


Figure 3. XPS spectra of P4VP-NR and NR. The inset shows the multiplex-scan spectra in the  $\text{N}_{1s}$  region.

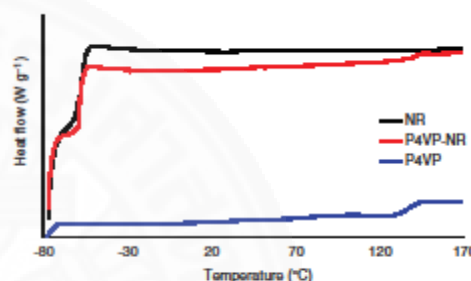


Figure 4. DSC thermograms of NR and P4VP-NR.

attributed to the aromatic protons of the pyridine rings. The FTIR spectrum of P4VP shows signals at  $2927$ ,  $1604$  and  $1417\text{ cm}^{-1}$ , which correspond to C-H stretches, C=N stretches and C=C stretches, respectively (Fig. 1), consistent with a previous report.<sup>37</sup>

Solid NR was prepared by coagulating NR latex in an acidic solution. P4VP and the solid NR were crosslinked using BPO as initiator and chloroform as solvent, as both P4VP and NR are readily soluble in this solvent. After the reaction, an insoluble polymer is formed, indicating the formation of a gel or crosslinked material. It is well known that free radical initiators can be used as crosslinking agents in NR because they can create free radicals on polymer chains via hydrogen abstraction processes.<sup>40–43</sup> The formation of free radicals on polymer chains leads to crosslinking reactions between polymer chains. After purification by Soxhlet extraction, photographs were taken of P4VP-NR and NR. The NR sample and P4VP powder are yellow and light brown, respectively (Fig. 2). The P4VP-NR sample is found to be darker than both constituent materials, indicating that P4VP-NR is not the same material as P4VP or NR. P4VP and NR are soluble in some organic solvents, for example chloroform and toluene, but the P4VP-NR sample does not dissolve in any solvents, but can only be swollen in, for example, chloroform and toluene. The formation of insoluble gel also suggests the formation of crosslinked material.

The FTIR spectra show signals of both P4VP and NR. Signals at  $1604$ ,  $1420$  and  $1000\text{ cm}^{-1}$  correspond to C=N, C=C and pyridine ring deformation of P4VP,<sup>28</sup> respectively, whereas the signal at  $1451\text{ cm}^{-1}$  corresponds to C=C stretching of the polyisoprene. P4VP-NR and NR were also characterized using XPS. XPS spectra of P4VP-NR and NR samples show signals of  $\text{O}_{1s}$ ,  $\text{C}_{1s}$ ,  $\text{Si}_{2s}$ , and  $\text{Si}_{2p}$  at  $532$ ,  $284$ ,  $153$  and  $102\text{ eV}$ , respectively (Fig. 3). The silicon signals

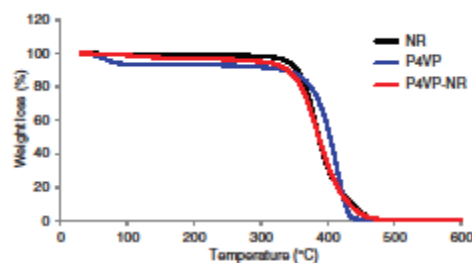


Figure 5. TGA thermograms of NR and P4VP-NR.

arise from the silicon substrate used for sample preparation. However, only the P4VP-NR sample shows a nitrogen signal at 399 eV. Hence, the XPS results also confirm the presence of P4VP in the crosslinked material. A blend sample between NR and P4VP was prepared and subjected to Soxhlet extraction in acetone in order to further confirm the formation of crosslinked material. From the NMR characterization, no P4VP signals are observed, suggesting that a physical mixing of the blend sample is unable to retain the P4VP. Hence, the presence of both P4VP and NR in the P4VP-NR sample must be due to the formation of a crosslinked or network structure inseparable by solvent extraction. The formation of insoluble products, the FTIR and XPS results and the polymer blend experiment thus confirm the formation of a crosslinked material between P4VP and NR through free radical crosslinking reaction.

The thermal properties of NR and P4VP-NR were characterized using DSC and TGA (Figs 4 and 5). The DSC thermograms show  $T_g$  of NR and P4VP at  $-58.9$  and  $137.2$  °C, respectively. P4VP-NR shows  $T_g$  of NR and P4VP components at  $-57.8$  and  $140.5$  °C. This suggests that the P4VP-NR sample still comprised amorphous domains of NR and P4VP in the crosslinked sample. The slightly

higher  $T_g$  values of P4VP-NR are due to the crosslinked structure restricting chain motions. From the TGA thermograms, it is found that NR is only slightly more thermally stable than P4VP-NR, as both start to lose weight at about 300 °C. The decomposition temperatures of the polymers, which were determined from the intersection of two tangents at the onset of the decomposition temperatures, are found to be about 352 °C for NR and 348 °C for P4VP-NR. NR is thus only slightly more stable than P4VP-NR.

In this study, the effects of reaction conditions and reagent concentrations on immobilization percentage were investigated. First, the immobilization percentage as a function of P4VP concentration was measured using a BPO concentration of 10 phr and reaction time of 24 h at 90 °C (Fig. 6(a)). It is found that, as the P4VP concentration is increased from 50 to 150 phr with respect to NR, the immobilization percentage increases from 35 to 90%. Second, the effect of BPO concentration on immobilization percentage was studied using a P4VP concentration of 100 phr and reaction time of 24 h at 90 °C (Fig. 6(b)). When the BPO concentration is increased from 5 to 15 phr, the immobilization percentage increases from 22 to 63% and then flattens out. Third, the effect of reaction temperature on immobilization percentage was investigated using a P4VP concentration of 100 phr, BPO concentration of 10 phr and reaction time of 24 h (Fig. 6(c)). It is found that when the reaction temperature is increased from 80 to 100 °C, which is an optimum working range for BPO,<sup>44</sup> the immobilization percentage increases from 55 to 77%. Lastly, the effect of reaction time on immobilization percentage was investigated using a P4VP concentration of 100 phr, BPO concentration of 10 phr and reaction temperature of 90 °C (Fig. 6(d)). When the reaction time is increased from 18 to 36 h, the immobilization percentage increases from 58 to 77%.

#### Determination of crosslink density

The crosslink density of the P4VP-NR samples was measured using the Flory-Rehner method. Crosslink density can be determined

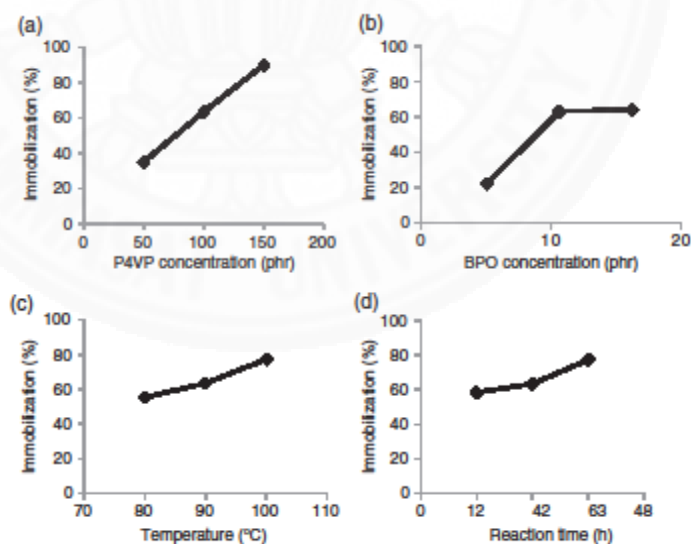


Figure 6. Immobilization percentage as a function of (a) P4VP concentration, (b) BPO concentration, (c) reaction temperature and (d) reaction time.

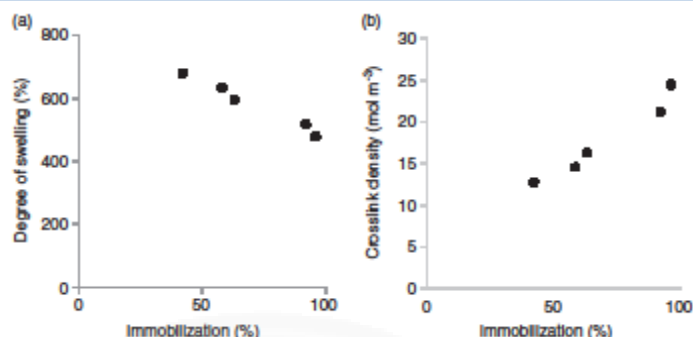


Figure 7. (a) Degree of swelling and (b) crosslink density as a function of immobilization percentage.

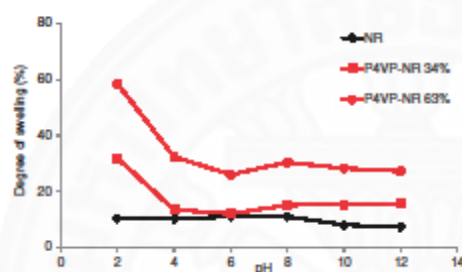


Figure 8. Degree of swelling of NR and P4VP-NR (immobilization percentage = 34 and 63%) in aqueous solutions with various pH values.

via equilibrium swelling in toluene solvent. It is found that the higher the immobilization percentage, the lower the degree of swelling. In addition, the crosslink density is proportional to the immobilization percentage. At an immobilization percentage of 42%, the crosslink density is 13%. This increases to 24% at an immobilization percentage of 96% (Fig. 7). The crosslink density is thus dependent on the proportion of P4VP in the crosslinked material.

#### pH responsiveness

The pH responsiveness of P4VP-NR was characterized in aqueous solutions for pH in the range 2–12. It is found that P4VP-NR shows hydrogel-like behaviour. It becomes more swollen than the pristine NR due to the presence of hydrophilic vinylpyridine units (Fig. 8). In addition, the P4VP-NR sample with higher immobilization percentage is more swollen than that with lower immobilization percentage. The degree of swelling of the P4VP-NR samples increases when the pH of the solution is below 4, whereas that of the NR sample does not change. Pyridine is a weak base in which the  $pK_a$  of its conjugate acid, pyridinium salt, is 4.7.<sup>45</sup> When the pH of solution is below 4.7, pyridine is converted into pyridinium salt containing positive charges. Due to the electrostatic repulsion of positive charges, the materials become swollen and absorb more water.<sup>28</sup> When the pH is increased above 4, the pyridine groups are deprotonated and become neutral, leading to less adsorption of water and a lower degree of swelling.

The pH responsiveness of P4VP-NR was confirmed by water contact angle measurements (Fig. 9). It is found that the NR sample

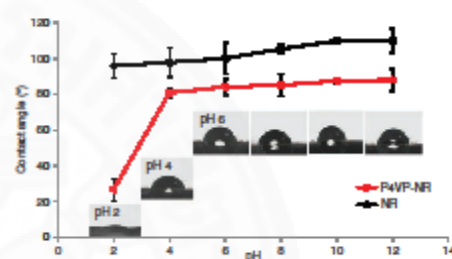


Figure 9. Contact angles of NR and P4VP-NR for solutions of various pH.

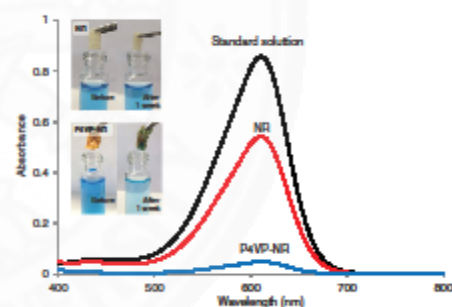


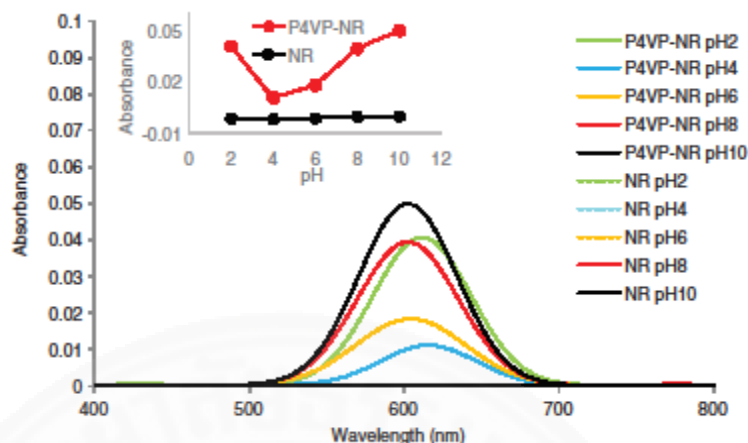
Figure 10. UV-visible spectra of standard indigo carmine solution and solutions after immersion of NR and P4VP-NR samples.

shows contact angles of around 95–110° through the pH range used in this experiment, consistent with previous reports.<sup>6,27</sup> The slight increase in contact angle is possibly due to the interaction with the surface protein of the latex. The P4VP-NR samples show an abrupt increase in contact angle from 28° to 80° when the pH is changed from 2 to 4. The contact angles remain steady after that. This result confirms that P4VP-NR is pH-responsive under acidic conditions.

#### Adsorption and desorption of indigo carmine

In this study, the adsorption and desorption of indigo carmine dye from P4VP-NR and NR were analysed. Indigo carmine was





**Figure 11.** UV-visible spectra of solutions after desorption of indigo carmine from NR and P4VP-NR. The inset shows the absorbance values at various pH.

chosen to represent a water-soluble anionic model drug. The rubber samples were incubated in indigo carmine solution for one week at room temperature. It is found that P4VP-NR can adsorb more dye than NR, as shown by a greater reduction of absorption intensity (Fig. 10). After dye adsorption, the rubber samples were taken out and then immersed in aqueous solutions with various pH values and the absorbance was measured to monitor the release of the indigo carmine. The absorbance of the NR samples does not change significantly as the pH is increased from 2 to 10, indicating that the NR is not pH-responsive (Fig. 11). For the P4VP-NR samples, significantly more dye is released when the pH values of the solution are 2, 8 and 10. At a pH of 2, the dye release is possibly due to the material becoming highly protonated, leading to a large free volume inside the material, thereby allowing the dye to be released. At a pH of 8 and 10, the dye release is due to the vinylpyridine groups becoming neutral, which is unfavourable for interactions between neutral rubber and anionic dye. These pH-response studies suggest that P4VP-NR material has potential applications in responsive drug release, separation membranes and activators for enzymes.<sup>46–48</sup>

#### Adsorption isotherm studies

In this study, the Langmuir, Freundlich, Temkin and Dubinin–Radushkevich isotherm models were used to investigate the interaction between adsorbate molecules and adsorbent surface, i.e. the interaction between indigo carmine and P4VP-NR, respectively. The Langmuir adsorption isotherm is commonly used to describe the formation of monolayer coverage on the surface of an adsorbent. The Freundlich adsorption isotherm describes the adsorption characteristics based on multilayer adsorption. The Temkin adsorption isotherm considers the indirect effects on adsorbate–adsorbent interaction, such as heat, which can influence the adsorption mechanism. Lastly, the Dubinin–Radushkevich model describes the adsorption on both homogeneous and heterogeneous surfaces based on pore filling mechanism. The mathematical equations of these four models are summarized in Table 1.<sup>49–51</sup> Linear regression analysis shows that the Langmuir adsorption isotherm yields the highest linear

**Table 1.** Mathematical equations for the Langmuir, Freundlich, Temkin and Dubinin–Radushkevich isotherm models<sup>a</sup>

Isotherm	Equation	Linear form
Langmuir	$Q_e = \frac{Q_0 K_L C_e}{1 + K_L C_e}$	$\frac{1}{Q_e} = \frac{1}{Q_0} + \frac{1}{Q_0 K_L C_e}$
Freundlich	$Q_e = K_f C_e^{1/n}$	$\log Q_e = \log K_f + \frac{1}{n} \log C_e$
Temkin	$Q_e = \frac{bT}{b_0} \ln(A_T C_e)$	$Q_e = B \ln A_T + B \ln C_e$
Dubinin–Radushkevich	$Q_e = (q_s) \exp(-K_{ad} \epsilon^2)$	$\ln Q_e = \ln(q_s) - (K_{ad} \epsilon^2)$

<sup>a</sup>  $C_e$  is the equilibrium concentration of adsorbate ( $\text{mg L}^{-1}$ ),  $Q_e$  is the amount of dye adsorbed per gram of adsorbent at equilibrium ( $\text{mg g}^{-1}$ ),  $Q_0$  is the maximum monolayer coverage capacity ( $\text{mg g}^{-1}$ ),  $K_L$  is the Langmuir isotherm constant ( $\text{L mg}^{-1}$ ),  $K_f$  is the Freundlich isotherm constant ( $\text{mg g}^{-1}$ ),  $n$  is the adsorption intensity,  $A_T$  is the Temkin isotherm equilibrium binding constant ( $\text{L mg}^{-1}$ ),  $b_0$  is the Temkin isotherm constant,  $R$  is the universal gas constant ( $8.314 \text{ J mol}^{-1} \text{ K}^{-1}$ ),  $T$  is the temperature at  $303.15 \text{ K}$ ,  $B$  is a constant related to heat of sorption ( $\text{J mol}^{-1}$ ),  $q_s$  is the theoretical isotherm saturation capacity ( $\text{mg g}^{-1}$ ),  $K_{ad}$  is the Dubinin–Radushkevich isotherm constant ( $\text{mol}^2 \text{ J}^{-2}$ ) and  $\epsilon$  is the Dubinin–Radushkevich isotherm constant.

$R^2$  value of 0.8 (Fig. 12). This study indicates that the interaction between indigo carmine and P4VP-NR likely takes place as monolayer adsorption. The maximum monolayer coverage capacity ( $Q_0$ ) and Langmuir isotherm constant ( $K_L$ ) determined from slope and intercept are  $1.55 \text{ mg g}^{-1}$  and  $0.25 \text{ L mg}^{-1}$ , respectively.

The isotherm constants provide evidence about the adsorption mechanism. The Freundlich isotherm gives a value of adsorption intensity ( $n$ ) of larger than 1, indicating that the adsorption of dye onto P4VP-NR is favourable (Table 2).<sup>52,53</sup> In addition, the value of mean sorption energy ( $E$ ) from the Dubinin–Radushkevich isotherm gives information about chemical and physical adsorption. The  $E$  value of  $1 \text{ kJ mol}^{-1}$  is in the range of  $1–8 \text{ kJ mol}^{-1}$ , revealing that the type of adsorption of indigo carmine on P4VP-NR is physical adsorption.<sup>51,54,55</sup>

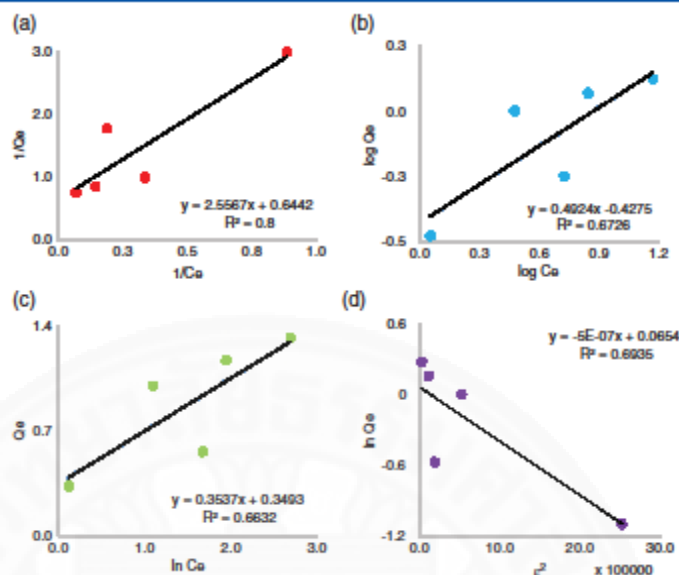


Figure 12. Linear adsorption isotherms based on (a) Langmuir, (b) Freundlich, (c) Temkin and (d) Dubinin–Radushkevich models.

Langmuir isotherm				Freundlich isotherm			
$Q_0$ (mg g <sup>-1</sup> )	$K_L$ (L mg <sup>-1</sup> )	$R_L$	$R^2$	$1/n$	$n$	$K_f$ (mg g <sup>-1</sup> )	$R^2$
1.552	0.252	0.284	0.8	0.4924	2.03	0.374	0.6726
Temkin isotherm				Dubinin–Radushkevich isotherm			
$A_T$ (L mg <sup>-1</sup> )	$b_T$	$B$	$R^2$	$q_s$ (mg g <sup>-1</sup> )	$K_{ad}$ (mol <sup>2</sup> J <sup>-2</sup> )	$E$ (kJ mol <sup>-1</sup> )	$R^2$
2.685	7075.24	0.3537	0.6632	1.068	$5 \times 10^{-7}$	1	0.6935

## CONCLUSIONS

Crosslinked materials of P4VP and NR were successfully prepared via free radical crosslinking reaction. The crosslinked materials were rubber-like with thermal properties close to those of unmodified NR. The materials showed pH responsiveness in acidic conditions, as confirmed by water swelling, water contact angle and dye release studies. Dye adsorption revealed monolayer adsorption characteristics. These pH-responsive, hydrogel-like rubbers will be useful for a variety of biomedical and sensing applications. Future work includes increasing the release rate of the crosslinked materials. Based on our work, it will also be possible to prepare other types of responsive or multi-stimuli-responsive rubbers through the reactions of multiple responsive materials, which will extend the properties and expand the range of applications of these rubbers.

## ACKNOWLEDGEMENTS

This work was financially supported by the Thailand Research Fund (TRF) and the Faculty of Science and Technology, Thammasat

University (TRGS880199). The authors acknowledge the Central Scientific Instrument Center (CSIC), Department of Chemistry, Faculty of Science and Technology, and Thammasat University.

## REFERENCES

- Graves DF, *Rubber*, in *Handbook of Industrial Chemistry and Biotechnology*, ed. by Kent JA, Springer, New York, pp. 689–718 (2007).
- Zhong J-P, Li S-D, Yu H-P, Wei Y-C, Peng Z, Qu J-L et al., *J Appl Polym Sci* **81**:1305–1309 (2001).
- dos Santos KAM, Suarez PAZ and Rubim JC, *Polym Degrad Stab* **90**:34–43 (2005).
- Chaikumpollert O, Sae-Heng K, Wakisaka O, Mase A, Yamamoto Y and Kawahara S, *Polym Degrad Stab* **96**:1989–1995 (2011).
- Hinchiranan N, Charmondusit K, Prassarakich P and Rempel GL, *J Appl Polym Sci* **100**:4219–4233 (2006).
- Kookarinnat C and Paoprasert P, *Iran Polym J* **24**:123–133 (2015).
- Zhong J-P, Li S-D, Wei Y-C, Peng Z and Yu H-P, *J Appl Polym Sci* **73**:2863–2867 (1999).
- Chanroj T and Paoprasert P, *Rubber Chem Technol* **89**:251–261 (2016).
- Phinyocheep P, Phetphaisit CW, Derouet D, Campistron I and Brosse JC, *J Appl Polym Sci* **95**:6–15 (2005).
- Chusijulit S, Yaowsang C, Na-Ranong N and Potiyaraj P, *J Appl Polym Sci* **100**:3948–3955 (2006).

- 11 Xue X, Wu Y, Wang F, Ling J and Fu X, *J Appl Polym Sci* **118**:25–29 (2010).
- 12 Xavier T, Samuel J, Manjoran KB and Kurian T, *J Elastom Plast* **34**:91–101 (2002).
- 13 Suksawad P, Yamamoto Y and Kawahara S, *Eur Polym J* **47**:330–337 (2011).
- 14 Nakason C, Kaesaman A and Supasanthikul P, *Polym Test* **23**:35–41 (2004).
- 15 Kangwansupamonkon W, Gilbert RG and Kiattkamjornwong S, *Macromol Chem Phys* **206**:2450–2460 (2005).
- 16 Kochthongrasamee T, Prasassarakich P and Kiattkamjornwong S, *J Appl Polym Sci* **101**:2587–2601 (2006).
- 17 Amnuaypanich S and Ratpolan P, *J Appl Polym Sci* **113**:3313–3321 (2009).
- 18 Juntuek P, Ruksakulpiwat C, Chumsamrong P and Ruksakulpiwat Y, *J Appl Polym Sci* **122**:3152–3159 (2011).
- 19 Pisuttisap A, Hinchiranan N, Rempel GL and Prasassarakich P, *J Appl Polym Sci* **129**:94–104 (2013).
- 20 Turner DT, *Polymer* **1**:27–40 (1960).
- 21 Lewis PM, *NR Technology* **17**:57–65 (1986).
- 22 Chen J-K and Chang C-J, *Materials* **7**:805–875 (2014).
- 23 Yoshida T, Lai TC, Kwon GS and Sako K, *Expert Opin Drug Deliv* **10**:1497–1513 (2013).
- 24 Almeida H, Amaral MH and Lobão P, *J Appl Pharma Sci* **02**:1–10 (2012).
- 25 Quitmann D, Gushterov N, Sadowski G, Katzenberg F and Tiller JC, *ACS Appl Mater Interfaces* **5**:3504–3507 (2013).
- 26 Heuwers B, Beckel A, Krieger A, Katzenberg F and Tiller JC, *Macromol Chem Phys* **214**:912–923 (2013).
- 27 Nuntahirun P, Yamamoto O and Paoprasert P, *Macromol Res* **24**:816–823 (2016).
- 28 Kavitha T, Kang I-K and Park S-Y, *Polym Int* **64**:1660–1666 (2015).
- 29 Ozay O, Ekici S, Aktas N and Sahiner N, *J Environ Manag* **92**:3121–3129 (2011).
- 30 El-Hamshary H, El-Garawany M, Assubaie FN and Al-Eed M, *J Appl Polym Sci* **89**:2522–2526 (2003).
- 31 Vrela P, Palacin S, Descours F, Bureau C, Derf FL, Lyskawa J et al, *Appl Surf Sci* **212**–213:792–796 (2003).
- 32 Cao L, Hu Y, Zhang L, Ma C, Wang X and Wang J, *J Supercrit Fluids* **58**:233–238 (2011).
- 33 Borah KJ and Borah PD, *Bull Korean Chem Soc* **32**:225–228 (2011).
- 34 Pardey AJ, Rojas AD, Yáñez JE, Betancourt P, Scott C, Chinae C et al, *Polyhedron* **24**:511–519 (2005).
- 35 Saijun D, Nakason C, Kaesaman A and Klinpituksa P, *Songklanakaraj Sci Technol* **31**:561–565 (2009).
- 36 Vudjung C, Chaisuwan U, Pangan U, Chaipugdee N, Boonyod S, Santawitee O et al, *Energy Procedia* **56**:255–263 (2014).
- 37 Flory PJ and Rehner Jr J, *J Chem Phys* **11**:512–520 (1943).
- 38 Flory PJ and Rehner Jr J, *J Chem Phys* **11**:521–526 (1943).
- 39 Cambridge University Engineering Department, Materials Data Book (2003). Available: <http://www-mdp.eng.cam.ac.uk/web/library/enginfo/cueddatabooks/materials.pdf> [10 October 2016].
- 40 Manaila E, Stelescu MD, Cracian G and Surdu L, *Polym Bull* **71**:2001–2022 (2014).
- 41 Halimatuddahlana, Ismail H and Akil HM, *Int J Polym Mater* **54**:1169–1183 (2005).
- 42 Liu H, Chuai C, Iqbal M, Wang H, Kalsoom BB, Khattak M et al, *J Appl Polym Sci* **122**:973–980 (2011).
- 43 Tamboli SM, Mhaske ST and Kale DD, *J Appl Polym Sci* **122**:973–980 (2011).
- 44 Paoprasert P, Moonrinta S and Kanokul S, *Polym Int* **63**:1041–1046 (2014).
- 45 Ana Arizaga GI and Piñol R, *J Colloid Interface Sci* **348**:668–672 (2010).
- 46 Tobis J, Boch L, Thomann Y and Tiller JC, *J Membr Sci* **372**:219–227 (2011).
- 47 Hanko M, Bruns N, Tiller JC and Heinze J, *Anal Bioanal Chem* **386**:1273–1283 (2006).
- 48 Bruns N, Banerwarth W and Tiller JC, *Biotechnol Bioeng* **101**:19–26 (2008).
- 49 Chen X, *Information* **4**:14–22 (2015).
- 50 Dada AO, Olalekan AP, Olatunya AM and Dada O, *IOSR J Appl Chem* **3**:38–45 (2012).
- 51 Zheng H, Liu D, Zheng Y, Liang S and Liu Z, *J Hazard Mater* **167**:141–147 (2009).
- 52 Hameed BH, Mahmoud DK and Ahmad AL, *J Hazard Mater* **158**:65–72 (2008).
- 53 Ho YS and McKay G, *Chem Eng J* **70**:115–124 (1998).
- 54 Saltak K, San A and Aydin M, *J Hazard Mater* **141**:258–263 (2007).
- 55 Zheng H, Wang Y, Zheng Y, Zhang H, Liang S and Long M, *Chem Eng J* **143**:117–123 (2008).

ISBN 978-81-933894-0-9  
5th International Conference on Advances in Chemical, Biological & Environmental Engineering  
(ACBEE-17)  
Singapore, 27-30 March, 2017

## Preparation and Characterization of Deproteinized Natural Rubber Grafted with 4-Vinylpyridine as pH Responsive Materials

Chanon Sansuk<sup>1</sup>, Sopitcha Phetrong<sup>1</sup>, and Peerasak Paoprasert<sup>1,a</sup>

<sup>1</sup> Department of Chemistry, Faculty of Science and Technology, Thammasat University, Pathumthani, Thailand

<sup>a</sup> Corresponding author : peerasak@tu.ac.th

*Abstract: Natural rubber is one of the renewable materials with excellent properties, including high elasticity and fatigue resistance. This work reports a method to introduce a pH-responsive function to natural rubber. 4-vinylpyridine was functionalized onto deproteinized natural rubber latex via graft copolymerization in the water medium. The grafted copolymer (4VP-g-DPNR) was characterized using Fourier-transform infrared spectroscopy, nuclear magnetic resonance spectrometer, and X-ray photoelectron spectroscopy. The pH-responsiveness of the functionalized materials was studied in aqueous solutions via water swelling experiment. It was found that the 4VP-g-DPNR sample became swollen under acidic conditions whereas the unmodified rubber did not change in any pH solutions. Based on these results, this work thus demonstrated a method to add the pH responsive function to natural rubber. The introduction of pH responsiveness into natural rubber will lead to new responsive rubber-based materials and widen their applications.*

*Keywords: Grafting, pH-responsive material, Natural rubber, Deproteinization, 4-vinylpyridine*

### 1. Introduction

Natural rubber (NR) from *Hevea brasiliensis* is one of the most valuable renewable resources. It has attracted significant interest in many fields, including the automobile, consumer, and medical sectors, mainly due to its outstanding elasticity and good mechanical properties [1]. Thailand is the largest producer and exporter in the world [2].

The graft copolymerization of a vinyl monomer onto NR is one of the most interesting and widely studied fields of research into adding value and function to NR. Graft copolymerization of NR is usually carried out via free radical method, which can be initiated by chemical initiator, high energy radiation, or UV illumination, under various conditions [3]. Several types of monomer have been reported producing a range of new rubber-based materials [4-9]. However, among these materials, NR with responsive functions is rare. Adding responsive functions to the unique properties of NR will expand the range of applications, for example, sensing devices and smart biomedical materials. Stimuli responsive materials are unique because they can sense and respond to changes in ambient conditions, such as pH, temperature, light, ionic strength, electric field, and magnetic field [10-12]. Changes in environmental conditions can trigger a change in the physical and chemical properties of stimuli-responsive materials, such as their size, shape, hydrophobicity/hydrophilicity, and degradation rate. The stimuli-responsive materials have numerous potential applications.

4-Vinylpyridine (4VP)-based polymers are known as pH-responsive materials that can potentially be used in many sensing and biomedical applications, such as in drug delivery and biosensors [13]. In addition, 4-vinylpyridine is a good ligand for the formation of complexes with metal ions, thereby allowing P4VP-based polymers to be used as metal absorbents [14, 15].



Therefore, in this work, a method for functionalizing 4-vinylpyridine (4VP) onto deproteinized natural rubber latex (DPNR) was demonstrated. 4VP was grafted onto DPNR via emulsion polymerization in the presence of potassium persulfate (KPS) as initiator and sodium dodecyl sulfate (SDS) as emulsifier. Thus, integration of 4VP and DPNR will expand the range of applications of rubber-based materials.

## 2. Materials and Methods

### 2.1. Materials

High-ammonia NR latex (60% dry rubber content) was purchased from Department of Agriculture, Thailand. All chemicals were purchased from Sigma-Aldrich. 4-vinylpyridine monomer (4VP) (95%, Acros) was purified by passing through silica gel columns prior to use. Deionized (DI) water was used throughout all experiments.

### 2.2. Preparation of Deproteinized Natural Rubber Latex

The deproteinized natural rubber latex (DPNR) was firstly prepared by incubation of the high-ammonia NR latex (60% dry rubber content) with 0.1% w/w urea in the presence of 1% w/w sodium dodecyl sulfate (SDS) for 30 min. Then, the incubated urea natural rubber latex was centrifuged at 10,000 rpm for 60 min. The recovered cream fraction (top layer) was re-dispersed in 1% w/w SDS to further wash the rubber particles. The washing process was repeated twice and then the recovered cream was re-dispersed in 1% w/w SDS to make DPNR latex [16].

### 2.3. Grafting of 4VP on DPNR

The DPNR latex (5 g) was firstly placed into a 250 mL two-neck round-bottom flask equipped with a mechanical stirrer and reflux condenser, followed by dilution with DI water (5 mL). A solution of potassium hydroxide (0.1 g) to maintain pH of the system and sodium dodecyl sulfate (0.1 g) as an emulsifier was then added. The 4VP (150 phr with respect to dry rubber content) monomer was then gradually dropped. The reaction mixture was continuously stirred for 30 min to allow rubber particles to swell with 4VP monomer and become homogeneous. After that, the reaction was heated to approximately 70 °C and a solution of potassium persulfate (10 phr with respect to dry rubber content) in distilled water was added. The reactions were allowed to proceed under agitation at 90 °C for 3 hours and then the reactor was discharged. The grafted latex was coagulated with 5 wt% acetic acid, washed several times with distilled water, and dried up in an oven at 60 °C for an overnight. The obtained product was purified by soxhlet extraction in acetone for 24 hours to remove the residue free monomer, homopolymer, and any contaminants, followed by dry at 60 °C for 24 hours.

The grafting ratio was calculated from the following equation:

$$\text{Grafting ratio (\%)} = \frac{I_{8.5}}{I_{5.1}} \times 100, \quad (1)$$

where  $I_{8.5}$  and  $I_{5.1}$  are the integrated signal area of the proton of pyridine ring of 4VP unit and the unsaturated methyne proton of polyisoprene, respectively.

### 2.4. Water swelling experiment

The P4VP-NR and dry NR were cut into small pieces (1x1 cm<sup>3</sup>). The samples were immersed in aqueous solutions with pH ranging from 2 to 12 for 24 hours at room temperature. The pH of the solution was adjusted using 0.1 M HCl and 0.1 M NaOH deionized water. After removing the surface liquid gently with tissue paper, the weight of materials was measured and the swelling percentage was according to the following equation:

$$\text{Swelling (\%)} = \frac{W_2 - W_1}{W_1} \times 100, \quad (2)$$

where  $W_1$  and  $W_2$  was the weight of the material before and after immersion, respectively.

### 2.5. Characterization

<sup>1</sup>H (400 MHz) Nuclear Magnetic Resonance (NMR) spectra were obtained using an AVANCE Bruker NMR Spectrometer with chloroform-d as a solvent. The Fourier transform infrared (FT-IR) spectra were obtained

using a Perkin Elmer FT-IR (Spectrum GX model) and NaCl salt windows. The CHN analyzer was obtained using Perkin-Elmer 2400 series CHNS/O Analyzer. The surface elements of the sample were investigated using an X-ray photoelectron spectrometer (XPS; AXIS ULTRA<sup>DLD</sup>, Kratos analytical, Manchester UK.) The base pressure in the XPS analysis chamber was about  $5 \times 10^{-9}$  torr. The samples were excited using X-ray hybrid mode at a  $700 \times 300 \mu\text{m}$  spot area with a monochromatic Al  $K_{\alpha 1,2}$  radiation at 1.4 keV.

### 3. Results and Discussion

#### 3.1. Analysis of grafted material

In this work, the graft copolymerization of 4VP onto natural rubber latex (NR) was prepared by emulsion polymerization. Prior to grafting reaction, NR was deproteinized to remove surface proteins in order to increase grafting efficiency. The DPNR was prepared using urea as surfactant. From CHN analyzer, the total nitrogen content in the as-prepared DPNR was reported as shown in Table 1. It was found that total nitrogen content of the as-prepared DPNR decreased, compared with untreated NR. Thus, in this work, urea and SDS were able to remove protein from NR, consistent with previous reports [17-19].

TABLE I: C, H, and N data of NR and DPNR.

Sample Name	Composition (%w/w)		
	Carbon	Hydrogen	Nitrogen
NR	84.79	12.68	0.76
DPNR	84.19	12.88	0.43

The graft copolymerization of 4VP and DPNR in water medium was carried out in the presence of potassium persulfate (KPS) as initiator and sodium dodecyl sulfate (SDS) as emulsifier. It is well-known that KPS thermally dissociates to generate free radicals as shown in Figure 1. Those free-radicals reacted with DPNR at the  $\alpha$ -methylene hydrogen atom via hydrogen abstraction processes to give polyisoprene radicals [6, 16]. The polyisoprene radicals then react with 4VP monomer during propagation to obtain 4VP-g-DPNR (Figure 2a). After the graft copolymerization and purification process, the photograph of the obtained 4VP-g-DPNR was taken, showing a yellowing solid rubber (Figure 2b).

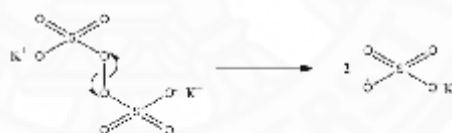


Fig. 1: Thermal decomposition of potassium persulfate.

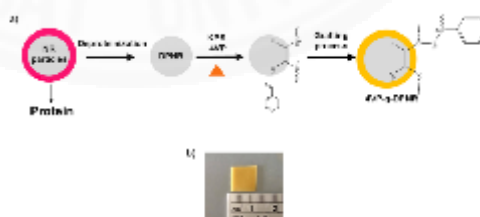


Fig. 2: Schematic representation of (a) grafting reaction between 4VP and DPNR using KPS and (b) photograph of DPNR-grafted 4VP. Sample size is approximately  $1 \times 1 \text{ cm}^2$ .

The FT-IR spectrum of the DPNR in Figure 3. exhibited the vibration bands of C=C stretching and bending at  $1662\text{ cm}^{-1}$  and  $841\text{ cm}^{-1}$ , CH<sub>3</sub> stretching at  $2961\text{ cm}^{-1}$ , CH<sub>2</sub> stretching at  $2916\text{ cm}^{-1}$ , CH<sub>2</sub> bending at  $1451\text{ cm}^{-1}$ , CH<sub>3</sub> bending at  $1376\text{ cm}^{-1}$ , and =C-H bending at  $835\text{ cm}^{-1}$ . [20] After the graft copolymerization and soxhlet extraction by acetone, the 4VP-g-DPNR showed the signatures of both P4VP and DPNR. The important characteristic bands for the grafted materials appeared at  $1604\text{ cm}^{-1}$ ,  $1420\text{ cm}^{-1}$ , and  $1000\text{ cm}^{-1}$ , corresponding to C=N, C=C, and pyridine ring deformation, respectively, [13], whereas the signal at  $1451\text{ cm}^{-1}$  corresponded to CH<sub>2</sub> bending of the polyisoprene, suggesting the occurrence of grafting process of 4VP onto DPNR.

The confirmation of the chemical structure was then investigated using <sup>1</sup>H-NMR. Figure 4. shows <sup>1</sup>H-NMR spectrum of 4VP-g-DPNR. The signal characteristic peak of DPNR appeared at 1.7, 2.0 and 5.1 ppm, which were assigned to methyl (-CH<sub>3</sub>), methylene (-CH<sub>2</sub>-), and unsaturated methane (=C-H-) protons of isoprene units, respectively. Moreover, broad signals around 6.5 and 8.5 ppm were attributed to the aromatic protons of the pyridine rings [21, 22]. These confirmed that 4VP was grafted onto DPNR. The grafting efficiency determined from the <sup>1</sup>H-NMR spectrum was 45%.

In addition, the chemical composition at the surface of the graft copolymer using an XPS technique is shown in Figure 5. Signals of O<sub>1s</sub>, C<sub>1s</sub>, Si<sub>2p</sub>, and Si<sub>2p</sub> were observed on DPNR sample at binding energies of 532 eV, 285 eV, 153 eV, and 102 eV, respectively. It can be seen that the chemical composition of the DPNR sample mainly consisted of carbon atoms and the presence of the small oxygen content may resulted from the impurities in the rubber latex [23]. Moreover, the silicon signals arose from the silicon substrate used for the measurement. Unlike the DPNR sample, only the 4VP-g-DPNR sample showed a nitrogen signal at 399 eV, which owing to the presence of nitrogen atom of pyridine ring in the grafted material [24]. Hence, in this work, the results from FT-IR, <sup>1</sup>H-NMR, and XPS on 4VP-g-DPNR sample indicated the successful graft copolymerization of 4VP on DPNR via using emulsion polymerization.

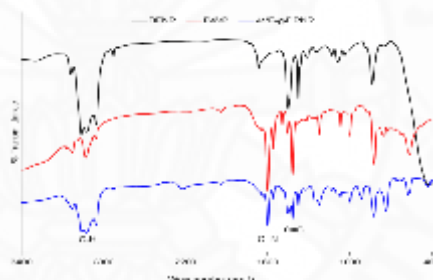


Fig. 3: FTIR spectra of DPNR, P4VP and 4VP-g-DPNR.

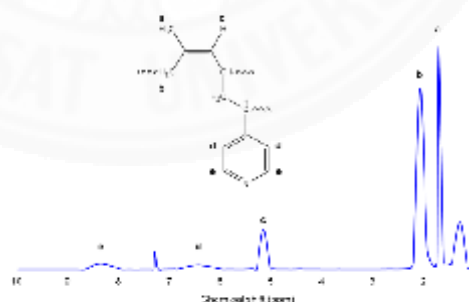


Fig. 4: <sup>1</sup>H-NMR spectrum of 4VP-g-DPNR.

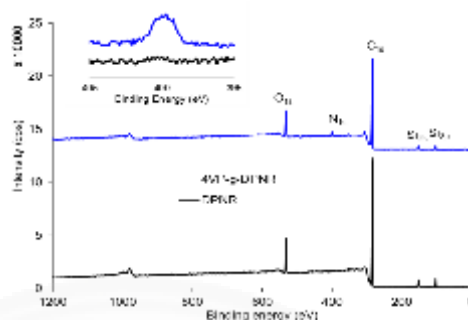


Fig. 5: XPS spectra of 4VP-g-DPNR and DPNR. The inset shows the multiplex-scan spectra in the  $N_{1s}$  region.

### 3.2. pH responsiveness

The pH responsiveness of DPNR and 4VP-g-DPNR samples was characterized in aqueous solutions for a pH range of 2-12. It was found that 4VP-g-DPNR sample became more swollen than the pristine DPNR sample due to the presence of hydrophilic vinylpyridine units (Figure 6). The swelling percentage of the 4VP-g-DPNR samples increased when the pH of the aqueous solution was below 4 whereas that of the DPNR sample did not change in any pH of the aqueous solution. Since, pyridine is a weak base in which the  $pK_a$  of 4.7 [25]. When the pH of solution is below 4.7, pyridine is protonated and converted into pyridinium salt containing positive charges. Since the electrostatic repulsion of positive charges, the materials become swollen and absorb more water. When the pH was higher than 4, the pyridine groups were deprotonated or became neutral, leading to a lower swelling percentage. In addition, it was also found that the swelling ratio increased as the grafting ratio increased owing to the greater amount of 4VP onto the samples.

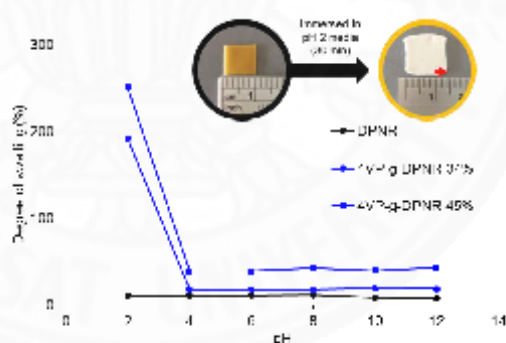


Fig. 6: Degree of swelling of DPNR and 4VP-g-DPNR (grafting ratio =34 and 45 %) in aqueous solutions with various pH values.

## 4. Conclusions

In this work, 4VP-g-DPNR was successfully prepared via emulsion polymerization. The materials showed pH responsiveness in acidic conditions when pH was below 4, as confirmed by water swelling. Based on our work, it will also be possible to prepare other types of responsive or multi-stimuli-responsive rubbers through



the reactions of multiple responsive materials, which will extend the properties and expand the range of applications of these rubbers.

## 5. Acknowledgement

This work is financially supported by the Thailand Research Fund (TRF) and the Faculty of Science and Technology, Thammasat University (TRG5880199). The authors acknowledge the Central Scientific Instrument Center (CSIC), Department of Chemistry, Faculty of Science and Technology, and Thammasat University. In addition, the authors would like to thank the reviewers and journal editors for useful comments and suggestions.

## 6. References

- [1] S. Kohjiya, and Y. Ikeda, *Chemistry, Manufacture and Applications of Natural Rubber*. Woodhead publishing., 2014.
- [2] C. Saengruksawong, S. Khamyong, N. Anongrak *et al.*, "Growths and Carbon Stocks of Para Rubber Plantations on Phonpisai Soil Series in Northeastern Thailand," *RUBBER THAI JOURNAL*, vol. 1, pp. 1-18, 2012.
- [3] M. Yeganeh-Ghotbi, and V. Haddadi-Asl, "Surface Modification of SBR and NR by Hydrophilic Monomers (I): Effect of Structural Parameters and Inhibitors," *Iranian Polymer Journal*, vol. 9, no. 3, pp. 183-189, 2000.
- [4] W. Kangwansupamonkon, R. G. Gilbert, and S. Kiatkamjornwong, "Modification of Natural Rubber by Grafting with Hydrophilic Vinyl Monomers," *Macromolecular Chemistry and Physics*, vol. 207, no. 6, pp. 2450-2460, 2006.
- [5] C. Nakason, A. Kaesaman, and P. Supasanthitkul, "The grafting of maleic anhydride onto natural rubber," *Polymer Testing*, vol. 23, pp. 35-41, 2004.
- [6] T. Kochthongrasamee, P. Prasassarakich, and S. Kiatkamjornwong, "Effects of Redox Initiator on Graft Copolymerization of Methyl Methacrylate onto Natural Rubber," *Journal of Applied Polymer Science*, vol. 101, pp. 2587-2601, 2006.
- [7] S. Amnuaypanich, and P. Ratpolsan, "Pervaporation membranes from natural rubber latex grafted with poly(2-hydroxyethyl methacrylate) (NR-g-PHEMA) for the separation of water-acetone mixtures," *Journal of Applied Polymer Science*, vol. 113, pp. 3313-3321, 2009.
- [8] P. Juntuek, C. Ruksakulpiwat, P. Chumsamrong *et al.*, "Glycidyl methacrylate grafted natural rubber: Synthesis, characterization, and mechanical property," *Journal of Applied Polymer Science*, vol. 122, pp. 3152-3159, 2011.
- [9] A. Pisuttisap, N. Hinchiranan, G. L. Rempel *et al.*, "ABS modified with hydrogenated polystyrene-grafted-natural rubber," *Journal of Applied Polymer Science*, 2013.
- [10] J.-K. Chen, and C.-J. Chang, "Fabrications and Applications of Stimulus-Responsive Polymer Films and Patterns on Surfaces: A Review," *Materials*, vol. 7, no. 2, pp. 805-875, 2014.
- [11] Y. T. L. TC, K. GS *et al.*, "pH- and ion-sensitive polymers for drug delivery.," *Expert Opinion on Drug Delivery*, vol. 10, no. 11, pp. 1497-1513, 2013.
- [12] H. Almeida, M. H. Amaral, and P. Lobão, "Temperature and pH stimuli-responsive polymers and their applications in controlled and selfregulated drug delivery," *Journal of Applied Pharmaceutical Science*, vol. 2, no. 6, pp. 01-10, 2012.
- [13] T. Kavitha, I.-K. Kang, and S.-Y. Park, "Poly(4-vinyl pyridine)-grafted graphene oxide for drug delivery and antimicrobial applications," *Polymer International*, vol. 64, no. 11, pp. 1660-1666, 2015.
- [14] O. Ozay, S. Ekici, N. Aktas *et al.*, "P(4-vinyl pyridine) hydrogel use for the removal of UO<sub>2</sub><sup>2+</sup> and Th<sup>4+</sup> from aqueous environments," *Journal of Environmental Management*, vol. 92, no. 12, pp. 3121-3129, 2011.
- [15] H. El-Hamshary, M. El-Garawany, F. N. Assubaie *et al.*, "Synthesis of poly(acrylamide-co-4-vinylpyridine) hydrogels and their application in heavy metal removal," *Journal of Applied Polymer Science*, vol. 89, pp. 2522-2526, 2003.
- [16] N. Pukkate, Y. Yamamoto, and S. Kawahara, "Mechanism of graft copolymerization of styrene onto deproteinized natural rubber," *Colloid and Polymer Science*, vol. 286, no. 4, pp. 411-416, 2008.

- [17] K. Nawamawat, J. T. Sakdapipnich, and C. C. Ho, "Effect of Deproteinized Methods on the Proteins and Properties of Natural Rubber Latex during Storage," *Macromolecular Symposia*, vol. 288, pp. 95-103.
- [18] Y. Yamamoto, P. T. Nghia, W. Klinklai *et al.*, "Removal of Proteins from Natural Rubber with Urea and Its Application to Continuous Processes" *Journal of Applied Polymer Science*, vol. 107, pp. 2329-2332, 2008.
- [19] N. Pukkate, T. Kitai, Y. Yamamoto *et al.*, "Nano-matrix structure formed by graft-copolymerization of styrene onto natural rubber," *European Polymer Journal*, vol. 43, no. 8, pp. 3208-3214, 2007.
- [20] S. Moolsin, P. Chaimee, and C. Predapattarachai, "EFFECTS OF THERMAL INITIATORS ON METHYL METHACRYLATE POLYMERIZATION IN NATURAL RUBBER LATEX," *Pure and Applied Chemistry International Conference*, 2015.
- [21] N. Nugay, Z. Küçükyavuz, and S. Küçükyavuz, "Anionic synthesis and characterization of poly(4-vinylpyridine)-poly(dimethylsiloxane) block copolymers," *Polymer International*, vol. 32, no. 1, pp. 93-96, 2007.
- [22] J.-J. Yuan, R. Ma, Q. Gao *et al.*, "Synthesis and Characterization of Polystyrene/Poly(4-vinylpyridine) Triblock Copolymers by Reversible Addition-Fragmentation Chain Transfer Polymerization and Their Self-Assembled Aggregates in Water," *Journal of Applied Polymer Science*, vol. 89, pp. 1017-1025 2003.
- [23] P. Wongthong, C. Nakason, Q. Pan *et al.*, "Modification of deproteinized natural rubber via grafting polymerization with maleic anhydride," *European Polymer Journal*, vol. 49, no. 12, pp. 4035-4046, 2013.
- [24] S. H. Goh, S. Y. Lee, X. Zhou *et al.*, "X-ray Photoelectron Spectroscopic Studies of Interactions between Poly(4-vinylpyridine) and Poly(styrenesulfonate) Salts," *Macromolecules*, vol. 31, pp. 4260-4264, 1998
- [25] A. Arizaga, G. Ibarz, and R. Piñol, "Stimuli-responsive poly (4-vinyl pyridine) hydrogel nanoparticles: Synthesis by nanoprecipitation and swelling behavior," *Journal of Colloid and Interface Science*, vol. 348 pp. 668-672, 2010.

## BIOGRAPHY

Name	Mr. Chanon Sansuk
Date of Birth	July 2, 1992
Educational Attainment	2014: Bachelor degree of Science, Major of Chemistry, Thammasat University
Work Position	Graduate student
Scholarship	Year 2015-2016: The scholarship for Talent student, Faculty of Science and Technology, Thammasat University

### Extracurricular activities

1. Participate and present poster in topic “Synthesis and characterization of poly(4-vinylpyridine)-functionalized natural rubber as pH responsive materials” at Pure and Applied Chemistry International Conference 2016 (PACCON2016), Bangkok, Thailand (9-11 February 2016)
2. Participate and present poster in topic “Preparation and pH responsive behavior of poly(4-vinylpyridine)-crosslinked natural rubber” at The 42<sup>nd</sup> Congress on Science and Technology of Thailand (STT 42), Centara grand at Central Plaza Ladprao, Bangkok, Thailand (30 November – 2 December 2016)
3. Participate and present poster in topic “Preparation and pH responsive behavior of poly(4-vinylpyridine)-crosslinked natural rubber” at the 3<sup>rd</sup> International Congress on Advance Materials (AM 2016), Centara grand at Central Plaza Ladprao, Bangkok, Thailand (27-30 November 2016)
4. Participate and oral presentation in topic “Preparation and Characterization of Deproteinized Natural Rubber Grafted with 4-Vinylpyridine as pH responsive materials at the 5<sup>th</sup> International Conference on Advances in Chemistry, Biological & Environmental Engineering (ACBEE-17), Ibis Singapore on Bencoolen, Singapore (29-30 March 2017)

## Publications

1. Chanon Sansuk, Sopitcha Phetrong, and Peerasak Paoprasert. Preparation of pH-responsive crosslinked materials from natural rubber and poly(4-vinylpyridine). *Polymer International*, 2017(66), pages 787-794. (Impact factor: 2.414)
2. Chanon Sansuk, Sopitcha Phetrong, and Peerasak Paoprasert. Preparation and Characterization of Deproteinized Natural Rubber Grafted with 4-Vinylpyridine as pH responsive materials. 5<sup>th</sup> International Conference on Advances in Chemistry, Biological & Environmental Engineering (ACBEE-17), March 29-30, 2017, Ibis Singapore on Bencoolen, Singapore. (oral presentation)

## Work Experiences

Teaching assistant in chemistry laboratory at  
Faculty of Science and Technology  
Thammasat University